Techniques for computing scattering amplitudes: Mellin space, Inverse Soft Limit, Bonus Relations.

by
Dhritiman Nandan
M. S., Brandeis University, 2008

A dissertation submitted in partial fulfillment of the requirements for the Degree of Doctor of Philosophy in the Department of Physics at Brown University

Providence, Rhode Island
May 2013

This dissertation by Dhritiman Nandan is accepted in its present form
by the Department of Physics as satisfying the dissertation
requirement for the degree of Doctor of Philosophy.

Date ______________ ____

Anastasia Volovich, Director

Recommended to the Graduate Council

Date ______________ ____

Antal Jevicki, Reader

Date ______________ ____

Chung-I Tan, Reader

Approved by the Graduate Council

Date ______________ ____

Peter M. Weber
Dean of the Graduate School

Curriculum Vitae

CONTACT INFROMATION

Email: dhriti@brown.edu, dhritiman.nandan@gmail.com

EDUCATION

2008-2013	Ph.D in Physics, Brown University, USA. Advisor: Prof. Anastasia Volovich.
2008	M.S. in Physics, Brandeis University, USA.
2005	Master of Science in Physics, Indian Institute of Technology Kanpur, India.
2002	Bachelor of Science in Physics *(with Honours)*, St. Xavier's College, Calcutta (Calcutta University), India.

PUBLICATIONS

1. "Star Integrals, Convolutions and Simplices ", arXiv:1301.2500 [hep-th], Accepted for publication in JHEP, with Miguel F. Paulos, Marcus Spradlin and

Anastasia Volovich.

2. "Generating All Tree Amplitudes in N=4 SYM by Inverse Soft Limit. ", arXiv:1204.4841 [hep-th], Published in JHEP 1208 (2012) 040 , with Congkao Wen.

3. "On Feynman Rules for Mellin Amplitudes in AdS/CFT.", arXiv:1112.0305 [hep-th], Published in JHEP 1205 (2012) 129, with Anastasia Volovich and Congkao Wen.

4. "Note on Bonus Relations for N=8 Supergravity Tree Amplitudes", arXiv:1011.4287 [hep-th], Published in JHEP 1102 (2011) 005, with Song He and Congkao Wen.

5. "A Grassmannian Etude in NMHV Minors", arXiv:0912.3705 [hep-th], Published in JHEP 1007:061,2010, with Anastasia Volovich and Congkao Wen.

CONFERENCES ATTENDED

1. "Amplitudes and Periods", Institut des Hautes Études Scientifiques, France, December 2012

2. "Scattering Without Space-Time", International Center for Theoretical Sciences, Bangalore, 2012

3. "Amplitudes 2011", University of Michigan, Ann Arbor, 2011

4. "The Fifth New England String Meeting", Brown University, Providence, 2011

5. "The Fourth New England String Meeting", Brown University, Providence, 2010

6. "The Third New England String Meeting", Brown University, Providence, 2008

SCHOOLS ATTENDED

1. CERN Winter School on Supergravity, Strings, and Gauge Theory 2013, CERN, February 2013

2. Mathematica Summer School on “Scattering Amplitudes and AdS/CFT", Perimeter Institute, Summer 2011

3. PITP Summer School on “Aspects of Supersymmetry", IAS, Princeton, Summer 2010

4. Summer School on Particles, Fields and Strings, PIMS, University of British Columbia, Summer 2008

SEMINARS AND TALKS GIVEN

1. “Generating All Tree Amplitudes by Inverse Soft Limit", at “Scattering Without Space-Time", ICTS, Bangalore, Fall 2012

2. “Grassmannian Etude in NMHV Minors", Brown University, Fall 2010.

3. “Generating All Tree Amplitudes by Inverse Soft Limit", Journal Club, Brown University, Fall 2012.

4. “Differential Equations for amplitudes in 2d kinematics- Review", Journal Club, Brown University, Summer 2012.

5. “Spinning Conformal Blocks in CFT- Review", Journal Club, Brown University, Spring 2012.

6. “BCJ for gauge and gravity theories- Review", Journal Club, Brown University, Fall 2010.

7. “Scattering Amplitudes in SYM" - Poster, Graduate Research Poster Session, Brown University, Fall 2011.

8. “Scattering Amplitudes, Grassmannians and Twistor String Theory " - Poster, Graduate Research Poster Session, Brown University, Fall 2010.

HONORS AND AWARDS

1. Research Assistantship, Brown University, 2009-2012.

2. Teaching Assistantship awarded by Department of Physics, Brown University, 2008 -2009(Fall and Spring).

3. Summer Research Assistantship, Brown University, 2008 Summer.

4. Teaching Assistantship awarded by Brandeis University, 2005-2007.

Acknowledgements

The long journey through graduate school would not have been a worthwhile and enjoyable experience without the support of many people!

I would like to take this opportunity to thank my advisor, Prof. Anastasia Volovich for her inspiring guidance during all these years. Her deep insights and perceptive analysis regarding physics has helped shape my understanding of the topics discussed in this thesis and beyond. Moreover, her enthusiasm and the constant support for all the different projects I undertook including various directions pursued independently, went a long way in making this a delightful experience.

The great joy of research is in imbibing and sharing new knowledge and I have been rather fortunate to get the chance to collaborate with amazing physicists. I owe a great deal to Prof. Mark Spradlin, Dr.Congkao Wen, Dr. Miguel Paulos and Dr. Song He for teaching me so many things during our fruitful collaborations! Their generosity in giving time to teach the subject is unparalleled.

It is a pleasure to acknowledge all the physics I learned from Prof. Antal Jevicki, Prof. David Lowe, Prof. Chung-I Tan and Prof. Mark Spradlin. Their willingness to share their profound insights on a wide range of topics and the rigorous and entertaining courses they taught at Brown has made this journey rather memorable.

The postdocs in the group played a great role in making this an exciting place and Dr. Klaus Larjo, Dr. Ari Pakman, Dr. Miguel Paulos, Dr. Alex Prygarin, Dr. Ilias Messamah and Dr. Cristian Vergu has been a great source for learning new ideas and interesting anecdotes! Special thanks are in order for Cristian for helping me to get up to speed with Mathematica skills!

My fellow students and also the senior grad students in the Brown HET Group were the perfect partners in crime and it was an absolute joy to share the office with them. Special thanks to Micheal Abbott, Ines Aniceto, Shubho Roy, Marko Djuric, Yorgos Papathanasiou, Chris Kalousious, Congkao Wen, Kewang Jin, Antun Skanata, Qibin Ye, Peter Tsang, John Golden, Timothy Raben, Jung-Gi Yoon! It was great fun to have many interesting conversations on everything under the sun, with Ata Karacki, Mike Luke, Mike Segala, Qibin Ye, Antun Skanata, Florian Sabou, Mirna Mihovilovic, Saptaparna Bhattacharyya, Ravi Singh, Alex Geringer-Sameth, Son Le and Alexandra Junkes!

Friends in various corners of the globe has been instrumental in keeping my sanity for all these years! It has been the greatest pleasure to have as friends, Sayak Mukherjee, Arnab Kundu, Rakhi Acharyya, Anwesha Tapadar, Arjun Bagchi, Dyotana Banerjee, Abhishek Roy, Abhishek Kumar, Amar Chandra, Jishnu Bhattacharyaa, Jaydip Sen, Dipromit Majumdar, Apratim Roy, Tathagata Sengupta, Satish Akella, Anish Mokashi, Tanmay Das, Sudeep Das, Junuka Deshpande, Aditee Dalvi and Priyanka Dalvi!

Thanks to Mary Ann Rotondo and Barbara Dailey for always helping out with the administrative issues!

I would like to thank my family, parents Sikha Nandan and Milan Nandan, and brother Debarshi Nandan for their continuous love and support.

Lastly, no thanks are enough for my wife Susmita Basak for always being there through all these years! This journey would not have been the same without her constant companionship!

Contents

List of Tables xiv

List of Figures xv

1 Introduction 1

1.1 Scattering Amplitudes 1

1.1.1 Review of recent progress 3

1.1.2 Outline 7

1.1.3 Kinematic variables for scattering amplitudes 10

1.1.4 Tree Level Amplitudes 14

1.2 AdS/CFT correspondence 20

1.2.1 Correlation functions in CFT 22

1.2.2 Embedding Space 22

2 Mellin Amplitudes for Correlation functions 24

2.1 Introduction 24

2.2 Feynman rules for Mellin amplitudes 26

2.3 Proof of Feynman rules 28

2.3.1 Maximal off-shell vertex 28

2.3.2 Evaluating the integrals 31

2.3.3 General case 40

2.4 Flat space limit 43

3 Star Integrals, Convolutions and Simplices 46

3.1 Introduction 46

3.2 Mellin amplitudes refresher 50

3.2.1 The Mellin amplitude 50

3.2.2 Feynman rules and convolutions 51

3.3 Star integrals 54

3.4 $2n$-gon loop integrals in $2d$ kinematics 60

3.4.1 Setup: splines 60

3.4.2 Applications: hexagon, octagon, and beyond 62

3.5 Elliptic functions and beyond 65

3.5.1 The double box 65

3.5.2 The triple box 69

4 Generating tree level amplitudes in $\mathcal{N} = 4$ SYM by Inverse Soft Limit 72

4.1 Introduction 72

4.2 Two-particle channel BCFW and ISL in SYM 75

4.2.1 Inverse soft factors and shifts 75

4.2.2 Examples 80

4.3 Recursion relation for adding particles 83

4.3.1 MHV 83

4.3.2 NMHV 86

4.3.3 NNMHV 92

4.3.4 N^{k}MHV 96

4.3.5 Amplitudes from ISL 98

4.4 BCFW shifts from ISL 100

4.5 Constructing form factors 104

4.6 Conclusion 108

5 Gravity Tree amplitudes using Bonus Relations 110

5.1 Introduction 110

5.2 A brief review of tree amplitudes in SUGRA and bonus relations . . . 114

5.2.1 Tree Amplitudes in SUGRA from BCFW Recursion Relations 114

5.2.2 Applying Bonus Relations to MHV Amplitudes 118

5.3 Applying Bonus Relations to Non-MHV Gravity Tree Amplitudes . . 119

5.3.1 General Strategy 119

5.3.2 NMHV Amplitudes 122

5.3.3 N^{2}MHV amplitudes 128

5.4 Generalization to all gravity tree amplitudes 134

5.5 Conclusion and outlook 139

A Appendix for Chapter 2 **141**

A.1 Useful integrals 141

A.2 Example: 9-points in ϕ^3 theory 142

B Appendix for Chapter 3 **147**

B.1 Details on the double box computation 147

B.2 Details on the triple box computation 150

B.2.1 Cross-ratios for eight-point functions 150

B.2.2 A Γ-function parameterization 152

C Appendix for Chapter 4 **154**

C.1 ISL in Momentum Twistor 154

C.2 Example of the ISL recursion relations 155

C.3 Two-particle channel BCFW and ISL in gravity 157

List of Tables

List of Figures

2.1 A general vertex for ϕ^n theory. 28

2.2 The Witten diagram for the scalar ϕ^n theory with a vertex having n off-shell legs and n vertices having 1 off-shell leg and $(n-1)$ on-shell legs. 29

2.3 A vertex with all off-shell legs in arbitrary Witten diagram. 40

3.1 The one-, two- and three-loop ladder diagrams (black) and their corresponding dual tree diagrams (blue). The external faces of the former, or equivalently the external vertices of the latter, are labeled $x_1, x_2, \ldots$ clockwise starting from x_1 as indicated. 52

3.2 The 'star' graphs for $n = 4, 6, 8$, in blue, correspond to the one-loop box, hexagon, and octagon integrals in $d = 4, 6, 8$ respectively. These are the basic building blocks for many integrals relevant to multi-loop scattering amplitudes in SYM theory since each one is simply $M = 1$ in Mellin space. 54

4.1 BCFW diagram of two particle channel corresponding to adding particle 1^+. 77

4.2 BCFW diagram of two particle channel corresponding to adding particle 1^-. 78

4.3 **(a):** For the $\langle 1\ n]$ shift we add particles $\{1, \ldots, m-1\}$ on the left side of the first diagram to make it $A_L^{\text{MHV}}(\widehat{1}, \ldots, m, \widehat{P})$ while the subamplitude A_R on the right can be of any type.
(b): For the $[1\ n\rangle$ shift we add particles $\{1, \ldots, m-1\}$ on the left side of the first diagram to make it$A_L^{\text{MHV}}(\overline{1}, \ldots, m, \widehat{P})$ 84

4.4 **(a):** For the $[1\ n\rangle$ shift we add particles $\{1, \ldots, m-1\}$ on the left side of the this diagram to build up $A_L^{\text{NMHV}}(\overline{1}, \ldots, m, \widehat{P})$ while A_R on the right can be of any type.
(b, c): These are the corresponding BCFW contributions to the $(m+1)$ point subamplitude A_L^{NMHV} in **(a)**. 87

4.5 **(a):** For the $\langle 1\ n]$ shift we add particles $\{1, \ldots, m-1\}$ on the left side of the first diagram to build up $A_L^{\text{NMHV}}(\widehat{1}, \ldots, m, \overline{P})$ while A_R on the right can be of any type.
(b, c): These the corresponding BCFW contributions to the $(m+1)$ point subamplitude A_L^{NMHV} from **(a)**. 90

4.6 **(a):** For the $[1\ n\rangle$ shift we add particles $\{1, \ldots, m-1\}$ on the left side of the first diagram to make it $A_L^{\text{NNMHV}}(\overline{1}, \ldots, m, \widehat{P})$ while the subamplitude A_R on the right can be of any type.
(b, c, d): In these three diagrams inside the box we consider the three different BCFW contributions that are possible for the $(m+1)$ point subamplitude A_L^{NNMHV} from **(a)**. 92

4.7 **(a):**For the $[1\ n\rangle$ shift we add particles $\{1, \ldots, m-1\}$ on the left side of the first diagram to make it$A_L^{\text{NNMHV}}(\overline{1}, \ldots, m, \widehat{P})$ while the subamplitude on the right can be of any type A_R.
(b,c,d): In these three diagrams inside the box we consider the three different BCFW contributions that are possible for the $(m+1)$ point subamplitude A_L^{NNMHV}, from (a) 95

4.8 **(a):** Contribution to a $(m+1)$point N^{k}MHV amplitude for $[1\ m+1\rangle$ shift.
(b): Contribution to a $(m+1)$point N^{k}MHV amplitude for $\langle 1\ m+1]$ shift. 97

4.9 **(a,b):** The two possible BCFW diagrams for the $[1\ n\rangle$ shift where F is the form factor and A is the amplitude. 104

5.1 Rooted tree diagram for tree-level SYM amplitudes 116

5.2 All factorizations contributing to (5.2.11) for the MHV amplitude. . . 118

5.3 Different types of diagrams for a general N^kMHV amplitude, where $k = p + q + 1$. We use a dashed line $- - --$ connecting three legs to denote a bonus-simplified lower-point amplitude, in which these three legs are kept fixed. For lower-point amplitudes without dashed lines, we use the usual $(n-2)!$ form. 121

5.4 Diagrams for NMHV amplitudes. 123

5.5 Diagrams for 5-point NMHV amplitude and the boundary term of 6-point NMHV amplitude. Fig. 5.5(a) and Fig. 5.5(b) are used to calculate the bonus-simplified 5-point right-hand-side amplitude of Fig. 5.5(c). 126

5.6 Diagrams for N^2MHV amplitudes. 131

5.7 Diagrams for 6-point N^2MHV amplitude. 133

5.8 Two relevant diagrams for computing new bonus coefficients for n-point N^kMHV amplitude. The rest of the bonus coefficients can be obtained recursively from the N^{k-1}MHV case. 136

A.1 A vertex with all off-shell legs in 9-point amplitude in ϕ^3 theory . . . 143

C.1 A particular BCFW diagram occuring in 10 point N^3MHV amplitude . . . 156

Chapter 1

Introduction

1.1 Scattering Amplitudes

The S-matrix is the transfer matrix between states that are well separated in spacetime. The elements of the S-matrix or the scattering amplitudes contain the description of all the physical processes of the theory. It has been shown in the $60's$ that we can study some general properties of this S-matrix like analyticity, unitarity and symmetries and deduce wonderful insights about the theory. But, the advent of QCD and the development of gauge theories in the seventies put this idea on hold. In spite of great success, unfortunately, gauge theories have a great deal of redundant degrees of freedom and these seriously complicate computations of scattering processes by perturbative techniques and often obscures the underlying symmetry and structure of the theory. This situation worsens in the case of gravity where the diffeomorphism symmetry brings in enormous redundancy. Even for pure Einstein gravity there is a proliferation of Feynman diagrams and even the number of terms for even a simple vertex grows tremendously as we increase the number of particles. This makes dealing with gravity amplitudes a daunting task. However, this is not the end of the tunnel! Even in this hopeless scenario an unexpected result was discovered by Parke and Taylor[1][1] when they were studying scattering of massless gluons in QCD. They could find a remarkably simple answer to an entire class of amplitudes, the ones where 2 of the gluons have negative helicity and rest positive and named the Maximally Helicity Violating(MHV) amplitudes. The compact result for such a $n-$ particle MHV amplitude is[2],

$$A(1^{+},\dots,i^{-},..j^{-},\dots,n)=\frac{\langle i\,j\rangle^{4}}{\langle 1\,2\rangle\langle 2\,3\rangle\dots\langle n\,1\rangle}. \tag{1.1.1}$$

The Parke-Taylor formula laid the foundation for the current advances in the study of scattering amplitudes of massless gauge theories. It is also known that due to Supersymmetric Ward identities, the amplitudes with one or no negative helicity gluons, vanish[5, 6, 7, 8]. This simple results coming at the end of a very complicated computational process opened a window for exploring new methods for describing the hidden structures of the gauge theory by studying scattering amplitudes. Before we go on to review some of the preliminary ideas that would be used often in the later chapters of the thesis, we would present a brief overview of the recent advancements in the study of scattering amplitudes.

[1] See [2, 3, 4] for similar results.

[2] The Spinor Helicity variables will be explained in details in the next section. It is sufficient to know for now that $\langle a\,b\rangle$ are Lorentz invariant combinations of some commuting spinors.

1.1.1 Review of recent progress

In the recent years, the resurgence of scattering amplitudes in gauge theories has been driven by the new knowledge of on-shell and Unitarity based techniques.

These ideas are as useful for probing the formal aspects of quantum field theories as they are for finding new computational techniques, that would assist in decoding the signals in the collider experiments. The LHC is one of the most ambitious endeavours to unravel the mysteries of fundamental interactions. It is expected to fill in the missing pieces in the Standard Model as well as push the frontiers of our knowledge and throw some light on the new physics beyond the Standard Model. However, in experiments studying very high energy scattering processes there is a profusion of background jets produced from QCD processes.In order to study the physical processes leading us to new physics, it is essential to know the cross-section of such multi-jet processes. Scattering amplitudes in QCD are very relevant for such computations, unfortunately, they are very difficult to compute. Recent studies have focused mostly on the $\mathcal{N} = 4$ Super Yang Mills(SYM) theory which share many properties with QCD . However, this theory is relatively easier for computational purposes because only planar diagrams contribute in the large N_c limit and moreover, the maximal supersymmetry imbues it with many simplifying structures.

In 2003 Witten[9] has shown that the $\mathcal{N} = 4$ SYM Theory can be obtained from a Topological String theory in twistor space and that the scattering amplitudes in SYM theory have a very simple and geometric interpretation in terms of the curves in twistor space. This idea has been taken forward in complementary directions by Roiban, Spradlin and Volovich[10] and Cachazo, Svrcek and Witten[11] to give different formulations for constructing tree level amplitudes of $\mathcal{N} = 4$ SYM. The spirit of the S-matrix program for studying analytic properties of scattering amplitudes was utilized in novel ways was Britto, Cachazo, Feng and Witten(BCFW)[12, 13]. They have shown that, factorization properties of tree level amplitudes can be used to construct amplitudes recursively from lower point amplitudes. This has unlocked a door in our ability to compute tree level amplitudes for a large number of particles. Numerous studies of these BCFW recursion relations established the recursion to hold for a large class of gauge theories as well as gravity theories. It has also been noticed that there also exists simple generalizations of BCFW for supersymmetric amplitudes in both $\mathcal{N} = 4$ SYM and $\mathcal{N} = 8$ Sugra[14].

The unitarity based method[15] provides a parallel direction to study loop amplitudes in gauge theories. The main idea is to reconstruct the full loop amplitude by cutting various propagators and then fusing on-shell tree amplitudes in new ways to do the reconstruction . These ideas and especially their generalizations for the case of supersymmetric theories greatly simplified one loop amplitude computations and also provided new techniques for multi-loop amplitudes. Especially these ideas and also knowledge about the nature of IR divergences for massless particles allowed Anastasiou, Bern, Dixon and Kosower[16] and Bern, Dixon and Smirnov(BDS)[17] to conjecture all loop MHV amplitudes to have a very simple iterative structure. The study of loop amplitudes in maximally supersymmetric theories has also led to the discovery of a remarkable symmetry by Drummond, Henn, Korchemsky and Sokatchev[18, 19], called the dual superconformal symmetry, which is completely obscured from the Lagrangian perspective. The conformal symmetry along with the dual superconformal symmetry closes on to an infinite dimensional symmetry called

Yangian. The Yangian symmetry of this planar sector of $\mathcal{N} = 4$ SYM is believed to be related to integrability properties of the theory in this regime.

On the other hand the gauge/gravity duality had shed more light on the holographic description of scattering amplitudes. Alday and Maldacena [20]have shown that at strong coupling scattering amplitudes can be determined by computing expectation values of lightlike Wilson loops in a dual space which would be the boundary of a minimal surface in the AdS space. Moreover, it was also realized that the working of the BDS proposal was the result of the hidden dual conformal symmetry and it can be viewed as the usual conformal symmetry for the dual Wilson loops[21]. In fact, the dual conformal symmetry has been understood from the AdS/CFT perspective as a fermionic T-dual description of the spacetime physics[22, 23]. The duality between Wilson loops and scattering amplitudes have also been extended to all types of amplitudes and many interesting connections were discovered between Correlation functions, Wilson loops and scattering amplitudes in this context[24, 25, 26].

In another very recent development Arkani-Hamed, Cachazo, Cheung and Kaplan[27] had furthered our understanding of the scattering amplitudes by writing down a dual formulation of the scattering amplitude, as a Grassmannian integral, for calculating the leading singularities to all loop orders. Shortly after, Arkani-Hamed, Bourjaily, Cachazo, Caron-Huot and Trnka [28] also opened a new direction for calculating loop level amplitude by writing down a BCFW recursion of the loop integrand at any loop order. They have used the new variables called momentum twistors, previously introduced by Hodges, and these are the most natural variables making dual Superconformal symmetry manifest[29, 30]. In fact, the Yangian symmetry has played a very important role in both cases. Recently, a better understanding of the this approach has been proposed, in terms of on-shell diagrams and their remarkable connections to ideas in combinatorics[31].

The study of these multiloop amplitudes using momentum twistors and the ABCCT formulation for the integrand makes the scenario more tractable than the existing methods, but still leaves us with the job of evaluating the full integral which can still be a formidable task. Fortunately, new ideas from the theory of motives introduced by Goncharov, Spradlin, Volovich and Vergu[32], make us view such a seemingly intractable scenario in a more favourable light. They have introduced the idea of "Symbols" for dealing with iterated integrals and this has also led to other insights relating multi-loop amplitudes and areas in mathematics like number theory or algebraic geometry.

Another very interesting development is due to Bern, Carrassco and Johansson[33], who show that gauge theory amplitudes can be written in a rather novel way by using a duality between color factors and "kinematic factors". This structure is also carried over to loop amplitudes.

The maximally supersymmetric theory of gravity in 4 dimensions, $\mathcal{N} = 8$ Supergravity(Sugra) has also shown many unexpected simplicities in the perturbative regime. The earlier mentioned BCFW recursion relation and their supersymmetric extension also apply to this theory. It is seen that gravity has an even better behavior under BCFW deformations, than gauge theory, which has led to it being dubbed as the "Simplest Quantum Field Theory" [14] with respect to the scattering amplitudes. This simplicity manifests itself in many extra relations between its tree level amplitudes called Bonus relations. There has been an ongoing debate on the finiteness of $\mathcal{N} = 8$ Sugra and using supersymmetry and other considerations the projected divergence has been predicted to show up at 7 loops[34, 35, 36, 37, 38]. The unitarity based methods have been very useful in trying to understand these issues.

A rather intriguing aspect of gravity amplitudes are the KLT relations[39], derived from string theory, relating gravity amplitudes to the square of Yang-Mills amplitudes. In the similar spirit the color-kinematic duality of gauge theory can be used to determine gravity as a double copy of gauge theory[40].

All these remarkable developments had strengthened the idea that the on-shell scattering amplitudes are rather unique observables in gauge theories as they are able to encode so many hidden symmetries and mathematical structure of the theory.

1.1.2 Outline

In the rest of this chapter we review various techniques and ideas that would be used often in the later chapters.

It has been noticed that the Mellin amplitudes of tree-level scalar correlation functions with any scalar interaction in the bulk can be built up by rules analogous to Feynman rules for scattering amplitudes. These rules were conjectured by Paulos[41] and Fitzpatrick, Kaplan, Penedones, Raju and van Rees[42]. So in effect we can get all the important information about the correlation function without doing any complicated position space integrals. In Chapter 2 I present our work with Volovich and Wen[43]. We have been able to derive these proposed Feynman rules for any scalar theory in the bulk . Another interesting analogy with scattering amplitudes is that the Mellin amplitudes are functions of variables which are analogous to Mandelstam invariants with some “momenta"- like variables defined in an auxiliary space and it has been proposed that the flat space limit of Mellin amplitudes actually give a holographic description of flat space S-matrix elements. In our work we also show that this proposal holds for the Feynman rules which would in effect give the holographic tree-level flat-space S-matrix elements.

Recently it has been observed by Paulos, Spradlin and Volovich[44] that the Mellin space representation is also a very useful way to deal with the boundary S-matrix in AdS/CFT in the perturbative regime especially all the dual conformal invariant multi-loop integrals that arise in $\mathcal{N} = 4$ SYM theory. In fact, such integrals in given spacetime dimensions can be related to integrals at lower loop level but in higher spacetime dimensions via some differential or integral operators using the Mellin space technique. A specific example of such a case would be the connection between one loop hexagon integral in six dimensions and the two loop double box in four dimensions. In Chapter3 I am exploring such scenarios with Paulos, Spradlin and Volovich.We probe the scenario that multi-loop integrals can be obtained as integro-differential operators acting on star integrals in Mellin space. We present some new computations of pentagon, hexagon and octagon stars to corroborate this idea. We also investigated whether one encounters a much more complicated basis of functions beyond generalized Polylogarithms, like elliptic functions, for the multi-loop integrals under consideration using the above-mentioned techniques.

A very interesting fact about amplitudes in gauge and gravity theories is that they have a very nice soft behavior(i.e. when the momentum of one of the particles vanishes). Under a soft limit a given amplitude is related to an amplitude with one lower number of external particles times an universal soft factor. In recent years though there has been some attempts to construct amplitudes by the reverse procedure i.e. by constructing amplitudes using the universal soft factors mentioned above while starting from an amplitude with lower number of external particles. This is called the Inverse Soft approach[27, 45]. In Chapter 4 I present my work from a paper with Wen[46], in which we were able to show explicitly that one can use the Inverse Soft procedure to construct tree level superamplitudes of $\mathcal{N} = 4$ SYM. This is a novel method of bootstrapping our way up to any amplitudes, starting from a three point amplitude, such that the soft behavior is manifest and this is the result of an exact recursion relation that we proposed in our paper. The recursion relation allows us to find the specific configuration for adding particles to construct any BCFW (Britto, Cachazo, Feng and Witten)[13] diagram term that constitute a tree level amplitude. A rather unique symmetry of $\mathcal{N} = 4$ SYM is the dual superconformal symmetry discovered by Drummond, Henn, Korchemsky and Sokatchev. This symmetry which is a part of the Yangian symmetry of this theory, is completely obscured from the Lagrangian picture . We also show that the Inverse Soft procedure is pretty robust and can even be extended to theories with no Yangian symmetry and we also showed that it is possible to construct Form Factors of $\mathcal{N} = 4$ SYM by the same prescription. We were able to extend the above ideas to $\mathcal{N} = 8$ supergravity for the graviton MHV amplitudes.

Scattering amplitudes in $\mathcal{N} = 8$ SUGRA also exhibit many other interesting properties. It has been recently pointed out by Arkani-Hamed, Cachazo and Kaplan[14] that there are reasons to believe that $\mathcal{N} = 8$ SUGRA to be even simpler than SYM. One particular interesting feature behind their claim is the fact that gravity amplitudes exhibit exceptionally soft behavior under BCFW shift, which leads to an interesting extra relation between gravity amplitudes, which is called bonus relation. These relations have been very useful in showing the equivalence of many different Maximally Helicity Violating(MHV) forms of gravity amplitudes. In Chapter5 I present our work with He and Wen[47], where we have extended the utilities of bonus relation beyond the MHV level to any N^{k}MHV amplitudes, which greatly simplifies the previous known results for all tree-level gravity scattering amplitudes and writes the final result as a permutation sum over $(n-3)!$ terms.

1.1.3 Kinematic variables for scattering amplitudes

In this dissertation we will be mostly studying a specific gauge theory, the $\mathcal{N}=4$ Super Yang-Mills(SYM) theory in 4 dimensions with a $SU(N_c)$ gauge group with t'Hooft coupling $\lambda = g^2 N_c$ where g is the Yang-Mills coupling constant. We will consider color-ordered partial amplitude at tree level. We consider the theory at large $N_c \to \infty$ limit such that only the planar Feynman diagrams contribute. In such a scenario it can be shown that only the single-trace terms are relevant and the amplitude can be expressed as,

$$\mathcal{A}_n(\{k_i, h_i, a_i\}) = g^{n-2} \sum_{\sigma \in S_n/Z_n} \mathrm{Tr}(T^{a_{\sigma(1)}} \cdots T^{a_{\sigma(n)}})\ A_n(\sigma(1^{h_1}), \ldots, \sigma(n^{h_n}))\,. \quad (1.1.2)$$

This procedure, called the color-ordering[2, 4, 48, 49], is a tremendous simplification since before this step amplitudes are functions of momenta, polarization vectors and color factor of each particle. By color-ordering one has factored out the color-dependency so we only need to compute the color-ordered partial amplitude $A_n(\sigma(1^{h_1}), \ldots, \sigma(n^{h_n}))$ multiplying each trace factor.

Spinor Helicity

Scattering amplitudes are functions of the momenta and polarization vectors of the particles. But due to the gauge freedom $\epsilon \to \epsilon + \alpha p$ these are not very good variables. In 4 dimensions though we can use the fact the massless particles can be only characterized by their helicity and momenta can be written using 2 component spinors. This leads to the spinor helicity method which turn out to be a very useful set of variables for writing the amplitudes. We will mostly follow [9, 50] for this review. Let us introduce this method, now;

We can turn the momentum 4− vectors, p^μ of a particle into a 2×2 matrix by using the complete set of Pauli matrices in the following way,

$$p^{\alpha\dot{\alpha}} = \frac{1}{2} p^\mu \sigma_\mu^{\alpha\dot{\alpha}}, \tag{1.1.3}$$

where , the Pauli matrices $\sigma_\mu^{\alpha\dot{\alpha}}$ are,

$$\sigma_1 = \begin{pmatrix} 0 & 1 \\ 1 & 0 \end{pmatrix}, \quad \sigma_2 = \begin{pmatrix} 0 & -i \\ i & 0 \end{pmatrix}, \quad \sigma_3 = \begin{pmatrix} 1 & 0 \\ 0 & -1 \end{pmatrix}, \quad \sigma_0 = \begin{pmatrix} 1 & 0 \\ 0 & 1 \end{pmatrix} \tag{1.1.4}$$

For the given choice of the Pauli matrices, we can write the massless on-shell condition for the momenta as,

$$det|p^{\alpha\dot{\alpha}}| = p^2 = 0, \tag{1.1.5}$$

which implies that the 2×2 matrix $p^{\alpha\dot{\alpha}}$ has rank at most 1 and it can be written in terms of the spinor helicity variables as,

$$p^{\alpha\dot{\alpha}} = \lambda^{\alpha}\tilde{\lambda}^{\dot{\alpha}}. \tag{1.1.6}$$

We note that for the complexified Minkowski space with signature $(+,+,-,-)$ the holomorphic and the anti-holomorphic spinor helicity variables λ and $\tilde{\lambda}$ are independent real variables. The Lorentz invariants can be written in terms of these variables in the following way,

$$\begin{aligned} \langle i\, j\rangle &= \epsilon_{AB}\lambda_i^A\Lambda_j^B \\ [i\, j] &= \epsilon_{\dot{A}\dot{B}}\tilde{\lambda}_i^{\dot{A}}\tilde{\lambda}_j^{\dot{B}}, \end{aligned} \tag{1.1.7}$$

where ϵ_{AB} and $\epsilon_{\dot{A}\dot{B}}$ are the antisymmetric invariant tensors. The Mandelstam invariants can be expressed as,

$$(p_i + p_j)^2 = s_{ij} = -2p_i \cdot p_j = \langle i\, j\rangle[i\, j], \tag{1.1.8}$$

and the more complicated invariants too can be defined in a similar way only in terms of the Lorentz invariant contractions of the holomorphic and anti-holomorphic spinors. We note here that these spinors give the wavefunctions of massless particles of helicity $-\frac{1}{2}$ and $\frac{1}{2}$ respectively. We can also construct the polarization vector for a gluon with a given helicity using the spinor variables. Corresponding to the positive helicity gluon one can define the polarization vector as, $\epsilon^+_{A\dot{A}} = \frac{\mu_A\tilde{\lambda}_{\dot{A}}}{\langle\mu\,\lambda\rangle}$ where the arbitrary spinor μ_A encodes the freedom to make different gauge choices. Similarly for negative helicity spinors we can define polarization vectors as $\epsilon^-_{A\dot{A}} = \frac{\lambda_A\tilde{\mu}_{\dot{A}}}{[\tilde{\lambda}\,\tilde{\mu}]}$. Now we can define any color-ordered partial amplitude as $A(\{p_1, h_1\}, \ldots, \{p_n, h_n\})$.

Twistor Space

The Twistor space[51, 52] has been used extensively for studying scattering amplitudes and Wilson loops in four dimensional maximally supersymmetric gauge theories. These variables unravel remarkable simplicity in the observables by making the conformal symmetry of the theory manifest and the twistor space can be naturally supersymmetrized. Let us do a quick review of the basic notion of twistor space and its relation with ordinary spacetime.

Twistor space is characterized by homogenized coordinates,

$$Z^A = \{\underbrace{\mu_a, \lambda^a}_{Z^a}, \eta^\alpha\} \tag{1.1.9}$$

where the bosonic twistor part Z^a is described by the two, $2-$component Weyl spinors, $\{\mu, \lambda\}$ which are related by the following incidence relation,

$$\mu^A = ix^{AB}\lambda_B, \quad \eta^\alpha = \theta^{\alpha B}\lambda_B \tag{1.1.10}$$

where the point $\{x, \theta\}$ is a spacetime point in the complexified Minkowski spacetime $\mathfrak{M}^{2|4}$. The incidence relation implies that 2 points in spacetime are null separated when the corresponding lines in twistor space intersect at a point. Hence, null spacetime lines correspond to points in twistor space.

Momentum Twistor

We had discussed earlier that scattering amplitudes in $\mathcal{N} = 4$ SYM possess an unique symmetry called the dual superconformal symmetry. Momentum twistors are variables which are twistors in this dual space. The momentum twistors, initialy introduced by Hodges[53] solves the momentum conservation. Let us first introduce the dual region momenta space where the dual superconformal symmetry acts. We can write the momentum of different particles as,

$$p_i = x_{i+1} - x_i \tag{1.1.11}$$

With the identification $x_{n+1} = x_1$, we can see that the momentum conservation is trivialized in this coordinates, $\sum_i p_i = 0$. Moreover, we consider the null separated region momenta, $(x_{i+1} - x_i)^2 = 0$ then we would also insure on-shell condition and by the above conditions we can see that the momenta can be joined end-to-end to form a closed polygon with null faces.

1.1.4 Tree Level Amplitudes

Tree Level Amplitudes can be determined by their analytic structures. In fact they can be treated as meromorphic functions determined by the poles which are given by the physical exchange of external particle channels.

BCFW Recursion relations

BCFW recursion relations[13] were initialy studied in the context of tree level amplitudes in $\mathcal{N} = 4$ SYM theory but it is generically valid for any QFT in any dimensions. Let us consider a color ordered $n-$particle amplitude $A(1, 2, \ldots n)$. We would like to study analytic structure of scattering amplitudes as functions of complex variable. Britto-Cachazo-Feng-Witten(BCFW) has taken two adjacent momenta and shifted them in such a way that momentum is conserved as well as the external particles remain on-shell.

$$\widehat{p_1}(z) \to p_1 - zq, \quad \overline{p_n}(z) \to p_n + zq, \tag{1.1.12}$$

such that

$$p_i.q = 0, \quad \text{and} \quad q^2 = 0. \tag{1.1.13}$$

The above deformations and the associated constraints can only be solved for complexified q or in complexified Minkowski plane. Using the parametrization of the momentum in complexified Minkowski plane by using the spinor-helicity variables we can find a solution for q and it can be written as,

$$\begin{aligned} \lambda_{\widehat{1}} &= \lambda_1 - z\lambda_n; \\ \tilde{\lambda}_{\overline{n}} &= \tilde{\lambda}_n + z\tilde{\lambda}_1; \end{aligned} \tag{1.1.14}$$

and $[1\ n\rangle$ to denote the parity flipped version of the above shifts, namely

$$\begin{aligned} \lambda_{\hat{1}} &= \tilde{\lambda}_1 - z\tilde{\lambda}_n; \\ \lambda_{\hat{n}} &= \lambda_n + z\lambda_1; \end{aligned} \tag{1.1.15}$$

The above form of the complexified amplitude $A(z)$ has a very nice behaviour as a meromorphic function in z which only has simple poles. Moreover, for tree amplitudes the simple poles are given by the physical factorization channels i.e. propagators, $P_{ik} = (\sum_{j=i}^{k} p_i)^2$, going on-shell in the Feynman diagrammatic expansion of the amplitude. Under the BCFW shifts the shifted propagators $\widehat{P}_{ik}^2(z) = 0$ has a solution only when one of the shifted momenta is contained in the setP_{ik} and it is given by

$$z* = \frac{P_{ik}^2}{[1|P_{ik}|n\rangle} \tag{1.1.16}$$

The residues at the above poles (1.1.16) of the amplitude also has a physical interpretation in terms of lower point amplitudes and hence the picture of the factorization of the amplitude about the physical poles are completely determined by the analytic and unitary properties of the amplitude. Generally we can write the amplitude factorized on physical kinematical channels as,

$$Res\,(A(z))\,|_{z=z*} = -\sum_{h_i} A_L^{h_i}(z*)\frac{i}{\widehat{P}_{ik}^2(z)} A_R^{-h_i}(z*) \tag{1.1.17}$$

where h_i is the helicity and we do a sum over all helicities and the lower point amplitudes are evaluated on the poles and are on-shell. Now, if for certain types of amplitudes in different theories like Yang-Mills or gravity $A(z \to \infty) \to 0$ we get a rather remarkable form of the amplitude due to the property of meromorphic functions. For the previous scenario we can integrate $A(z)$ over a closed contour $\mathcal{C}$ which encloses all the simple poles $z*$,

$$\frac{1}{2\pi i}\int_{\mathcal{C}} \frac{dz}{z} A(z) = A(0) + \sum_{z \exists z*} Res \frac{A(z)}{z} = 0. \tag{1.1.18}$$

So the physical amplitude $A(0)$ is computed in terms of lower point amplitudes in a recursive manner,

$$A = A(0) = \sum_{h_i} A_L^{h_i}(z*) \frac{i}{P_{ik}^2} A_R^{-h_i}(z*). \tag{1.1.19}$$

This is the famous BCFW recursion relation for tree-level amplitudes and it has been a very powerful technique since it is a very general property about factorization of amplitudes of physical theories which satisfy certain conditions under very large deformations in some complex deformations. The two theories which we would be dealing with in this thesis has the following behavior under such deformations,

$$\begin{aligned} \text{Yang} - \text{Mills}: \quad A(z) \to \frac{1}{z} \\ \text{Gravity}: \quad M(z) \to \frac{1}{z^2}, \end{aligned} \tag{1.1.20}$$

and hence they can both be constructed by this recursion relation. It is important to note that the seed of this recursion is determined by the 3− point amplitudes in both theories. Unlike in Minkowski space where the 3− point amplitudes vanish, in complexified Minkowski it is not the case and the 3− point amplitudes determined by the Poincare symmetry only are the basic building blocks of any amplitude. Another interesting observation is that when we sum over all possible helicities in the BCFW recursion we get many terms contributing to the particular amplitude and many of them have poles which are not present in the physical amplitude, called 'spurious poles'. But, remarkably, the sum of all the terms add up to cancel such spurious poles and only the physical poles are present.

SUSY Amplitudes

Now we will review the extension of the BCFW for the case of super-symmetric theories. We will see that SUSY in fact makes all amplitudes behave in a much better way for both gravity and gauge theories. But before explicitly showing this nice feature for both $\mathcal{N}=4$ and $\mathcal{N}=8$ SUGRA let us build the framework for dealing explicitly with supersymmetric $\mathcal{N}=4$ SYM since we will be concerned with many aspects of this theory during rest of the thesis, moreover the power of supersymmetry shows itself in all its glory for this particular gauge theory. The key idea behind the great progress in understanding the scattering amplitudes in this particular theory, is the existence of the on-shell superspace first introduced by Nair[54], where by making the symmetries of the theory manifest.This allows us to treat different helicity amplitudes on the same footing. But in order to do that let us first observe that the on-shell superspace lets us package the different field contents of the $\mathcal{N}=4$ SYM theory into a single super-wavefunction $\Psi(\eta,p)$ by introducing Grassmann variables η^A ($A=\{1,\ldots,4\}$) transforming under the fundamental representation of R symmetry group $SU(4)$. So we can write this wavefunction as,

$$\begin{aligned}\Psi(\eta,p) &= G^+(p)+\eta^A\Gamma_A(p)+\frac{1}{2!}\eta^A\eta^B S_{AB}(p)+\frac{1}{3!}\eta^A\eta^B\eta^C\epsilon_{ABCD}\overline{\Gamma}^D(p)\\ &\quad +\frac{1}{4!}\eta^A\eta^B\eta^C\eta^D\epsilon_{ABCD}G^-(p).\end{aligned} \tag{1.1.21}$$

Using the above wave-function for each particle, we can define superamplitude as,

$$\mathcal{A}_n\Big(\lambda, \tilde{\lambda}, \eta\Big) = \mathcal{A}\left(\Psi_1 \ldots \Psi_n\right). \tag{1.1.22}$$

We note that we can project out the particular type of particle we have in the amplitude by expanding out in the Grassmann variable η and collecting the correct component. Let us mention the nice and compact form of the MHV superamplitude which is a generalization of the Parke-Taylor formula[54],

$$\mathcal{A}_n^{\text{MHV}}(\lambda, \tilde{\lambda}, \eta) = \frac{\delta^{(4)}(p)\, \delta^{(8)}(q)}{\langle 1\,2\rangle\langle 2\,3\rangle \ldots \langle n\,1\rangle}\,, \tag{1.1.23}$$

where $q = \sum_{i=1}^{n}\ \lambda_i^{\alpha}\, \eta_i^{A}$, is the supermomentum and the superdelta function, $\delta^{(8)}(q)$ imposes supermomentum conservation as expected. In order to write down the superamplitude for any number of particles we can factor out the MHV superamplitude (1.1.23) and express it in a compact form as,

$$\mathcal{A}_n = \mathcal{A}_n^{\text{MHV}} \mathcal{P}_n, \tag{1.1.24}$$

where $\mathcal{P}_n$ is expanded as a polynomial in the Grassmann parameters η such that,

$$\mathcal{P}_n = \mathcal{P}_n^{\text{MHV}} + \mathcal{P}_n^{\text{NMHV}} + \ldots \mathcal{P}_n^{\overline{MHV}}. \tag{1.1.25}$$

Note that, $\mathcal{P}_n^{\text{MHV}} = 1$ while $\mathcal{P}_n^{\text{NMHV}}$ has Grassmann degree 4 and the remaining terms increase in Grassmann degree in units of 4 up to $\mathcal{P}_n^{\overline{MHV}}$ which is of degree $4n - 16$.

Now the SUSY BCFW recursion is a very simple extension and we have an integral over the Grassmann parameter of the shifted propagator,

$$\mathcal{A} = \sum_{P_i} \int d^4 \eta_{P_i} \mathcal{A}_L(z^*) \frac{1}{P_i^2} \mathcal{A}_R(z^*) \,. \tag{1.1.26}$$

. But here we also have to shift the Grassmann parameter to conserve supermomentum so the total BCFW shift is,

$$\begin{aligned} \lambda_{\hat{1}} &= \lambda_1 - z\lambda_n; \\ \tilde{\lambda}_{\overline{n}} &= \tilde{\lambda}_n + z\tilde{\lambda}_1; \\ \eta_{\overline{n}} &= \eta_n + z\eta_1, \end{aligned} \tag{1.1.27}$$

It has been seen that under SUSY BCFW shifts, all amplitudes $\mathcal{A}(z)$ are better behaved as $z \to \infty$ [55, 56, 14].

1.2 AdS/CFT correspondence

One of the foremost examples of the gauge/gravity duality is the AdS/CFT duality, proposed by Maldacena[57]making a remarkable connection between gauge theories and string theory. His conjecture states that in $D = 4$, $\mathcal{N} = 4$SYM gauge theory with gauge group $SU(N_c)$, where N_c is the number of colors and the t'Hooft coupling is $\lambda = g^2 N_c$($g^2$is the SYM coupling constant) is equivalent to Type IIB string theory in 10 dimensions with $AdS_5 \times S_5$ boundary conditions. Especially, in the large N limit, i.e. $N_c \to \infty$ and the t'Hooft coupling is fixed then this gauge theory is dual to a weakly coupled Type IIB supergravity theory in $AdS_5 \times S_5$. This novel idea led to tremendous insights into exploring fundamental issues in quantum gravity and also turned out to be a very effective way of dealing with strongly coupled field theories. This conjecture has been made even more precise and it has been posited that the partition function for fields in the weakly coupled gravity theory in Euclidean AdS gives the correlation function of the corresponding operator in the Euclidean CFT at the boundary, i.e.,

$$\mathcal{Z}_{\rm bulk}[\psi(\vec{x},z)|_{z=0}=\psi_0(\vec{x})]=\langle e^{\int d^4x\psi_0(\vec{x})\mathcal{O}(\vec{x})}\rangle_{\rm CFT} \tag{1.2.1}$$

Over the last decade AdS/CFT has been tested intensively at the planar limit and even though it is not proved but seems to be true beyond reasonable doubt. In fact this idea has provided new insights in different strongly coupled field theories like in Quark Gluon plasmas or theories interesting for condensed matter physics. As has been mentioned earlier it can also be used to give a holographic description of perturbative scattering amplitudes for gauge theories!

AdS/CFT allows us to compute CFT correlation functions at strong coupling via computing Witten diagrams in AdS space. The Mellin space representation(a multi-dimensional extension of Mellin transform) of conformal correlation functions, proposed by Mack[58, 59], is very similar in spirit to the momentum space representation of flat-space scattering amplitudes: they both seem like a natural framework for describing those physical observables. In AdS/CFT, computation of Witten diagrams is a daunting task in position space but the Mellin space representation of correlation functions of CFT's with gravity duals makes their properties completely transparent and much easier to handle.

1.2.1 Correlation functions in CFT

Correlation functions in CFT are very nicely constrained by the conformal group at least for smaller number of operators. We just quickly mention that the 2 point functions of primary operators are completely fixed by conformal symmetry and it is,

$$\begin{aligned} \langle \mathcal{O}(x_1)\mathcal{O}'(x_2)\rangle &= \frac{1}{x_{12}^{2\Delta_{\mathcal{O}}}}, \quad \mathcal{O}=\mathcal{O}' \\ &= 0, \quad \text{otherwise} \end{aligned} \tag{1.2.2}$$

where the $\Delta_{\mathcal{O}}$ is the conformal dimension of the operator $\mathcal{O}$. Even the 3 point function is constrained upto a structure constant C_{ijk},

$$\langle \mathcal{O}_i(x_1)\mathcal{O}_j(x_2)\mathcal{O}_k(x_3)\rangle = \frac{C_{ijk}}{x_{12}^{\Delta_1+\Delta_2-\Delta_3}x_{23}^{\Delta_2+\Delta_3-\Delta_1}x_{31}^{\Delta_3+\Delta_1-\Delta_2}}. \tag{1.2.3}$$

1.2.2 Embedding Space

Now we will give a very short review of the the embedding space/ambient space method[60, 61]. We would consider Euclidean AdS_{d+1} of radius R,and the coordinates being X_I, defined as a hyperboloid which is preserved by the $SO(d+1,2)$ symmetry,

$$X^A X_A = -R^2, \quad X^0 > 0 \tag{1.2.4}$$

and embedded in Minkowski spacetime in $(d+2)$ dimensions. The conformal boundary of this AdS spacetime can be thought of as a projective light-cone,

$$P^A P_A = 0, \quad P\ \lambda P, \tag{1.2.5}$$

such that the points $P \in \mathfrak{M}^{d+2}$ and $\lambda \in \mathfrak{R}$. In AdS/CFT we are interested in the dual d dimensional CFT whose correlations functions are given by the $SO(d+1,1)$ invariants of the projective coordinates $P's$ and with a homogeneity of weight Δ at each point. The usual expressions for Euclidean CFT in $\mathfrak{R}^d$ one just needs to use the Poincare coordinates on the light cone section for the external points,

$$P \equiv (P^+, P^-, P^\mu) = \{1, x^2, x^\mu\}, \quad , \mu \in \{1, \ldots, d-1\}, \tag{1.2.6}$$

such that Lorentz invariant physical distances are now given by,

$$(x_i - x_j)^2 = (P_i - P_j)^2 = P_{ij} = -2P_i \cdot P_j \tag{1.2.7}$$

Chapter 2

Mellin Amplitudes for Correlation functions

2.1 Introduction

AdS/CFT is a powerful tool [57, 62, 63] which among other things allows us to compute CFT correlators at strong coupling via Witten diagrams in AdS space. In practice these computations are still quite challenging in position space and generally require a lot of work, see [64, 65, 66, 67, 68, 69, 70, 71, 72, 73, 74, 75, 76, 77, 78, 79, 80]. Recently it has been argued that taking the Mellin transform of correlation functions drastically simplifies the computations and the resulting expressions have nice mathematical structure, see e.g. [59, 58, 81, 41, 42, 82, 83, 84]. The correlation functions of primary scalar operators for a CFT can be written in Mellin space as

$$\langle \mathcal{O}(x_1)\mathcal{O}(x_2)\ldots\mathcal{O}(x_n)\rangle \sim \int \mathrm{d}\delta_{ij} M(\delta_{ij}) \prod_{1\leq i<j\leq n} \Gamma(\delta_{ij})\,(x_{ij}^2)^{-\delta_{ij}}, \tag{2.1.1}$$

where $M(\delta_{ij})$ is called the Mellin amplitude and parameters δ_{ij} can be parametrized as $\delta_{ij} = k_i \cdot k_j$. Mellin amplitudes have many similarities to scattering amplitudes in flat space, in particular the large AdS radius limit of the Mellin amplitude was argued to be equivalent to the scattering amplitudes in flat space [81, 42], such that k_i plays the role of momentum in flat space,[1] suggesting that Mellin amplitudes could be used to provide a holographic definition of the S-matrix, see [85, 86, 87, 88, 89, 90, 91, 92, 93, 94] for related discussion.

More recently in [41] and [42], the authors studied various aspects of the Mellin representation of AdS correlators. In particular, a set of Feynman rules, for computing Mellin amplitudes for any theory of scalar field at tree-level, was proposed and checked for a few non-trivial correlators in ϕ^3 and ϕ^4 theories in [41] as well as recursively via a factorization formula for ϕ^3 theory in [42].

In this note we will consider a scalar field with ϕ^n interaction at tree level and offer a direct proof of the Feynman rules for Mellin amplitudes by evaluating all the Witten diagram integrals explicitly. We hope that our results will be useful for better understanding of the structure of Mellin amplitudes and for the future development of similar rules for fields with spin and for loop amplitudes. We have also checked that the Mellin space Feynman rules reduce to the usual Feynman rules in the flat

[1] The quantities k_i's are also called “Mellin momentum" or “fictitious momentum" but for the sake of brevity we will just refer to them as “momentum" in the rest of the paper and we stress that this interpretation is precise only when we look at the flat space limit of the Mellin amplitude and not in general.

space limit.

The chapter is organized as follows. In section 2.2 we review the conjectured Feynman rules for Mellin amplitudes. In section 2.3 we use particular forms of the bulk-to-boundary and bulk-to-bulk propagators to compute the Witten diagram with the maximal off-shell vertex for a ϕ^n theory and show that they lead to the conjectured Feynman rules for Mellin amplitudes. Then we demonstrate that we get the same Feynman rules for such a vertex embedded in a very general Witten diagram of the ϕ^n theory. In section 2.4 we show that these Feynman rules reduce to the usual Feynman rules in the flat space limit. We discuss some useful formulas and a non-trivial example in Appendix A.

Note added: While the paper, resulting from this chapter's work, was in preparation, the paper [95] appeared which checks the formula for the off-shell n-pt vertex of the ϕ^n theory via recursion relations.

2.2 Feynman rules for Mellin amplitudes

Let us first review the Feynman rules for Mellin amplitudes corresponding to any tree level Witten diagram in AdS$_{d+1}$ for a ϕ^n scalar theory, as proposed in [41]. To compute the Mellin amplitude one has to put together propagators and vertices following a few simple steps:

− Assign a "momentum" k_i to every line such that the external lines of the Witten diagram have $-k_i^2 = \Delta_i$ and at each vertex we have conservation $\sum_i k_i = 0$,[2] where

[2] The vector k has such properties because it solves the constrains of δ_{ij}, namely $\delta_{ij} = \delta_{ji}$ and

Δ_i is the conformal dimension of the corresponding field.

– Assign an integer m_i to each internal line with the propagator

$$\mathcal{P}_i = \frac{-1}{2m_i!\Gamma(1+\Delta_{m_i}+m_i-h)}\,\frac{1}{k_i^2+(\Delta_{m_i}+2m_i)}, \qquad (2.2.1)$$

where $h = d/2$.

– The factor for a vertex connecting lines with dimension Δ_i and integers m_i, (see Fig. 2.1) is given by

$$V^{\Delta_1\ldots\Delta_n}_{[m_1,\ldots,m_n]} = g^{(n)}\,\Gamma\left(\frac{\sum_{i=1}^n \Delta_i - 2h}{2}\right)\left(\prod_{i=1}^n (1-h+\Delta_i)_{m_i}\right)$$
$$F_A^{(n)}\left(\frac{\sum_{i=1}^n \Delta_i - 2h}{2}, \{-m_1,\ldots,-m_n\}, \{1+\Delta_1-h,\ldots,1+\Delta_n-h\}; 1,\ldots,1\right) \quad (2.2.2)$$

where $g^{(n)}$ is the coupling in the $g^{(n)}\phi^n$ theory, $(a)_m = \frac{\Gamma(a+m)}{\Gamma(a)}$ is the Pochhammer symbol and $F_A^{(n)}$ is the Lauricella function of n variables

$$F_A^{(n)}(y, \{a_1,\ldots,a_n\}, \{b_1,\ldots,b_n\}; x_1,\ldots,x_n) = \sum_{l_i=0}^{\infty}\left((y)_{\sum_{i=1}^n l_i}\prod_{i=1}^n \frac{(a_i)_{l_i}}{(b_i)_{l_i}}\frac{x_i^{l_i}}{l_i!}\right) \quad (2.2.3)$$

– Finally, sum over all positive integers m_i to obtain the Mellin amplitude.

We note here that the vertex given above is the most general type of vertex (or the maximal off-shell vertex) when all legs are off-shell[3], but the theory would also have vertices with less number of off-shell legs. The vertex factor in such cases can be simply obtained from the general case by taking some of the m_i's to zero,

---

$\sum_{j\neq i}\delta_{ij} = -\Delta_i^2$.

[3] The legs connecting to the AdS boundary directly are referred to as the on-shell legs, while those that do not connect to the boundary are the off-shell legs.

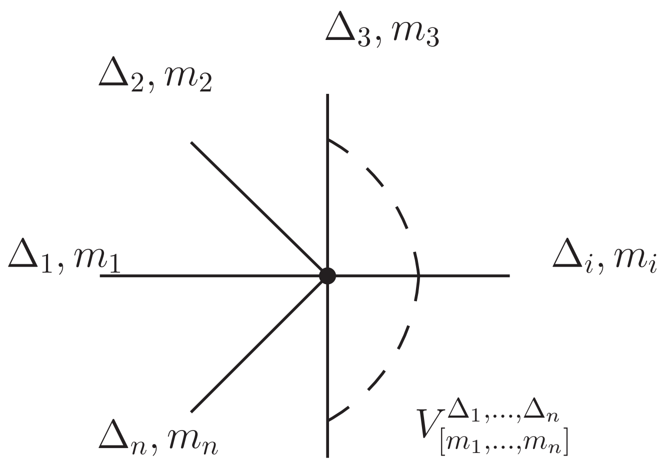

Figure 2.1: A general vertex for ϕ^n theory.

corresponding to the legs going on-shell. Also, note that the Lauricella function of m variables can be written in a series form as in (2.2.3) which is convergent for $\sum_i |x_i| < 1$. For the vertex above, all n variables x_i take a particular value 1, which is the Lauricella function evaluated at that particular point, which is well-defined via analytic continuation.

2.3 Proof of Feynman rules

2.3.1 Maximal off-shell vertex

In this section we consider a Witten diagram for the scalar ϕ^n theory in AdS_{d+1} which has a vertex with the maximal number of off-shell legs (see Fig. 2.2) and prove the Feynman rules for this case which we described in the previous section.

Let X^I be the coordinates of the Euclidean AdS_{d+1} space, embedded in a $d+2$

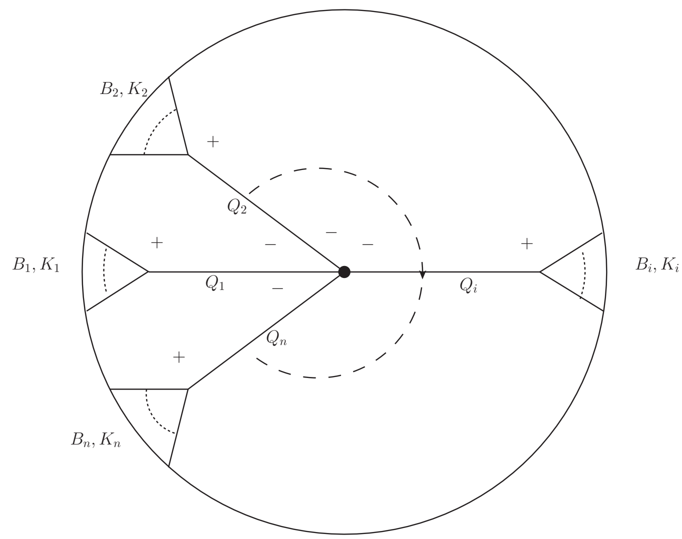

Figure 2.2: The Witten diagram for the scalar ϕ^n theory with a vertex having n off-shell legs and n vertices having 1 off-shell leg and $(n-1)$ on-shell legs.

dimensional Minkowski space such that $X^2 = -R^2$, where R is the AdS radius and the point on the boundary P^A defined on the light-cone such that $P^2 = 0$. The bulk-to-boundary propagator between a point P on the boundary and X in the bulk for a scalar field of dimension Δ is given by[4]

$$E(P, X) = \frac{1}{2\pi^h \Gamma(1 + \Delta - h)} \int_0^{+\infty} \frac{\mathrm{d}t}{t} t^\Delta \, e^{2tP \cdot X}. \tag{2.3.1}$$

The bulk-to-bulk propagator between the points X_1 and X_2 can be written as an integral over a point Q on the boundary of the AdS, the integrand being the product

[4]We will drop the normalization factor $\frac{1}{2\pi^h \Gamma(1+\Delta-h)}$ from (2.3.1) for subsequent calculations, since it is not relevant. Moreover this factor goes into the overall normalization factor in the definition of Mellin amplitudes and according to (2.1.1) we have ignored it in this note and the inclusion of this factor would allow us to write (2.1.1) as an equality.

of two bulk-to-boundary propagators of states with non-physical dimension $h \pm c$

$$G_{BB}(X_1, X_2) = \int_{-i\infty}^{+i\infty} \frac{\mathrm{d}c}{2\pi i} f_\Delta(c) \int_{\partial AdS} \mathrm{d}Q \int \frac{\mathrm{d}s}{s} \frac{\mathrm{d}\bar{s}}{\bar{s}} s^{h+c} \bar{s}^{h-c}\, e^{2sQ\cdot X_1 + 2\bar{s}Q\cdot X_2} \tag{2.3.2}$$

where

$$f_\Delta(c) \equiv \frac{1}{2\pi^{2h}[(\Delta - \widehat{)}^2 - c^2]} \frac{1}{\Gamma(c)\Gamma(-c)}. \tag{2.3.3}$$

To simplify the notations, let us call each set of external $(n-1)$ legs in Fig. 2.2 as a block, and denote it as B_i with $i = 1, \ldots, n$. Equations (2.3.2) and (2.3.1) give us the building blocks of any arbitrary Witten diagram in the ϕ^n theory. Fig. 2.2 can be constructed using two types of n-point correlation functions, built out of (2.3.1) and (2.3.2), which are given as

$$\begin{aligned} A_n(B_i, Q_{i,+}) &= g^{(n)} \int_0^{+\infty} \prod_{i=1}^{n-1} \frac{\mathrm{d}t_i}{t_i} t_i^{\Delta_i} \frac{\mathrm{d}s_i}{s_i} s_i^{\widehat{+}c_i} \int_{AdS} \mathrm{d}X_i\, e^{2(B_i + s_i Q_i)\cdot X_i}, \qquad (2.3.4) \\ A_n(Q_{1,-}, \ldots, Q_{n,-}) &= g^{(n)} \int_0^{+\infty} \prod_{i=1}^{n} \frac{\mathrm{d}\bar{s}_i}{\bar{s}_i} \bar{s}_i^{\widehat{-}c_i} \int_{AdS} \mathrm{d}X_i\, e^{2(\sum_{k=1}^n \bar{s}_k Q_k)\cdot X_i}, \end{aligned}$$

where the blocks of $(n-1)$ legs, which we call B_i, are typically given as,

$$B_i = \sum_{k=(i-1)(n-1)+1}^{i(n-1)} t_k P_k. \tag{2.3.5}$$

We note that in general B_i can also contain fewer legs, (in which case the Witten diagram gives a vertex with fewer off-shell legs) so the limits of the summation in (2.3.5) would change according to the diagram under consideration. Moreover in

Fig. 2.2 the label K_i indicates

$$K_i \equiv k_{a_i} + \ldots + k_{a_i+n-1} \tag{2.3.6}$$

the sum of the momenta of all the fields in the block B_i where k_{a_i} is the momenta of each field.

Now, let us write the expression for the Witten diagram in Fig. 2.2 using the n-point correlation functions (2.3.4) as the building blocks and we get

$$\begin{aligned} A &= \int_{-i\infty}^{+i\infty} \prod_{i=1}^{n} \frac{\mathrm{d}c_i}{(2\pi i)^n} f_{\Delta_i}(c_i) \int_{\partial AdS} \prod_{i=1}^{n} \mathrm{d}Q_i \Big(A_n(B_i, Q_{i,+}) \ldots A_n(B_n, Q_{n,+}) A_n(Q_{1,-}, \ldots, Q_{n,-}) \Big) \\ &= (g^{(n)})^{n+1} \int_{-i\infty}^{+i\infty} \prod_{i=1}^{n} \frac{\mathrm{d}c_i}{(2\pi i)^n} f_{\Delta_i}(c_i) \int \prod_{i=1}^{n(n-1)} \frac{\mathrm{d}t_i}{t_i} t_i^{\Delta_i} \int \prod_{i=1}^{n} \frac{\mathrm{d}s_i}{s_i} \frac{\mathrm{d}\bar{s}_i}{\bar{s}_i} s_i^{h+c_i} \bar{s}_i^{h-c_i} \\ &\times \int_{\partial AdS} \prod_{i=1}^{n} \mathrm{d}Q_i \int_{AdS} \prod_{i=1}^{n+1} \mathrm{d}X_i \exp\Big((2 \sum_{i=1}^{n} X_i \cdot (B_i + s_i Q_i) + 2X_{n+1} \cdot (\sum_{i=1}^{n} \bar{s}_i Q_i) \Big), \end{aligned} \tag{2.3.7}$$

where A is the $n(n-1)$ point correlation function.

2.3.2 Evaluating the integrals

Integrals over X_i

The integrations over the bulk points X_i can be done by applying (A.1.1) from the Appendix, which gives us the result,

$$\begin{aligned} A = (g^{(n)})^{n+1} (\pi^h)^{n+1} \int_{-i\infty}^{+i\infty} \prod_{i=1}^{n} \frac{\mathrm{d}c_i}{(2\pi i)^n} f_{\Delta_i}(c_i) \int \prod_{i=1}^{n(n-1)} \frac{\mathrm{d}t_i}{t_i} t_i^{\Delta_i} \int \prod_{i=1}^{n} \frac{\mathrm{d}s_i}{s_i} \frac{\mathrm{d}\bar{s}_i}{\bar{s}_i} s_i^{h+c_i} \bar{s}_i^{h-c_i} \\ \int_{\partial AdS} \prod_{i=1}^{n} \mathrm{d}Q_i \Big(\prod_{i=1}^{n} \Gamma(\frac{\Delta_{B_i} + (h+c_i) - 2h}{2}) \Big) \Gamma(\frac{\sum_{i=1}^{n} (h-c_i) - 2h}{2}) e^{E_Q} \end{aligned} \tag{2.3.8}$$

where $\Delta_{B_i} = \sum_{j\in B_i} \Delta_j$ and Δ_j is the conformal dimension of the field j and the exponent in the above integrand is given by,

$$E_Q = \sum_{i=1}^{n}(B_i + s_i Q_i)^2 + (\sum_{i=1}^{n} \overline{s_i} Q_i)^2. \tag{2.3.9}$$

Integrals over Q

To perform the Q_i integrals we first expand (2.3.9) and rewrite it as,

$$E_Q = \sum_{i=1}^{n}\Big(B_i^2 + 2s_i Q_i \cdot B_i\Big) + 2\sum_{1\le i<j\le n} \overline{s}_i\overline{s}_j Q_i \cdot Q_j. \tag{2.3.10}$$

Now we will integrate out the Q_i's successively.

First we will do the Q_1 integral using (A.1.2) and using the on-shell condition, $Q_i^2 = 0$ to simplify the result, we finally get,[5]

$$\begin{aligned} E_{Q_1} &= \sum_{i=1}^{n} B_i^2 + (s_1 B_1)^2 \\ &+ 2\Bigg((1+\overline{s}_1^2)(\sum_{1<i<j}^{n} \overline{s}_i\overline{s}_j Q_i \cdot Q_j) + \sum_{i\neq 1}^{n}(s_i B_i + \overline{s}_i(\overline{s}_1 s_1 B_1)) \cdot Q_i\Bigg), \end{aligned} \tag{2.3.11}$$

where the notation E_{Q_k} is used to denote the exponent obtained as a result of doing the set of successive integrals from Q_1 to Q_k, i.e.

$$\int_{\partial AdS} \prod_{i=1}^{k} \mathrm{d}Q_i e^{E_Q} = e^{E_{Q_k}}.$$

[5] At each step of doing the Q integral we will get a $2\pi^h$ factor which we would drop in the following steps to help us reduce clutter.

Next, we perform the Q_2 integral in a similar way and we find that E_{Q_2} can be written as

$$\begin{aligned} E_{Q_2} &= \sum_{i=1}^{n} B_i^2 + (s_1 B_1)^2 + (s_2 B_2 + \overline{s}_2(\overline{s}_1 s_1 B_1))^2 + 2\Bigg((1+\overline{s}_1^2)(1+\overline{s}_2^2(1+\overline{s}_1^2))(\sum_{2<i<j}^{n} \overline{s}_i \overline{s}_j Q_i \cdot Q_j)\Bigg) \\ &+ 2\Bigg(\sum_{i \neq \{1,2\}}^{n} \Bigg(s_i B_i + \overline{s}_i\Big((\overline{s}_1 s_1 B_1) + (1+\overline{s}_1^2)\overline{s}_2(s_2 B_2 + \overline{s}_2(\overline{s}_1 s_1 B_1))\Big)\Bigg) \cdot Q_i\Bigg). \end{aligned} \tag{2.3.12}$$

We continue integrating out the Q_i's successively as in the last few steps and integrating the p_{th} step the result is of the form,

$$\begin{aligned} E_{Q_p} &= \sum_{i=1}^{n} B_i^2 + \sum_{i=1}^{p} \Big(\overline{s}_i Y_{i-1} + s_i B_i\Big)^2 + 2\Bigg((\prod_{m=1}^{p} g_m)(\sum_{p<i<j}^{n} \overline{s}_i \overline{s}_j Q_i \cdot Q_j)\Bigg) \\ &+ 2\Bigg(\sum_{i \neq \{1,2,\ldots,p\}}^{n} (s_i B_i + \overline{s}_i Y_p) \cdot Q_i\Bigg), \end{aligned} \tag{2.3.13}$$

where we have defined the functions Y_i and g_i as,

$$\begin{aligned} Y_l &= \sum_{i=1}^{l} \frac{(\prod_{k=1}^{l} g_k)}{g_i} s_i \overline{s}_i B_i \quad \text{and} \\ g_l &= (1 + \overline{s}_l^2 \prod_{k=0}^{l-1} g_k) \quad \text{with} \quad g_0 = 1. \end{aligned} \tag{2.3.14}$$

After integrating out all the Q_i's using (2.3.13) we finally get the exponent of the integrand in (2.3.8) as,

$$E_{Q_n} = \sum_{i=1}^{n} B_i^2 + \sum_{l=1}^{n} \Big(\overline{s}_l Y_{l-1} + s_l B_l\Big)^2. \tag{2.3.15}$$

Integrals over t_i

Let us first expand the term in the parentheses in (2.3.15), and with the help of (2.3.14) we get

$$E_{Q_n} = \sum_{i=1}^{n}(1+s_i^2 F_i)B_i^2 + \sum_{1\leq i<j\leq n} \frac{2(s_i\bar{s}_i s_j\bar{s}_j)(B_i\cdot B_j)}{g_i g_j}\Big(\prod_{l=1}^{n} g_l\Big). \qquad (2.3.16)$$

where

$$F_i = 1 + \frac{\bar{s}_i^2}{g_i^2}\Big(\sum_{l=i+1}^{n} \bar{s}_l^2 \Big(\prod_{k=1}^{l-1} g_k^2\Big)\Big). \qquad (2.3.17)$$

Next, we will apply Symanzik star formula (A.1.3) to our integral (2.3.8) in order to obtain the Mellin amplitude $M(\delta_{ij})$.

Let us recall that B_i's are given as $\sum t_l P_l$, so the exponent of the integrand would only have terms quadratic in t coming from expanding the B_i^2 and $B_i\cdot B_j$ terms in (2.3.16)[6]. Using (A.1.3), we can see that the full result of the Witten diagram integral gives,

$$\begin{aligned} A &= (g^{(n)})^{n+1}\frac{(\pi^h)^{n+2}}{2(2\pi i)^{\frac{1}{2}n(n-3)}}\int \mathrm{d}\delta_{ij}\prod_{1\leq i<j\leq n}\Gamma(\delta_{ij})\,(P_{ij})^{-\delta_{ij}}\int_{-i\infty}^{+i\infty}\prod_{i=1}^{n}\frac{\mathrm{d}c_i}{(2\pi i)^n} \\ &\times \Bigg(\Big(\prod_{i=1}^{n}\Gamma\Big(\frac{\Delta_{B_i}+(h+c_i)-2h}{2}\Big)\Big)\Gamma\Big(\frac{\sum_{i=1}^{n}(h-c_i)-2h}{2}\Big)f_{\Delta_i}(c_i)\mathcal{M}(k_i,c_i)\Bigg) \end{aligned} \qquad (2.3.18)$$

where we introduce a new notation $\mathcal{M}(k_i, c_i)$ and call it as the Mellin integrand which

[6] In the embedding formalism, $P_{ab} = -2P_a\cdot P_b$ and $P_a^2 = 0$

is given as

$$\mathcal{M}(k_i, c_i) \;=\; \int \prod_{i=1}^{n} \frac{ds_i}{s_i}\frac{d\overline{s}_i}{\overline{s}_i}\, s_i^{h+c_i+a_i}\overline{s}_i^{h-c_i+a_i}(g_i)^{b_i}\Big(1+s_i^2 F_i\Big)^{d_i}, \qquad (2.3.19)$$

such that the Mellin amplitude can be given in terms of the Mellin integrand as,

$$\begin{aligned} M(\delta_{ij}) \;&=\; \int_{-i\infty}^{+i\infty} \prod_{i=1}^{n} \frac{\mathrm{d}c_i}{(2\pi i)^n}\Big(\prod_{i=1}^{n}\Gamma(\frac{\Delta_{B_i}+(h+c_i)-2h}{2})\Big) \\ &\times\; \Gamma(\frac{\sum_{i=1}^{n}(h-c_i)-2h}{2})f_{\Delta_i}(c_i)\mathcal{M}(k_i,c_i). \qquad (2.3.20)\end{aligned}$$

Note that in the Mellin integrand $\mathcal{M}(k_i, c_i)$ we have used k_i instead of δ_{ij}, and recall that $\delta_{ij} \equiv k_i \cdot k_j$.

Furthermore, a few words about the exponents a_i, b_i and d_i are in order. With respect to the i_{th} propagator in Fig. 2.2, a_i is the product of the momenta flowing through the propagator i from both sides. So according to our convention of Fig. 2.2, where K_i is the sum of all momenta of the fields contained in the block B_i, i.e. $K_i \equiv k_{a_i} + \ldots + k_{a_i+n-1}$, we get

$$a_i \equiv -(K_i \cdot \sum_{m\neq i} K_m) = K_i^2. \qquad (2.3.21)$$

The exponent b_i is the sum of all possible products of the momenta flowing through the propagators connecting the propagator i on the $\overline{s}_i$ side i.e.

$$b_i \equiv -(\sum_{m,n\neq i, m\neq n} K_m \cdot K_n), \qquad (2.3.22)$$

while d_i is the sum of all possible products of the momenta flowing from the other direction, namely s_i side,

$$d_i \equiv -\frac{a_i - \Delta_{B_i}}{2}, \tag{2.3.23}$$

recall that $\Delta_{B_i} = \sum_{j \in B_i} \Delta_j$.

Integrals over s_i and $\bar{s}_i$

The integral $\mathcal{M}(k_i, c_i)$ in (2.3.19) can be greatly simplified using a set of transformations which are the generalization of the transformations used in [41]. Firstly, we rescale s_i^2 by a factor of F_i, then (2.3.19) becomes

$$\mathcal{M}(k_i, c_i) = \prod_{i=1}^{n} \int \frac{ds_i}{s_i} s_i^{h+c_i+a_i} (1+s_i^2)^{d_i} \int \frac{d\bar{s}_i}{\bar{s}_i} F_i^{-\frac{h+c_i+a_i}{2}} \bar{s}_i^{h-c_i+a_i} g_i^{b_i}. \tag{2.3.24}$$

Then we can make a set of consecutive transformations on $\bar{s}$'s, to simplify the integral further,

$$\begin{aligned} \bar{s}_j^2 &\to x_j \\ x_2 &\to \frac{x_2}{1+x_1} \\ &\vdots \\ x_n &\to \frac{x_n}{(1+x_1)(1+x_2)\dots(1+x_{n-1})} \\ x_1 &\to \frac{x_1}{(1+x_2)(1+x_3)\dots(1+x_n)} \\ &\vdots \\ x_{n-1} &\to \frac{x_{n-1}}{1+x_n}. \end{aligned} \tag{2.3.25}$$

Under the above set of transformations we find that g_i, F_i and x_i(or $\overline{s}_i^2$) transform as,

$$\begin{aligned} g_i &\rightarrow \frac{1+\sum_{j=i}^n x_j}{1+\sum_{j=i+1}^n x_j}, \\ F_i &\rightarrow \frac{(1+x_i)(1+\sum_{j=i+1}^n x_j)}{1+\sum_{j=i}^n x_j}, \\ x_i &\rightarrow \frac{x_i(1+\sum_{j=i}^n x_j)}{(1+\sum_{j=i+1}^n x_j)(1+\sum_{j=1}^n x_j)}. \end{aligned} \tag{2.3.26}$$

We also find that the exponent of $(1+\sum_{j=i+1}^n x_j)$ is given by

$$(\frac{h+c_i+a_i+h-c_i+a_i}{2}+b_i)-(\frac{h+c_{i-1}+a_{i-1}+h-c_{i-1}+a_{i-1}}{2}+b_{i-1}),$$

and this vanishes when we use the definition of a_i and b_i from (2.3.21) and (2.3.22). Hence all the terms of the form $(1+\sum_{j=i+1}^n x_j)$ do not have any contribution to the exponent. Finally we are left with a very simple integral given as

$$\mathcal{M}(k_i,c_i)=\prod_{i=1}^n\int\frac{ds_i}{s_i}s_i^{h+c_i+a_i}(1+s_i^2)^{d_i}\int\frac{dx_i}{x_i}x_i^{\frac{h-c_i+a_i}{2}}(1+x_i)^{-\frac{h+c_i+a_i}{2}}(1+\sum_{j=1}^n x_j)^q, \tag{2.3.27}$$

where $q=\frac{1}{2}(\sum c_i-(n-2)h)$.

The s_i integrals give the Gamma functions,

$$\prod_{i=1}^n\int\frac{ds_i}{s_i}s_i^{h+c_i+a_i}(1+s_i^2)^{d_i} = \prod_{i=1}^n\frac{\Gamma(\frac{h+c_i+a_i}{2})\Gamma(\frac{\Delta_{B_i}-c_i-h}{2})}{\Gamma(\frac{\Delta_{B_i}-a_i}{2})}, \tag{2.3.28}$$

where we have used the fact that $k_i^2=-\Delta_i$ and also the definition of a_i and d_i from (2.3.21) and (2.3.23)to get the final form of the result.

To perform the x_i integrals, we will do a series expansion of the factor $(1+\sum_{j=1}^n x_j)^q$ in (2.3.27) as,

$$\begin{aligned}(1+\sum_{j=1}^{n} x_j)^q &= \sum_{m_1,\ldots,m_n=0}^{\infty} \prod_{k=1}^{n} (-q+\sum_{j=1}^{k-1} m_j)_{m_k} \prod_{k=1}^{n} \frac{(-x_k)^{m_k}}{m_k!} \\ &= \sum_{m_1,\ldots,m_n=0}^{\infty} \prod_{k=1}^{n} (-q)_{\sum_i m_i} \prod_{k=1}^{n} \frac{(-x_k)^{m_k}}{m_k!}.\end{aligned} \tag{2.3.29}$$

Then the x_i integrals can be performed easily, which leads to

$$\begin{aligned}\Pi_{i=1}^n \quad & \int \frac{dx_i}{x_i} x_i^{\frac{h-c_i+a_i}{2}} (1+x_i)^{-\frac{h+c_i+a_i}{2}} (1+\sum_{j=1}^{n} x_j)^q \\ = \quad & F_A^{(n)}\left(-q, \left\{\frac{h-c_1+a_1}{2}, \ldots, \frac{h-c_n+a_n}{2}\right\}, \{1-c_1, \ldots, 1-c_n\}; 1, \ldots, 1\right) \\ \times \quad & \prod_{i=1}^{n} \frac{\Gamma(c_i)\Gamma(\frac{h-c_i+a_i}{2})}{\Gamma(\frac{h+c_i+a_i}{2})}.\end{aligned} \tag{2.3.30}$$

So the Mellin integrand (2.3.27) is now given by the product of (2.3.28) and (2.3.30).

We can now do the final integration over the c variables to get the Mellin amplitude,

$$M(k_i) = \int_{-i\infty}^{+i\infty} \left(\prod_{i=1}^{n} \frac{dc_i}{2\pi i} f_{\Delta_i}(c_i) \Gamma(\frac{\Delta_{B_i}+c_i-h}{2})\right) \Gamma(\frac{(n-2)h-\sum_{i=1}^n c_i}{2}) \mathcal{M}(k_i, c_i). \tag{2.3.31}$$

As pointed out in [41], we can do this integral by determining the poles in the kinematics, namely, the a_i's and their corresponding residues. They can be determined by pinching of the contour by two poles, $c_i = \pm(\Delta_i - h)$ from $f_{\Delta_i}(c_i)$ and $c_i = a_i + h + 2n_i$ from $\Gamma(\frac{h-c_i+a_i}{2})$ with positive integer n_i, for each c_i integration. The above mentioned residues can be cast in a simple form and we can write the full result for (2.3.31) in the following form,

$$M(k_i) = \sum_{n_1,\ldots,n_n=0}^{\infty} (\prod_{i=1}^{n} \mathcal{P}_i) V^{\Delta_1,\ldots,\Delta_{n-1},\Delta_{n_1}}_{[0,\ldots,0,n_1]} \ldots V^{\Delta_{(n-1)^2+1},\ldots,\Delta_{n(n-1)},\Delta_{n_n}}_{[0,\ldots,0,n_n]} V^{\Delta_{n_1},\ldots,\Delta_{n_n}}_{[n_1,\ldots,n_n]} \tag{2.3.32}$$

where the simple poles in a_i can be read off from the terms, $\frac{1}{a_i+(\Delta_{n_i}+2n_i)}$, appearing in $\mathcal{P}_i$.

One may worry about other possible poles, including the poles $\pm c_i = \Delta_{B_i} - h + 2m$ from $\Gamma(\frac{\Delta_{B_i} \pm c_i - h}{2})$, and the pole from $\Gamma(\frac{(n-2)h - \sum_i c_i}{2})$. Firstly the pole from $\Gamma(\frac{(n-2)h - \sum_i c_i}{2})$ is canceled by $(-q)_{\sum n_i}$ in the Lauricella function, and as for the other pole, we note that after pinching off $c_i = -(\Delta_{B_i} - h + 2m)$ with $c_i = a_i + h + 2n_i$, this pole is canceled out by $\Gamma(\frac{\Delta_{B_i} + a_i}{2})$ in $I_s(c_i)$.

Furthermore, it has been argued in [42] that the correlation function in Mellin space has good behavior at large a_i, and poles and the corresponding residues are enough to determine the whole function, so (2.3.32) is the complete result of the integral (2.3.31), and it leads to the Feynman rules stated earlier in section 2.

For a ϕ^n theory, there are also vertices with less than n off-shell legs. In fact one can have vertices with $n, (n-1), \ldots, 1$ and 0 off-shell legs. We can obtain the results of these cases from the vertex with a maximal number of off-shell legs in Fig. 2.2 by taking some of B_i's to be a single leg connecting directly to the boundary. The result of this Witten diagram can be obtained by simply removing s_n and $\bar{s}_n$ and noticing that for a single leg on the boundary we have $(t_n P_n)^2 = 0$. If we take m out of n B_i's to be single legs, the result is actually in the same form of the ϕ^{n-m} theory, as one would have expected.

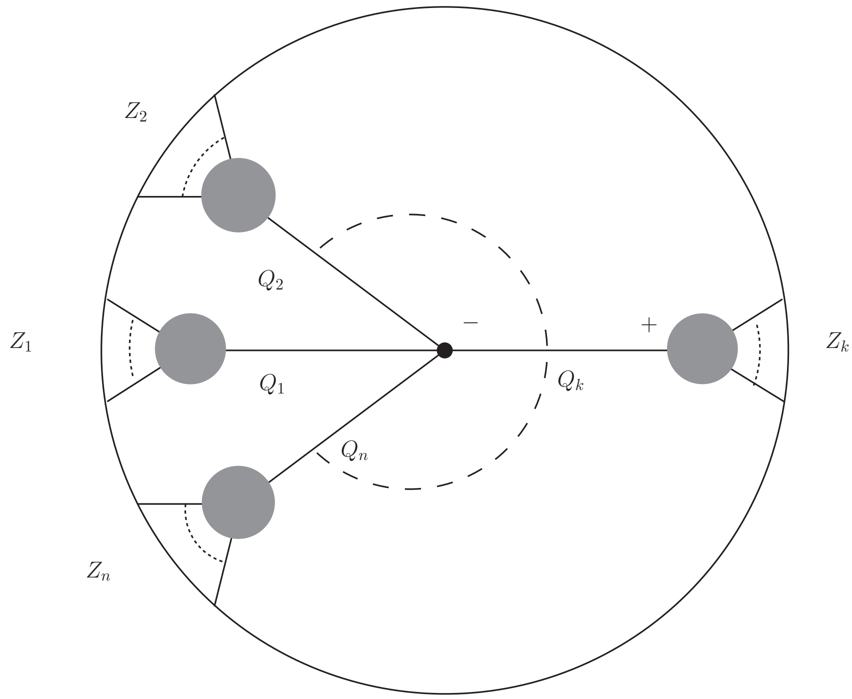

Figure 2.3: A vertex with all off-shell legs in arbitrary Witten diagram.

2.3.3 General case

Let us consider the most general case of a maximal off-shell vertex in an arbitrary Witten diagram in a scalar ϕ^n theory, as in Fig. 2.3. Here, the off-shell leg Q_k, is connected to the set of on-shell fields in the block named Z_k with $k = 1, \ldots, n$ via many propagators and vertices. All these intermediate propagators and vertices are collectively denoted by the blob attached to Q_k. We also assume that we had already done the Q integrations for all the propagators inside each blob connected to the block Z_k and the contribution from this to the exponent in the integrand of the $s, \bar{s},$ and c integrals is labeled as $\mathcal{B}_k^Z$. We note that this quantity depends on the variables $s, \bar{s}$ associated with all the propagators in the blob of the k_{th} block Z_k and all the t_kP_k's associated with the on-shell fields contained in this block,[7] but most importantly it does not contain the variables associated with the propagator Q_k i.e. s_k and $\bar{s}_k$.

We note that Fig. 2.2 is a special case of Fig. 2.3 if the k_{th} blob contains only one maximal vertex of ϕ^n theory with $(n-1)$ on-shell legs and then $\mathcal{B}_k^Z \equiv B_k$.

Now it is obvious that just as in the previous section, the contribution to the Mellin exponent after doing the integrations over Q_1 to Q_n can be written as,

$$E_{Q_n} = \sum_{i'} (\mathcal{D}_{i'})^2 + \sum_{l=1}^{n} \left(\bar{s}_l \mathcal{Y}_{l-1}^Z + s_l \mathcal{B}_l^Z \right)^2, \tag{2.3.33}$$

where

$$\mathcal{Y}_n^Z \quad = \quad \sum_{i=1}^{n} \frac{(\prod_{k=1}^{n} g_k)}{g_i} s_i \bar{s}_i \mathcal{B}_i^Z \tag{2.3.34}$$

and $\mathcal{D}_{i'}$ is defined as follows. Since the Q_1 to Q_n integrations affect the form of $\mathcal{B}_i^Z$, obtained from the previous Q integrations, at each step of these integrations we will get some complicated functions which we denote as $\mathcal{D}_{i'}$. We note that these do not have any dependence on the s and $\bar{s}$ variables associated with the maximal vertex and are not of any interest for the remaining calculation[8]. The other definitions being the same as in (2.3.14). Even though, it seems that this situation is much more complicated than before we note that none of the $\mathcal{B}_k^Z$'s depend on the s_k and $\bar{s}_k$'s associated with the vertex under consideration and moreover the $\mathcal{B}_k^Z$'s are also linear in the $t_kP_k \in Z_k$ and hence we can apply Symanzik star formula, to perform

[7]We will label all the variables associated with the propagators in the blob with a primed index.

[8]In Appendix. B we do a specific example of a general Witten diagram and there we also give an explicit form of these $\mathcal{D}_{i'}$'s for that special case.

the t_i integrals, as before by expanding the square. Now, let us focus on the second sum in (2.3.33) and since it has the same form as (2.3.15), the analysis is similar to the one in the previous section but with a few added subtleties. In particular, when applying Symanzik star formula, the contributions from the $\mathcal{B}_i^Z \cdot \mathcal{B}_j^Z$ term will be same as that of the $B_i \cdot B_j$ term before, with $i \neq j$, but the contributions from $\mathcal{B}_i^Z \cdot \mathcal{B}_i^Z$ would be different from the analogous term in the previous section.[9]

So all of the analysis in the previous section still holds as we can isolate the integrations for this particular vertex and write the Mellin integrand as,

$$\mathcal{M}(k_j) \quad = \quad \int ds \mathcal{V}(s) \int \prod_{j=1}^{n} \frac{ds_j}{s_j} \frac{d\bar{s}_j}{\bar{s}_j} \, s_j^{h+c_j+a_j} \bar{s}_j^{h-c_j+a_j} g_j^{-b_j} \prod_{j=1}^{n} H_j(s_j^2 F_j, s), \tag{2.3.35}$$

where we denote $\int ds\mathcal{V}(s)$ as the integrals irrelevant to the vertex. Even though $H_i(s_i^2 F_i, s)$ can be a complicated function, for the s and $\bar{s}$ relevant to the vertex we are interested in, they are always of the form $s_j^2 F_j$. So we can rescale s_i^2 by a factor of F_i for $i = 1, 2, \ldots, n$,[10] and after rescaling, $H_i(s_i^2 F_i, s)$ will be included in the irrelevant integral $\int ds\mathcal{V}(s)$. So at the end we arrive at the integral related to the vertex we are interested in i.e. the $\bar{s}$ dependent part

$$\mathcal{M}(k_i)\Big|_{\bar{s}} \quad = \quad \int \prod_{i=1}^{n} \frac{d\bar{s}_i}{\bar{s}_i} \, \bar{s}_i^{h-c_i+a_i} g_i^{-b_i} \prod_{i=1}^{n} F_i^{\frac{-h+c_i+a_i}{2}}, \tag{2.3.36}$$

which is exactly the same as the $\bar{s}$ part of the integral in (2.3.24) and hence gives the same form of the maximal off-shell vertex.

[9] The reason is that some terms in $\mathcal{B}_i^Z \cdot \mathcal{B}_i^Z$ could mix the contributions from the first sum, $\sum_{i'}(\mathcal{D}_{i'})^2$, in (2.3.33), however there is no such kind of mixing for the term of the form $\mathcal{B}_i^Z \cdot \mathcal{B}_j^Z$, because there cannot be any term in $\sum_{i'}(\mathcal{D}_{i'})^2$ to have this form, since the ith blob had never talked to jth blob before.

[10] Note $F_n = 1$, so when $j = n$ there is no rescaling.

2.4 Flat space limit

In this section we consider the flat space limit of the Mellin space Feynman rules. We will show that these rules give rise to the usual Feynman rules for scattering amplitudes in the flat space limit. This limit can also be considered as a consistency check of the AdS Feynman rules. The flat space limit corresponds to the large δ_{ij} behavior of the Mellin amplitudes. As had been discussed in [81] and [42], in this limit the Mellin amplitudes are related to the S-matrix in flat space by the following relation[11]

$$M(\delta_{ij}) \approx \int_0^\infty d\beta\, \beta^{\frac{1}{2}\sum\Delta_i - h - 1} e^{-\beta}\, T(p_i \cdot p_j = 2\beta\delta_{ij})\ , \qquad \delta_{ij} \gg 1\ , \tag{2.4.1}$$

where $T(p_i \cdot p_j = 2\beta\delta_{ij})$ is the flat space S-matrix as a function of the kinematic invariants $p_i \cdot p_j$ and β is an integration parameter. We will study the case of large δ_{ij} limit with Δ_i fixed. In order to confirm that the AdS Feynman rules indeed reduce to the usual flat space Feynman rules of ϕ^n theory in this limit, we only need to show that

$$\sum_{\{n_i\}} M(n_1, \ldots, n_s) = \frac{(-1)^s}{2^s}\Gamma(\frac{1}{2}\sum\Delta_i - h - s), \tag{2.4.2}$$

where $\sum_{\{n_i\}} M(n_1, \ldots, n_s)$ related to the Mellin amplitude by

$$M(\delta_{ij}) \approx \sum_{\{n_i\}} M(n_1, \ldots, n_s) \prod_{i=1}^{s} \frac{1}{k_i^2}, \tag{2.4.3}$$

[11] Notice it is slightly different from Eq. (127) in [42], because we define the Mellin amplitudes by a different normalization factor.

where $\frac{1}{k_i^2}$ is the propagator, s is the number of propagators, and the summation over $\{n_i\}$ become clear shortly. The above equation (2.4.2) follows directly from (2.4.1) by using the definition of the flat space massless scalar scattering amplitudes.

We will use the AdS Feynman rules (2.2.3) to compute the left hand side of (2.4.1). As in the case of ϕ^3 theory [42], we can always start from the bulk propagators closer to the external legs in the Witten diagram and perform the sum over $\{n_i\}$ recursively. To do so for a general ϕ^n theory, we need the following identity, which will be proved shortly,

$$\sum_{n_{I_1},n_{I_2},\ldots,n_{I_m}=0}^{\infty} \frac{V^{(1)}(n_{I_1})V^{(1)}(n_{I_2})\ldots V^{(1)}(n_{I_m})V^{(m+1)}(n_{I_1},n_{I_2},\ldots,n_{I_m},n_o)}{P_{n_{I_1}}P_{n_{I_2}}\ldots P_{n_{I_m}}} \tag{2.4.4}$$
$$= \frac{(-1)^m}{2^m}((m+1)-\frac{\sum\Delta_i}{2}+\Delta_{n_o})_{n_o}\Gamma(\frac{\sum\Delta_i}{2}-h-m),$$

where $P_n \equiv -2n!\Gamma(1+\Delta_n+n-h)$, and $V^{(1)}(n_I)$ denotes the vertex with one off-shell leg where this leg is labeled as n_I, and we follow a similar logic to define $V^{(m+1)}(n_{I_1},n_{I_2},\ldots,n_{I_m},n_o)$, which denotes the vertex with $(m+1)$ off-shell legs. Finally, the summation in $\sum\Delta_i$ indicates the sum over all the external on-shell legs. The identity (2.4.4) can be proved by performing the summation in the following order: first we sum over l_1, the summation variable in the Lauricella function $F_A^{(n)}$ then the corresponding n_{I_1}, next we do the sum over l_2 then n_{I_2} and so on. At each step of the sum we can apply the identity,

$$\sum_{n=0}^{\infty} \frac{(a)_n(b)_n}{n!(c)_n} = \frac{(c-b)_{-a}}{(c)_{-a}}. \tag{2.4.5}$$

We note here that $((m+1)-\frac{\sum\Delta_i}{2}+\Delta_{n_o})_{n_o}$ in (2.4.4) has the same dependence on

n_o as $V^{(1)}(n)$ does. So the summation on n_o in a general Witten diagram can be done by applying the above identities again. At the end of the day, we will be left with a sum involving only factors of the form of $V^{(1)}(n)$. It can be shown that the answer for the final sum of any Witten diagram is indeed given as Eq. (2.4.2).

Chapter 3

Star Integrals, Convolutions and Simplices

3.1 Introduction

In the last chapter we have discussed that the correlation functions of Conformal Field Theories (CFT's) in AdS/CFT at strong coupling have properties analogous to flat space scattering amplitudes in an auxiliary space called Mellin space, first introduced by Mack [59, 58] and further studied in the works [81, 41, 42, 43, 95, 96, 97]. An application of this formalism in the context of flat space conformal integrals has appeared in [44]. In this context we will now discuss multi-loop scattering amplitudes of $\mathcal{N} = 4$ supersymmetric Yang-Mills theory with $SU(N)$ gauge group in the planar ($N \to \infty$) limit . As we have reviewed earlier such amplitudes possess a remarkable set of symmetries, superconformal and dual superconformal symmetries which close onto a larger group of Yangian symmetry.

One of the important outcomes of using these symmetries has been the tremendous progress in our knowledge about the structure of multi-loop amplitudes. As mentioned earlier, the integrand of the theory has been constructed recursively by using this symmetry. It is now understood that the dual conformal symmetry invariant loop integrals need to be understood much better.

A very interesting application of the Mellin space formalism is in the context of flat space conformal integrals and has been introduced in [44]. In particular, it was shown that a large class of conformal integrals—including those corresponding to position space correlation functions in ϕ^4 theory, which correspond to various kinds of box integrals—have a very simple Mellin representation which can be constructed in terms of Feynman rules. Using these, it is straightforward to see that there are simple integro-differential relations between various kinds of multi-loop integrals and lower loop ones, all the way down to a set of basic building blocks: the one-loop n-gon integrals in n dimensions, also known as the n-point star integral. These relations generalize various differential relations between integrals of different loop order which have long been very useful in the study of scattering amplitudes (see in particular [98, 99, 100] for some recent examples relevant to SYM theory).

These results suggest that it is of pressing importance to understand the star integrals in detail (a close relative of our star integrals, with massless external legs but massive propagators, has been studied and evaluated explicitly in several cases in [101]). In this note we take some modest steps in this direction. Firstly, it has been realized that such integrals compute volumes of simplices in hyperbolic space [102, 103, 104, 105] (a different relation between amplitudes and volumes has been explored in [106, 31]).

We can therefore use Schläfli's formula, which determines the differential of the volume of an $(n-1)$-simplex in terms of the volumes of $(n-3)$-simplices (a motivic version of Schläfli's formula [107] has been similarly applied to compute symbols of star integrals in [108]). As one application, we integrate the formula explicitly to find the $d=5$ pentagon integral. The result is remarkably simple, being simply a sum of logarithms with unit coefficients. The $d=6$ hexagon and $d=8$ octagon are addressed next. In these cases finding the full answer appears much more difficult (some special cases of the $d=6$ hexagon have been explicitly evaluated in [109, 99, 110, 111]) and we will content ourselves with finding analytic results when the external kinematics are restricted to two dimensions. We apply the results of the recently developed spline technology for loop integrals [105], which tells us that in such kinematics, these integral can be written out as sums of box integrals with determined coefficients.

The fully massive $d=6$ hexagon ($d=8$ octagon) integral plays a role in determining the fully massive double (triple) box integrals in four dimensions. The relation of the $d=6$ hexagon to the double box has been worked out in [44]. In this note we do the same for the triple box and the octagon. We find the former is given as a double integral of the latter. Crucially, the hexagon and octagon integrals being integrated over are ratios of polylogarithm functions divided by certain square roots. We argue this has implications for the class of functions in terms of which higher loop integrals can be expressed.

This chapter is organized in the following way. In Section 3.2 we review general ideas about Mellin amplitudes and the consequences of the existence of Feynman rules for Mellin amplitudes. Namely, we discuss the connections of multi-loop Feynman amplitudes with products of Mellin amplitudes, and its implications for the position space results. We stress that from this it is clear that we need to have a better understanding of n-gons in n dimensions or the “star" integrals to understand the fully massive loop integrals of $\mathcal{N} = 4$ SYM. In Section 3.3 we discuss these star diagrams in more detail reviewing some known results as well as presenting some new analytic results for pentagons in five dimensions. For more complicated diagrams like the $d = 6$ hexagon and the $d = 8$ octagon it is very difficult to get explicit results for general kinematics. So, in Section 3.4 we extensively discuss the analytic results for $2n$-gons using a restrictive kinematic localized in two dimensions. We do this by using the technology of splines to simplify such computations and present explicit results for two examples, the $d = 6$ hexagon and the $d = 8$ octagon. In Section 3.5 we determine the representation of the triple box integral as a double integral of the $d = 8$ octagon. Both in this case and for the double box, the integrand has a square root in the denominator which we know explicitly. We study various kinematic limits which tell us whether or not one should expect to see elliptic, or even more complicated, functions rather than the generalized polylogarithms which are much more familiar in multi-loop computations. Our results agree with the analysis of [112]. Some details about our results for the $d = 6$ hexagon and the $d = 8$ octagons in $2d$ kinematics are collected in the Appendices B.

3.2 Mellin amplitudes refresher

3.2.1 The Mellin amplitude

The multi-dimensional Mellin transform formalism was introduced in the work of Mack [59, 58] and quickly applied to both AdS/CFT [41, 42, 43, 95, 96, 97] and flat space calculations [44, 113]. The Mellin transform can be applied to any conformally invariant function of several points x_i, with given conformal weights Δ_i. This could be a conformally invariant correlation function or a conformally invariant integral (in applications to SYM theory scattering amplitudes, these are usually called *dual* conformal as a reminder that the relevant conformal symmetry is that in momentum space, rather than position space). For instance, we can write

$$\langle \phi_{\Delta_1}(x_1) \cdots \phi_{\Delta_n}(x_n) \rangle = \int [\mathrm{d}\delta_{ij}]\, M(\delta_{ij}) \prod_{i<j}^{n} \Gamma(\delta_{ij})\, x_{ij}^{-\delta_{ij}} \tag{3.2.1}$$

where $x_{ij} \equiv (x_i - x_j)^2$ and the δ_{ij} parameters satisfy the constraints

$$\sum_{i \neq j} \delta_{ij} = 0, \qquad \delta_{ii} = -\Delta_i. \tag{3.2.2}$$

The function $M(\delta_{ij})$ is usually called the Mellin transform of $\langle \phi_{\Delta_1}(x_1) \cdots \phi_{\Delta_n}(x_n) \rangle$. After solving the constraints, the integral becomes an ordinary multi-variable Mellin transform in terms of $n(n-3)/2$ independent variables. The integration is over a set of complex variables c_i, each running from $-i\infty$ to $+i\infty$ along an appropriate contour. The constraints (3.2.2) guarantee that the variables x_{ij} in the integrand combine into cross-ratios, thereby imposing conformality. It is important to note that the constraints can formally be solved by introducing a set of Mellin momenta

k_i, satisfying momentum conservation, $\sum_i k_i = 0$, such that

$$\delta_{ij} = k_i \cdot k_j, \qquad k_i^2 = -\Delta_i. \tag{3.2.3}$$

This parametrization provides some intuition for the δ_{ij} parameters. In fact, in practice it is convenient to work with Mandelstam type variables, $s_{i_1 \ldots i_p} = -(k_{i_1} + \ldots + k_{i_p})^2$, *e.g.* $s_{12} = -(k_1 + k_2)^2 = \Delta_1 + \Delta_2 - 2\delta_{12}$.

3.2.2 Feynman rules and convolutions

In [44] a subset of us found that Mellin transforms of the kind of (dual conformally invariant) integrals that appear in SYM theory scattering amplitude computations have an extremely simple form. Consider for example a momentum space diagram whose position space dual is the same as a position space correlation function in ϕ^4 theory (three examples are shown in Figure 3.1, with the dual graphs shown in blue). The Mellin amplitude is obtained from the dual graph by the simple rules:

- To each external leg associate a Mellin momentum k_i such that $k_i^2 = -1$.
- Momentum flows through the diagram being conserved at each vertex.
- To each internal leg with momentum k associate a propagator $1/(k^2 + 1)$.

In other words, the Mellin amplitude looks just like a momentum space amplitude for massive ϕ^4 theory, with $m^2 = 1$. This 1 is nothing but the canonical dimension of ϕ, $\Delta = (d - 2)/2 = 1$.

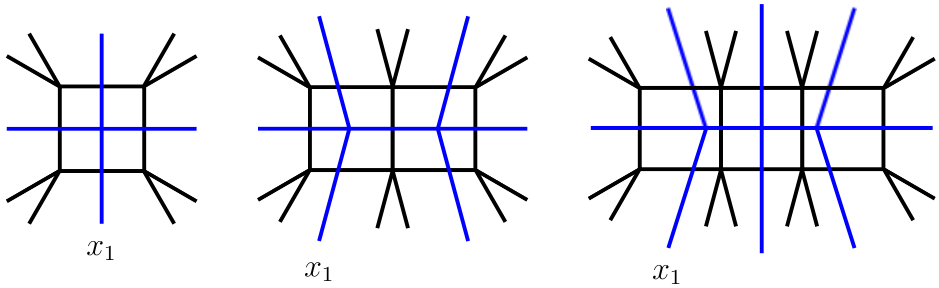

Figure 3.1: The one-, two- and three-loop ladder diagrams (black) and their corresponding dual tree diagrams (blue). The external faces of the former, or equivalently the external vertices of the latter, are labeled $x_1, x_2, \ldots$ clockwise starting from x_1 as indicated.

According to these rules we have, for example, the following very simple results for the Mellin amplitudes of the box, double box, and triple box integrals shown in Figure 3.1:

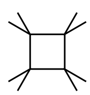

$$\Longrightarrow \qquad M = 1, \tag{3.2.4}$$

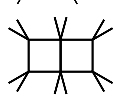

$$\Longrightarrow \qquad M = \frac{1}{1 - s_{123}}, \tag{3.2.5}$$

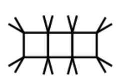

$$\Longrightarrow \qquad M = \frac{1}{1 - s_{123}} \frac{1}{1 - s_{567}}. \tag{3.2.6}$$

The Feynman-like rules nicely express Mellin amplitudes as products of simple factors. We can use this to our advantage since a product in Mellin space maps back into position space as a convolution of the individual position space expressions. That is, suppose we have two functions $f(x), g(x)$ with Mellin transforms $M^f(s), M^g(s)$,

$$M^f(s) = \int_0^{+\infty} \frac{\mathrm{d}x}{x}\, x^s\, f(x), \qquad M^g(s) = \int_0^{+\infty} \frac{\mathrm{d}x}{x}\, x^s\, g(x). \tag{3.2.7}$$

Then the position space representation for the product $M^f(s)M^g(s)$ is

$$\begin{aligned} h(x) &= \oint \frac{\mathrm{d}s}{2\pi i}\, M^f(s)M^g(s)x^{-s} = \oint \frac{\mathrm{d}s}{2\pi i} \int_0^{+\infty} \frac{\mathrm{d}y}{y}\, y^s\, f(y)M^g(s)x^{-s} \\ &= \int_0^{+\infty} \frac{\mathrm{d}y}{y}\, f(y)g(x/y). \end{aligned} \tag{3.2.8}$$

Accordingly, we can split the computation of higher-loop integrals into two steps: first we compute the position space expression corresponding to the Mellin transform, which is just a product of propagators; and the second, more difficult step is to evaluate the position space expression of the product of Γ functions appearing in (3.2.1). But the latter is nothing but the same as computing a diagram whose Mellin amplitude is $M = 1$, which corresponds to the n-legged star graph, examples of which are shown in Figure 3.2.

In SYM theory amplitude calculations we are also often interested in diagrams with various numerator factors. These can be translated into Mellin space as differential operators acting on the Mellin amplitude. Therefore we expect that a large class of integrals which appear in SYM theory scattering amplitude computations, to all loop order, can be expressed as integro-differential operators acting on just one class of elementary object: the n-point star integral in position space ϕ^n theory, or equivalently the one-loop n-gon Feynman integral in n dimensions. This makes it clear that studying these objects is an important first step in understanding the analytic structure of a large class of multi-loop integrals.

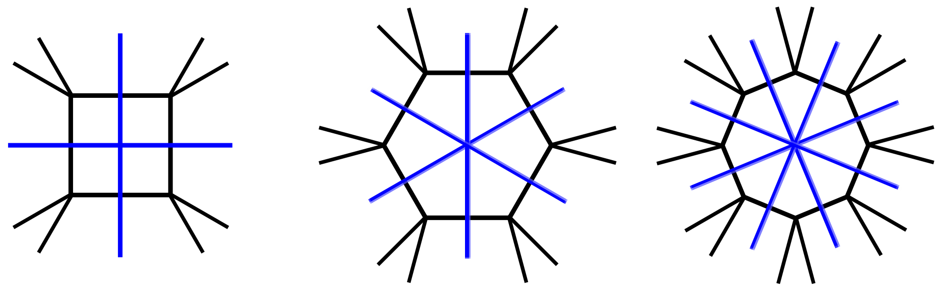

Figure 3.2: The 'star' graphs for $n = 4, 6, 8$, in blue, correspond to the one-loop box, hexagon, and octagon integrals in $d = 4, 6, 8$ respectively. These are the basic building blocks for many integrals relevant to multi-loop scattering amplitudes in SYM theory since each one is simply $M = 1$ in Mellin space.

3.3 Star integrals

It is convenient to use the embedding formalism [60, 61]. This amounts in practice to defining $d+2$-dimensional null vectors P^M to describe d-dimensional coordinate vectors x^μ, via

$$P^M = (P^+, P^-, P^\mu) = (1, x^2, x^\mu). \tag{3.3.1}$$

It is easy to check then that $P_{ij} \equiv -2P_i \cdot P_j = (x_i - x_j)^2 = x_{ij}^2$.

The n-gon star integrals are defined by

$$I^{(n)} = \int \frac{\mathrm{d}^d x}{i\pi^{d/2}} \prod_{i=1}^{n} \frac{1}{(x_i - x)^2} = \int \frac{\mathrm{d}^d Q}{i\pi^{d/2}} \prod_{i=1}^{n} \frac{1}{(-2P_i \cdot Q)}. \tag{3.3.2}$$

They are simply related to volumes $V^{(n-1)}$ of ideal hyperbolic $(n-1)$-simplices [102, 103, 104, 105] according to

$$V^{(n-1)} = \frac{\sqrt{|\det P_{ij}|}}{2^{\frac{n}{2}}\Gamma\left(\frac{n}{2}\right)} I^{(n)}. \tag{3.3.3}$$

Let us now consider the first few cases.

Triangle

It is straightforward to do the integral directly in this case, and one finds

$$I^{(3)} = \frac{\Gamma\left(\frac{1}{2}\right)^3}{\sqrt{P_{12}\, P_{13}\, P_{23}}}. \tag{3.3.4}$$

Using formula (3.3.3) above this gives $V^{(2)} = \pi$, which is indeed correct: the area of a hyperbolic ideal triangle is precisely equal to π.

Box

The simplest non-trivial star integral is the first one in Figure 3.2, corresponding to the four-dimensional box function. The result for this well-known integral is given by

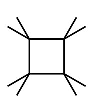

$$= \frac{\mathrm{Li}_2(x_+/x_-) - \mathrm{Li}_2\left(\frac{1-x_+}{1-x_-}\right) + \mathrm{Li}_2\left(\frac{1-1/x_+}{1-1/x_-}\right) - (x_+ \leftrightarrow x_-)}{\sqrt{\det x_{ij}^2}} \tag{3.3.5}$$

in terms of

$$x_\pm = \frac{1}{2}\left(1 + u_1 - u_2 \pm \sqrt{1 - 2u_1 + u_1^2 - 2u_2 - 2u_1 u_2 + u_2^2}\right) \tag{3.3.6}$$

and the two cross-ratios

$$u_1 = \frac{x_{13}^2 x_{24}^2}{x_{14}^2 x_{23}^2}, \qquad u_2 = \frac{x_{12}^2 x_{34}^2}{x_{14}^2 x_{23}^2}. \tag{3.3.7}$$

The numerator in (3.3.5) is nothing but the Bloch-Wigner function (see *e.g.* [104]), which indeed is known to compute the volume of an ideal hyperbolic tetrahedron.

Pentagon

The next-simplest case, not shown in Figure 3.2, is the one-loop pentagon integral in five dimensions, which as far as we are aware has not been explicitly evaluated in the literature (the one-loop pentagon integral in four dimensions has been evaluated in [114]). Surprisingly, we find that it takes a very simple form.

The pentagon integral corresponds to the volume of a hyperbolic 4-simplex. Such a volume depends on five cross-ratios, which in turn are built out of the five coordinates x_i. Let us take concretely

$$u_1 = \frac{P_{14}\,P_{23}}{P_{13}\,P_{24}}, \quad u_2 = \frac{P_{25}\,P_{34}}{P_{24}\,P_{35}}, \quad u_3 = \frac{P_{13}\,P_{45}}{P_{14}\,P_{35}}, \quad u_4 = \frac{P_{15}\,P_{24}}{P_{14}\,P_{25}}, \quad u_5 = \frac{P_{12}\,P_{35}}{P_{13}\,P_{25}} \tag{3.3.8}$$

To obtain an expression which only depends on cross-ratios we consider the rescaled integral

$$\tilde{I}^{(5)} = \sqrt{P_{13}\,P_{14}\,P_{24}P_{25}P_{35}}\,I^{(5)}. \tag{3.3.9}$$

The computation of the volume is most straightforwardly done using Schläfli's formula. The formula relates the differential of a hyperbolic simplex in terms of its co-dimension 2 simplicial faces and associated angle differentials—since each co-dimension 2 face is defined by the intersection of two hyperplanes (which lie along co-dimension 1 faces), there is therefore an associated angle. This angle can be represented in terms of the vectors normal to said hyperplanes.

More concretely, if we have a simplex whose vertex representation is given by the P_i vectors, its hyperplane representation is given in terms of vectors W_i which are normal to these hyperplanes. In particular, $W_i \cdot P_j = \delta_{ij}$. In terms of these we can write Schläfli's formula as

$$\mathrm{d}V_k = \frac{-1}{2i(k-1)} \sum_{i<j}^{n} V^{(ij)}_{(k-2)} (-1)^{i+j} \,\mathrm{d}\log\left(\frac{W_i \cdot W_j + \sqrt{(W_i \cdot W_j)^2 - W_i^2 W_j^2}}{W_i \cdot W_j - \sqrt{(W_i \cdot W_j)^2 - W_i^2 W_j^2}}\right) \tag{3.3.10}$$

where $V^{(ij)}_{(d-2)}$ corresponds to the volume of the $d-2$ simplex spanned by all the P_k vectors except for the pair P_i, P_j.

This formula is particularly simple in the case $k = 4$. In this case the $V_{(k-2)}$ become volumes of ideal hyperbolic triangles. But this is simply π! The integration of Schläfli's formula depends on the kinematic region under consideration. We work in the Euclidean region where all $(x_i - x_j)^2$ are positive, and if we define

$$\begin{aligned} \Delta^{(5)} &= \frac{1}{2} \frac{\det P_{ij}}{P_{13}\, P_{14}\, P_{24} P_{25} P_{35}} \\ &= 1 - [u_1(1 - u_3(1 + u_4) + u_2 u_4^2) + \text{cyclic}] - u_1 u_2 u_3 u_4 u_5, \end{aligned} \tag{3.3.11}$$

then for $\Delta^{(5)} < 0$ we have

$$V_{(4)} = \frac{\pi}{6} \sum_{1 \le i < j \le n} (-1)^{i+j} \log\left|\frac{W_i \cdot W_j - \sqrt{(W_i \cdot W_j)^2 - W_i^2 W_j^2}}{W_i \cdot W_j + \sqrt{(W_i \cdot W_j)^2 - W_i^2 W_j^2}}\right|, \tag{3.3.12}$$

and using (3.3.3) this gives

$$\tilde{I}^{(5)} = \frac{\pi^{\frac{3}{2}}}{2\sqrt{-\Delta^{(5)}}} \left(\sum_{1\leq i<j\leq 5} (-1)^{i+j} \log \left| \frac{W_i \cdot W_j - \sqrt{(W_i\cdot W_j)^2 - W_i^2 W_j^2}}{W_i \cdot W_j + \sqrt{(W_i\cdot W_j)^2 - W_i^2 W_j^2}} \right| \right) \tag{3.3.13}$$

The pentagon has a cyclic permutation symmetry under the action of $g : u_i \to u_{i+1}$. We can then finally write the remarkably simple and manifestly symmetric form:

$$\tilde{I}^{(5)} = \frac{\pi^{\frac{3}{2}}}{2\sqrt{-\Delta^{(5)}}} (1+g+g^2+g^3+g^4) \left\{ \log \left| \left(\frac{r-\sqrt{-\Delta^{(5)}}}{r+\sqrt{-\Delta^{(5)}}} \right) \left(\frac{s-\sqrt{-\Delta^{(5)}}}{s+\sqrt{-\Delta^{(5)}}} \right) \right| \right\} \tag{3.3.14}$$

with

$$r = \frac{(1-u_2)(1-u_5) - u_1(2-u_3-u_4-u_3u_5-u_2u_4+u_1u_3u_4)}{2}, \tag{3.3.15}$$

$$s = \frac{(1-u_5)(1-u_2u_5) - u_1\,(1+u_5-2\,u_3u_5+u_4+u_2u_4u_5+u_1u_4)}{2\,\sqrt{u_1u_5}} \tag{3.3.16}$$

Hexagon and beyond

Using Schläfli's formula (see [107, 108] for further details), one can easily express the differential (or, if one likes, the symbol) of the n-dimensional n-gon integral as a sum of certain $n-2$-dimensional $n-2$-gons. However, it is in general a difficult task to integrate this formula analytically. The structure of the differential equation makes it clear however that it can always be expressed in terms of generalized polylogarithm functions [107]; in particular,

- $I^{(2n)}$ can be expressed in terms of functions of transcendentality degree n,
- and $I^{(2n+1)}$ can be expressed in terms of functions of degree $n-1$.

One way to understand the apparent inconsistency of the transcendentality counting in the two cases is that the odd-dimensional integrals always contain an overall factor of $\pi^{3/2}$, as we saw explicitly for the pentagon in (3.3.14). Taking this factor into account, the m-dimensional m-gon integral always has total degree $m/2$. We remind the reader that all generalized polylogarithms of degree less than 4 can be expressed in terms of the classical polylogarithms Li_m, so non-classical polylogarithms first appear in the $d = 8$ octagon integral (for general kinematics).

We turn now to the $d = 6$ hexagon integral, which has received attention in the literature [109, 99, 110, 108, 111] in part due to its interesting relationships (via differential equations) to other integrals relevant to SYM theory scattering amplitudes [99]. However it remains an interesting outstanding problem to fully evaluate the $d = 6$ hexagon in general kinematics, where the integral depends on 9 independent cross-ratios (we present a choice of cross-ratios in Appendix B.1). To date the closest we have to this is the analytic formula for the special case of the "three-mass easy" hexagon [111] (an expression for its symbol was given in [108]). In this case three of the nine cross-ratios are set to zero. The formula presented in [111] therefore computes the $d = 6$ hexagon on a six-dimensional subspace of the full nine-dimensional cross-ratio space.

Motivated by the desire to simplify the evaluation of otherwise difficult integrals, and by the vast body of recent work on SYM theory amplitudes in two-dimensional kinematics (see for example [115, 116, 117, 100, 118]), in this paper we therefore carry out explicit computations of the $d = 6$ hexagon and the $d = 8$ octagon in $2d$ kinematics. Here, due to Gram determinant constraints, the nine cross-ratios for the hexagon (and the twenty cross-ratios for the general octagon) are constrained to take values in a six-dimensional (ten-dimensional) subspace of the full parameter space. We present explicit parametrizations of the cross-ratios in terms of six (ten) free variables in Appendices B.1 and B.2. Our result for the $d = 6$ hexagon in $2d$ kinematics is in a sense complementary to that of [111] since the two six-dimensional subspaces are disjoint inside the full nine-dimensional parameter space of the generic $d = 6$ hexagon.

3.4 $2n$-gon loop integrals in $2d$ kinematics

3.4.1 Setup: splines

In this section we evaluate $2n$-gon loop integrals in two-dimensional kinematics. To do this we shall use the methods developed recently in [105] based on spline technology, which the reader should consult for further details. With these, it can be shown that the one-loop star integral (3.3.2) can be written in the form

$$I^{(n)} = 2 \int_{\mathbb{M}^D} e^{X^2}\, \mathcal{T}(X; \{P_i\}) \tag{3.4.1}$$

where the spline is defined by

$$\mathcal{T}(X; \{P_i\}) = \int_0^{+\infty} \prod_{i=1}^{n} \mathrm{d}t_i \, \delta^{(D)}(X - \sum_{i=1}^{n} t_i P_i). \tag{3.4.2}$$

This expression follows by noticing that the spline is the Laplace transform of the integrand. Here we are interested in $2d$ kinematics, so we set $D = d + 2 = 4$. We shall also only consider even-dimension integrals and therefore set $n \to 2n$. The computation of the spline depends on the various linear relationships between the P_i's. Here we shall assume that the vectors are generic, i.e. that every set of four vectors spans $\mathbb{M}^4$.

Under these conditions the spline can be written as a sum of terms, each corresponding to a particular linearly independent set of vectors. Not all such sets need be considered though. It is sufficient to take the set $\mathcal{B}$ of so-called unbroken basis, which for generic kinematics amounts to the set of basis which include the vector P_1. To each such basis, b, there corresponds a piece in the spline, which is therefore made up of $N = (n-1)!/(n-4)!3!$ terms. Each term is labeled by its unbroken basis, b, and the coefficients can also be easily computed. In this manner we find

$$\mathcal{T}(X;\{P_i\}) = \sum_{b\in\mathcal{B}} \frac{\left(W_1^{(b)}\cdot X\right)^{2n-4}}{\prod_{i=1}^{2n-4} W_1^{(b)}\cdot \widehat{P}_i^{(b)}} \frac{\chi_{(b)}(X)}{\sqrt{\det b^T b}}. \tag{3.4.3}$$

Some explanations are in order. Firstly, $\widehat{P}_i^{(b)}$ denotes the ith vector *not* in the basis b. Secondly the vectors $W_i^{(b)}$ are defined by

$$W_i^{(b)}\cdot P_j = \delta_{ij}, \quad \forall P_j \in b. \tag{3.4.4}$$

We can think of b itself as a matrix whose columns are the vectors $P_i \in b$. This allows us to compute the determinant. Finally, $\chi_{(b)}(X)$ is the characteristic function of the cone spanned by the vectors in b, which can be written as

$$\chi_{(b)}(X) = \prod_{i=1}^{4} \Theta(W_i^{(b)}\cdot X). \tag{3.4.5}$$

To proceed we must evaluate the Gaussian-type integral in (3.4.1). We could evaluate it directly, since the spline is homogeneous in $|X| = \sqrt{-X^2}$. This would give us a sum of integrals of X polynomials over AdS tetrahedra. However, instead of doing this we can use the presence of the exponential to integrate by parts the terms of the form $W \cdot X$. At the end of this procedure, there are no such factors left, but there are however several types of terms, depending on how many times we differentiate the characteristic functions $\chi_{(b)}(X)$. In particular, one set of terms does not involve derivatives of at all:

$$I^{(n)} \quad = \quad \frac{(n-4)!!}{2^{\frac{n}{2}-2}} \sum_{b \in \mathcal{B}} \frac{\left(W_1^{(b)}\right)^{n-4}}{\prod_{i=1}^{n-4} W_1^{(b)} \cdot \widehat{P}_i^{(b)}} \int_{\mathbb{M}^4} e^{X^2} \, \frac{\chi_{(b)}(X)}{\sqrt{\det b^T b}} + \dots \, . \tag{3.4.6}$$

This is interesting, as the integrals above are nothing but box integrals, with four external legs P_i corresponding to the elements in the basis b. Accordingly, the kind of terms above are simply a sum of box integrals, namely dilogarithms. In contrast, the $\dots$ represent terms which have an even number of derivatives of $\chi_{(b)}(X)$. We have explicitly checked that all such terms cancel between themselves for $n = 3, 4$. To understand why, notice that those terms involve for example integrals over lines in AdS, which leads to single logarithmic terms. In order to have an expression of uniform transcendentality, it must be that these terms actually add up to zero.

3.4.2 Applications: hexagon, octagon, and beyond

To see in detail how we can perform the computation of these coefficients, let us set $n = 3$ and consider the particular basis made up of elements P_1, P_2, P_3, P_4. We then have

$$
\begin{aligned}
W_1^{(1234),M} &= \frac{\epsilon^M_{\ \ NPQ} P_2^N P_3^P P_4^Q}{\epsilon_{ABCD} P_1^A P_2^B P_3^C P_4^D} \\
\Rightarrow \frac{\left(W_1^{(1234)}\right)^2}{\left(W_1^{(1234)} \cdot P_5\right)\left(W_1^{(1234)} \cdot P_6\right)} &= \frac{\delta^{MNP}_{ABC} P_{2,M} P_{3,N} P_{4,P} P_2^A P_3^B P_4^C}{\delta^{MNPQ}_{ABCD} P_{5,M} P_{2,N} P_{3,P} P_{4,Q} P_6^A P_2^B P_3^C P_4^D}
\end{aligned}
\tag{3.4.7}
$$

with $\delta^{A_1 \ldots A_N}_{B_1 \ldots B_N}$ the totally antisymmetric product of N delta functions. It is important to notice that this expression, when multiplied by the inverse of $\sqrt{\det b^T b}$, will have total homogeneity -1 in each of the vectors P_i. Although we have focused on a particular term, this is a generic feature. It guarantees that, if we multiply I_{2n} by $P_{14}P_{25}P_{36}$, each term in the sum is separately conformally invariant, and can hence be written in terms of the nine cross-ratios of a conformal six point function (though we must keep in mind the result is only valid for $2d$ kinematics, which imposes non-linear relations on these cross-ratios). We give a choice for these in Appendix B.1, together with a $2d$ kinematics parametrization for them in terms of 6 independent variables $\chi_i^{\pm}, i = 1, 2, 3$. In terms of the latter, we can write the contribution of the particular basis (1234) to I_6 as

$$
\begin{aligned}
I_6 &= \frac{(2n-4)!!}{2^{n-2}} \frac{\chi_1^- \chi_2^- \chi_1^+}{\left(\left(\chi_1^- - \chi_2^-\right)\chi_1^+ + \left(\chi_1^- + 1\right)\chi_2^- \chi_3^+\right)\left(-\chi_1^+ + \chi_3^+ + \chi_1^-\left(\chi_3^+ + 1\right)\right)} \times \\
&\quad \times \frac{\left(\chi_1^- + 1\right)\left(\chi_1^+ - \chi_3^+\right)\left(\chi_3^+ + 1\right)^2}{\left(\chi_3^+\left(\chi_3^+ - \chi_1^+\right) + \chi_1^-\left((\chi^+)_3^2 + \chi_1^+ - \chi_2^+\left(\chi_3^+ + 1\right)\right)\right)} \times B + \ldots, \\
B &= 2\,\mathrm{Li}_2\left(\frac{\chi_1^+ - \chi_3^+}{\chi_2^+ - \chi_3^+}\right) + 2\,\mathrm{Li}_2\left(\frac{\chi_1^- - \chi_3^+}{\chi_3^+ \chi_1^- + \chi_1^-}\right) + \\
&\quad \log\left(\frac{\chi_1^-\left(\chi_1^+ - \chi_3^+\right)\left(\chi_3^+ + 1\right)}{\left(\chi_1^- - \chi_3^+\right)\left(\chi_2^+ - \chi_3^+\right)}\right) \log\left(-\frac{\chi_1^-\left(\chi_1^+ - \chi_2^+\right)\left(\chi_3^+ + 1\right)}{\left(\chi_1^- + 1\right)\left(\chi_2^+ - \chi_3^+\right)\chi_3^+}\right) + \\
&\quad \log\left(\frac{\chi_3^+ - \chi_1^-}{\chi_1^-\left(\chi_3^+ + 1\right)}\right) \log\left(\frac{\chi_3^+ - \chi_1^+}{\chi_2^+ - \chi_3^+}\right) + \frac{\pi^2}{3}
\end{aligned} \tag{3.4.8}
$$

Overall, there are a total of ten such terms. The total result is too cumbersome to reproduce here, but in the online version of this note we include a Mathematica notebook with the full result.

The computation of the $d = 8$ octagon integral in $2d$ kinematics is entirely analogous to what we have just done. There are now a total of 35 terms in the spline, each corresponding to a box integral with a certain coefficient. The $d = 8$ octagon depends on 20 cross-ratios which in $2d$ kinematics can be parametrized in terms of 10 independent parameters. The details of this kinematics have been included in Appendix B.2. The full expression for $I^{(8)}$ for the $d = 8$ octagon have been included in the attached Mathematica file since it is very lengthy.

It is straightforward to consider generalizations of the results above and consider $2n$-dimensional integrals in $2m$ kinematics, for $n > m+1$. Under such circumstances one finds the $2n$-dimensional integral decomposes (for generic $2m$-dimensional kinematics) into a sum of $(2n-1)!/(2n-2m)!(2m-1)!$ $2m$-integrals with well defined coefficients.

For instance, the general even-dimensional integral in $4d$ kinematics is given by

$$I^{(2n)} \;=\; \frac{(2n-6)!!}{2^{n-2}} \sum_{b\in\mathcal{B}} \frac{\left(W_1^{(b)}\right)^{2n-6}}{\prod_{i=1}^{n-6} W_1^{(b)}\cdot \widehat{P}_i^{(b)}} \int_{\mathbb{M}^6} e^{X^2}\, \frac{\chi_{(b)}(X)}{\sqrt{\det b^T b}} + \dots . \tag{3.4.9}$$

For the $d=8$ octagon the number of unbroken basis made up of six vectors is 21 and accordingly the $d=8$ octagon is a sum of 21 $d=6$ hexagon integrals.

3.5 Elliptic functions and beyond

3.5.1 The double box

One of the motivations for this work was to make an attempt to begin exploring integrals which evaluate to functions outside the class of generalized polylogarithm functions. Elliptic functions of this type have been encountered before in explicit QCD computations [119], and have been argued to appear in SYM theory as well starting with a double box integral contribution to the 2-loop 10-point N^{3}MHV amplitude [112].

Using the convolution tricks explained in Section 3.2.2, it was shown in [44] that the 3 to 3 exchange diagram in position space of ϕ^4 theory, which is the same as the double box Feynman integral, can be expressed as a one-fold integral of the 6-point star (the $d=6$ hexagon integral):

$$I_{3,3}(u_1,\dots,u_8,u_9) = \int_{u_8}^{+\infty} \frac{\mathrm{d}u_8'}{u_8'}\, \tilde{I}^{(6)}(u_1,\dots,u_8',u_9). \tag{3.5.1}$$

with $\tilde{I}^{(6)} = x_{14}^2 x_{25}^2 x_{36}^2 I^{(6)}$ and the double box integral,

$$I_{3,3} = \int \frac{\mathrm{d}^4 x_a \mathrm{d}^4 x_b}{(i\pi^2)} \frac{x_{14}^2 x_{25}^2 x_{36}^2}{x_{1a}^2 x_{2a}^2 x_{3a}^2 x_{4b}^2 x_{5b}^2 x_{6b}^2 \, x_{ab}^2}. \tag{3.5.2}$$

Thanks to our results in Section 3.4 we are now in possession of a simple formula giving the $d = 6$ hexagon in $2d$ kinematics. One therefore may hope that this should suffice for determining the double box in the same kinematical regime. However the formula above demands that the integration is done keeping all cross-ratios fixed except one, and it is easy to check that this is impossible in $2d$ kinematics, since the number of independent cross-ratios in this case is reduced because of Gram determinant identities. It is somewhat unfortunate that in order to recover a lower-dimensional kinematics result we have to take a detour through the full, generic result. Similar remarks hold for higher loop integrals: although we are only interested in $4d$ kinematics at the end of the day, our convolution formulae nevertheless require a detour through a higher-dimensional regime.

The symbol of the fully general $d = 6$ hexagon is known [107, 108], but it is rather complicated, and integrating it in general remains an interesting open problem. Since obtaining the full result seems to be currently out of reach, what can we say about it? Well, firstly we know what form the final expression has to take. We know that the $d = 6$ hexagon integral is related to the volume of a 5-simplex living in an AdS_5 submanifold of AdS_7. Denoting this volume by V_5, we have from formula (3.3.3) (and neglecting numerical factors):

$$I^{(6)}(x_i) \simeq \frac{V_5}{\sqrt{\det x_{ij}^2}}. \tag{3.5.3}$$

Schläfli's formula tells us that the differential volume of the 5-simplex is fixed entirely in terms of that of the 3-simplex, and from this we know that the result will take the form

$$I^{(6)}(x_i) \simeq \frac{\mathrm{Li}_3(\ldots)+\ldots}{\sqrt{\det x_{ij}^2}}, \tag{3.5.4}$$

where in the numerator of course $\mathrm{Li}_3()$ is shorthand for various terms of the correct transcendentality, such as $\mathrm{Li}_2()\log(), \log()\log()\log()$ and $\zeta(3)$, with complicated functions of the cross-ratios as arguments.

Our expression for the double box integral then becomes

$$I_{3,3}(u_i) = \int_{u_8}^{+\infty} \frac{\mathrm{d}u_8'}{u_8'} \frac{\mathrm{Li}_3(\ldots)+\ldots}{\sqrt{\Delta^{(6)}}}. \tag{3.5.5}$$

with $\Delta^{(6)} = \frac{\det x_{ij}^2}{(x_{14}^2 x_{25}^2 x_{36}^2)^2}$. In general, $\Delta^{(6)}$ is a third-order polynomial in u_8,

$$\Delta^{(6)} = \left[4\, u_1 u_2 u_5 u_6 u_7 u_9 u_8^3 + \text{lower-order terms in } u_8\right]. \tag{3.5.6}$$

Therefore, if any three cross-ratios are set to zero (and both u_3 and u_4 must be included in the three), then the determinant necessarily reduces to a second-order polynomial in u_8. This is important, since the order of the polynomial determines whether we should expect elliptic functions to appear in the final expression for the double box after integrating (3.5.5). Indeed, if we get rid of the polylogarithms for a second, the integral

$$\int \frac{\mathrm{d}u_8}{u_8\sqrt{(u_8-a)(u_8-b)(u_8-c)}} \tag{3.5.7}$$

leads to elliptic functions for generic a, b, c. If any pair of roots degenerates, or if the polynomial becomes second order instead of cubic, we would obtain logarithms instead. Because of this, it seems almost certain that the final integrated expression for the double box will contain elliptic functions, in general kinematics.

Let us look at a particular limit of the general kinematics where we actually expect to start seeing the elliptic functions in the final result. For the $d = 6$ hexagon the “minimal massive" case where we go beyond polylogarithms would be the case of 4 massive legs. Say we have $x_{61}^2 = 0$ and $x_{34}^2 = 0$. In this case we have $u_3 = u_4 = 0$, and as argued above this is the largest number of vanishing cross-ratios we can have while staying within the realm of elliptic functions. This configuration is exactly the case appropriate to the 10-point double box integral shown in Figure 6 of [112]. Now if we further set the other cross-ratios (apart from u_8) to some constant, generic values, then (3.5.7) certainly gives an elliptic function, so we would expect the same to be true for the double box in (3.5.5). However any other case with a smaller number of massive legs only gives polylogarithms, never elliptic functions, because for such cases the polynomial inside the square root degenerates from cubic to at most quadratic order. It might be interesting (and certainly easier) to derive the hexagon integral with u_8 arbitrary, $u_3 = u_4 = 0$ and all other cross-ratios set to some carefully chosen kinematic values. This would be sufficient to plug into formula (3.5.5) and check if elliptic functions actually do occur there.

3.5.2 The triple box

Let us now consider the triple box integral. In the dual position space this looks like a tree-level diagram involving 8 particles and two internal propagators (shown in Figure 3.1). Accordingly we expect it to be given by a two-fold integral of the 8-point star integral. This is what we shall proceed to show just now.

To begin with, we need a basis of cross-ratios which can describe a conformally invariant function of 8 points. For fully generic kinematics (in general dimension) we expect $8 \times 5/2 = 20$ independent cross-ratios. We list a choice of such cross-ratios in Appendix B.2.1. Next, we consider the Mellin representation of the triple box. According to the rules we set out in Section 3.2 it is the product of two propagators. Once the constraints (3.2.2) are solved, we get an ordinary multi-dimensional transform in terms of the 20 independent cross-ratios. In this way we find

$$I_{3,2,3} = \int_{-i\infty}^{+i\infty} \left(\prod_{i=1}^{20} \frac{\mathrm{d}c_i}{2\pi i} \, u_i^{c_i} \right) \frac{1}{(2+2c_{12})(2+2c_9)} \times \prod_{i<j}^{8} \Gamma(\delta_{ij}). \tag{3.5.8}$$

with

$$I_{3,2,3} = \frac{1}{4} \int \frac{\mathrm{d}x_a \mathrm{d}x_b \mathrm{d}x_c}{(i\pi)^3} \frac{x_{15}^2 x_{26}^2 x_{37}^2 x_{48}^2}{x_{1a}^2 \, x_{2a}^2 \, x_{3a}^2 \, x_{4b}^2 \, x_{5b}^2 \, x_{6c}^2 \, x_{7c}^2 \, x_{8c}^2 \, x_{ab}^2 \, x_{bc}^2} \tag{3.5.9}$$

For the reader's benefit we provide in Appendix B.2.2 an explicit formula for the product of 28 Γ-functions written out in terms of 20 independent variables c_i.

We don't need to display all those details here since we already know that the position space expression corresponding to the product of gamma functions is nothing but the $d = 8$ octagon integral. We have therefore only to compute the (much simpler) position space expressions corresponding to the propagator factors. For instance,

$$\int_{-i\infty}^{+i\infty} \frac{\mathrm{d}c_{12}}{2\pi i} \frac{u_{12}^{c_{12}}}{2(1+c_{12})} = \frac{\Theta(1-u_{12})}{2\,u_{12}} \tag{3.5.10}$$

with $\Theta(x) = 1$ for $x > 0$, and zero otherwise. In this manner we conclude that

$$I_{3,2,3}(u_1,\ldots,u_{20}) = \frac{1}{u_9\,u_{12}} \int_{u_9}^{+\infty} \mathrm{d}u_9' \int_{u_{12}}^{+\infty} \mathrm{d}u_{12}'\, \tilde{I}^{(8)}(u_1,\ldots,u_9',\ldots,u_{12}',\ldots,u_{20}) \tag{3.5.11}$$

with $\tilde{I}^{(8)} = x_{15}^2 x_{26}^2 x_{37}^2 x_{48}^2 I^{(8)}$. Of course, this equation can be turned around to write a (very simple) differential equation expressing the octagon as a second derivative of the triple box.

Finally let us remark on the $d = 8$ octagon integral. It is again given by the volume of a hyperbolic simplex, and accordingly we have something of the schematic form

$$\tilde{I}^{(8)}(u_i) = \frac{\mathrm{Li}_4(\ldots) + \ldots}{\sqrt{\Delta^{(8)}}}. \tag{3.5.12}$$

with $\Delta^{(8)}$ now given by $\frac{\det x_{ij}^2}{(x_{15}^2 x_{26}^2 x_{37}^2 x_{48}^2)^2}$. Of course we emphasize that the numerator will be a linear combination of (generalized) polylogarithm functions of degree four, including not just $\mathrm{Li}_4()$ but also for example $\mathrm{Li}_{2,2}()$, $\mathrm{Li}_2()\mathrm{Li}_2()$, etc. If we evaluate the determinant, we find

$$\Delta^{(8)} = \frac{u_1 u_2^3 u_3 u_4^2 u_5^2 u_6 u_7^2\, u_8^3 u_{10} u_{11}^3}{u_{13}\, u_{14}\, u_{16}^2\, u_{18}\, u_{19}} \,(u_9^3 u_{12}^3 + \ldots) \tag{3.5.13}$$

where the $\ldots$ stands for terms of lower degree in u_9 or u_{12}. For general kinematics the first integration with respect to u_9 will make elliptic functions appear, while it is reasonable to expect that (again, in general kinematics) the second integration will lead to an even more complicated class of functions, beginning as we see at three loops.

Chapter 4

Generating tree level amplitudes in $\mathcal{N} = 4$ SYM by Inverse Soft Limit

4.1 Introduction

It has been known for a long time that, for gauge theories and gravity, under the soft limit scattering amplitudes of any number of external particles reduces to amplitudes with one less number of external particle times an universal soft factor[120]. It is an amazing fact that amplitudes of gauge theories and gravity behave nicely under the soft limit. The study of soft limit of scattering amplitudes in field theories has been remarkably successful in understanding their structure. In fact, soft limit (as well as collinear limit) have been extensively used as strong constraints for helping to fix the scattering amplitudes [121, 122, 123, 124, 125, 126, 127, 128, 16, 17, 129, 130].

In recent years there had been a surging interest in understanding how to build up amplitudes by adding particles starting from an amplitude with lower number of particles, which is exactly the reverse mechanism of taking a soft limit. So, under this paradigm, also called the “Inverse Soft", the soft behaviour of scattering amplitudes are just enough to restrict the structure of amplitudes. This phenomenon was first observed and suggested in [45, 131], where the scattering amplitude was described in terms of the Hodges’ diagram representation [132], and later was introduced as one of the important ingredients in the Grassmannian approach to the scattering amplitudes [133, 134, 27, 28, 135, 136, 137, 138, 30, 139]. For the applications of Inverse Soft Limit (ISL) in understanding various aspects of the scattering amplitudes in $\mathcal{N} = 4$ Super Yang-Mills (SYM) theory and $\mathcal{N} = 8$ super gravity as well, see for instance [140, 141, 142, 143, 144, 145].

Moreover, it is known that from the point of view of the Grassmannian, ISL [134, 28] is a natural way of constructing Yangian-invariants [19]. Since tree-level amplitudes in $\mathcal{N} = 4$ SYM are Yangian invariant we should be able to construct these amplitudes by the above mentioned ISL, but unfortunately a systematic way of doing this had so far eluded us. In this paper we address this issue. In a recent paper [146] some progress had been made in carrying out this program for few simple non-supersymmetric amplitudes in $\mathcal{N} = 4$ SYM. This process is related to the two particle factorization channel of BCFW recursion relations. In this paper we generalize their results and show that all superamplitudes in $\mathcal{N} = 4$ SYM at tree level can be constructed by an explicit prescription of ISL, namely by a systematic way of adding a series of particles to lower-point superamplitudes to arrive at higher-point superamplitudes.

By analysing and examining the BCFW diagrams carefully, we are able to obtain recursion relations of how to construct an arbitrary BCFW diagram by adding particles from any side of that diagram, consequently any arbitrary amplitude will be ISL constructible in a concrete way. It is clear that the amplitudes constructed solely by adding particles not only have manifest Yangian symmetry, but also make the soft limit transparent.

The ISL in $\mathcal{N} = 4$ SYM is closely tied to the ideas of Grassmannian formalism, Hodges' diagrams, as well as Yangian invariance, and indeed the amplitudes constructed by ISL are guaranteed to have Yangian symmetry, as we mentioned. However the canonical configuration for adding particles obtained from the proposed recursion relations is quite independent of those ideas. In fact our way of adding particles can be straightforwardly generalized to another interesting class of physical observables, the form factors [147], for which all of above mentioned ideas may fail. So the ISL prescription constructed in this paper is quite general. On the other hand, the fact that ISL can be applied to the form factors may indicate that there might also exist hidden symmetries in form factors. In fact, indeed the tree-level solutions for form factors resemble the tree-level solutions for $\mathcal{N} = 4$ SYM theory [148], which is known to be manifestly dual conformal invariant.[1]

This chapter is organized as follows. In Section 4.2 we review the idea that two particle factorization channel of BCFW recursion relations is related to the notion of adding a particle to a tree amplitude in $\mathcal{N} = 4$ SYM by ISL. We also present a few non-trivial examples of constructing amplitudes using the ISL method. Then we move on to section 4.3 where we determine the canonical configuration for adding particles

[1]We would like to thank Gang Yang for the discussion on this topic.

to construct BCFW terms, and consequently a concrete prescription to generate any tree level superamplitudes of $\mathcal{N} = 4$ by this method is given. This canonical configuration takes the form of a set of recursion relations where we can generate a higher point configuration from lower point ones. In section 4.4, the BCFW shifts of a BCFW diagram have been shown to be in one-to-one correspondence with certain multiple shifts in the ISL picture. We go on to extend the ISL paradigm to construct form factors of $\mathcal{N} = 4$ SYM in section 4.5. Example using our recursion relation and discussions on the extension of the ISL method to gravity amplitudes and ISL in the momentum-twistor language are presented in the Appendix C.

4.2 Two-particle channel BCFW and ISL in SYM

4.2.1 Inverse soft factors and shifts

In [146] it was shown that the notion of adding a particle to a tree-level amplitude by ISL is related to the two particle factorization channel of BCFW recursion relations. In this section we review and extend their results for the supersymmetric BCFW recursion relations. Before we proceed let us mention that we would be using the symbol $\langle 1\ n]$ to denote the following BCFW shifts

$$\begin{aligned}
\lambda_{\hat{1}} &= \lambda_1 - z\lambda_n; \qquad (4.2.1)\\
\tilde{\lambda}_{\overline{n}} &= \tilde{\lambda}_n + z\tilde{\lambda}_1;\\
\eta_{\overline{n}} &= \eta_n + z\eta_1,
\end{aligned}$$

and $[1\ n\rangle$ to denote the parity flipped version of the above shifts, namely

$$\begin{aligned} \lambda_{\bar{1}} &= \tilde{\lambda}_1 - z\tilde{\lambda}_n; \\ \lambda_{\widehat{n}} &= \lambda_n + z\lambda_1; \\ \eta_{\bar{1}} &= \eta_1 - z\eta_n. \end{aligned} \tag{4.2.2}$$

We note here that we encounter two different BCFW diagrams for two particle factorization channel, and we will soon explain that they correspond to the cases where we add a positive and a negative helicity particles to a lower-point amplitude in the non-supersymmetric case, which are respectively called k preserving and k increasing inverse-soft operations in the supersymmetric case (see the discussion in Appendix A.), here k denotes the degree of R-charges of N^{k}MHV[2] amplitudes.

Let us start the discussion with $\langle 1\ n]$ BCFW shifts, see Fig.(4.1), we have

$$A(\widehat{1}, 2|3, \cdots, \overline{n}) = \int d^4\eta_{\widehat{P}} A_L(\widehat{1}, 2, -\widehat{P}) \frac{1}{s_{12}} A_R(\widehat{P}, 3, \ldots, \overline{n}). \tag{4.2.3}$$

Note that because of the particular choice of the BCFW shift, the three-point amplitude $A_L(\widehat{1}, 2, -\widehat{P})$ must be a $\overline{\text{MHV}}$ amplitude, namely the parity flipped version of the maximally-helicity-violating (MHV) amplitudes. It is straightforward to find that this BCFW diagram can be written as,

$$A(\widehat{1}, 2|3, \cdots, \overline{n}) = \mathcal{S}_+(n\ 1\ 2) A_R(2', 3, \ldots, n'), \tag{4.2.4}$$

[2]The meaning of this notation will become clear shortly.

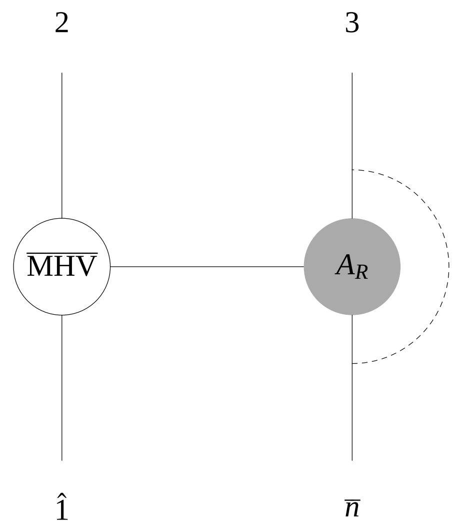

Figure 4.1: BCFW diagram of two particle channel corresponding to adding particle 1^+.

where the soft factor $\mathcal{S}_+(n\ 1\ 2)$ is defined as,

$$\mathcal{S}_+(n\ 1\ 2) = \frac{\langle n2\rangle}{\langle n1\rangle\langle 12\rangle}. \tag{4.2.5}$$

Here the primed particle labels, $2'$ and n', represent the following shifts on particles 2 and n,

$$\tilde{\lambda}_2 \to \tilde{\lambda}_2 + \frac{\langle 1n\rangle}{\langle 2n\rangle}\tilde{\lambda}_1,\ \tilde{\lambda}_n \to \tilde{\lambda}_n + \frac{\langle 12\rangle}{\langle n2\rangle}\tilde{\lambda}_1; \tag{4.2.6}$$
$$\eta_2 \to \eta_2 + \frac{\langle 1n\rangle}{\langle 2n\rangle}\eta_1,\ \eta_n \to \eta_n + \frac{\langle 12\rangle}{\langle n2\rangle}\eta_1.$$

The shifts ensure the momenta and supercharge conservation after adding particles. As indicated in $\mathcal{S}_+(n\ 1\ 2)$, this case will often be called as adding a positive particle 1^+, although we are dealing with a supersymmetric amplitude.

A similar calculation for the parity flipped version of the previous case i.e. for (4.2.2),

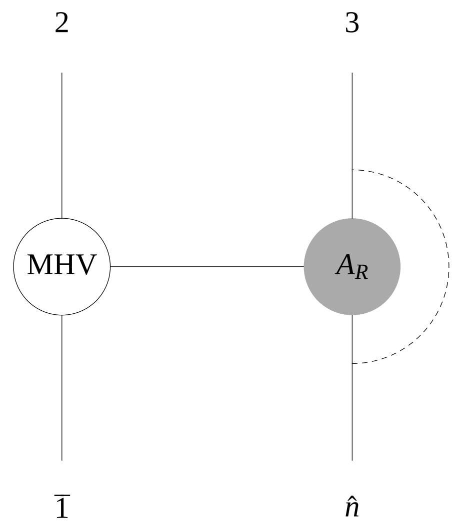

Figure 4.2: BCFW diagram of two particle channel corresponding to adding particle 1^-.

see Fig.(4.2), leads to another kind of soft factor, which is given as

$$\begin{aligned} \mathcal{S}_-(n\ 1\ 2) &= \frac{[n2]}{[n1][12]}\delta^4(\eta_1 + \frac{[n1]}{[2n]}\eta_2 + \frac{[12]}{[2n]}\eta_n) \\ &= \frac{1}{[n1][12][n2]^3}\delta^4([12]\eta_n + [2n]\eta_1 + [n1]\eta_2), \end{aligned} \tag{4.2.7}$$

with the following ISL shifts

$$\lambda_n \rightarrow \lambda_n + \frac{[21]}{[2n]}\lambda_1,\ \lambda_2 \rightarrow \lambda_2 + \frac{[1n]}{[2n]}\lambda_1. \tag{4.2.8}$$

We note that $\frac{[n2]}{[n1][12]}$ is the soft factor for removing a negative particle, while the extra fermionic delta function takes care of increasing the R-charge. Moreover the higher-point superamplitude we get by adding particle 1^- is given by

$$A(\bar{1}, 2|3, \ldots, \hat{n}) = \mathcal{S}_-(n\ 1\ 2)A(2', \ldots, (n-1), n'), \tag{4.2.9}$$

again $2'$ and n' indicate the shifts on 2 and n according to (4.2.8).

Let us conclude this subsection with remarks on how to generate general BCFW diagrams with multiple-particle channels according to ISL. It is clear that the previous discussion only allows us to rewrite BCFW diagrams with two-particle channel in the ISL form. To deal with a BCFW diagram with a multiple-particle channel, some attempt has been made in [146], where the goal is to build up a general BCFW diagram by adding particles to a two-particle-channel BCFW diagram. For instance let us consider a typical BCFW diagram for the $[1\ n\rangle$ shift,

$$A_L(\overline{1}, 2, \cdots, m, \widehat{P})\frac{1}{P^2}A_R(-\widehat{P}, m{+}1, \cdots, n{-}1, \widehat{n}). \tag{4.2.10}$$

The idea is to start with a two-particle-channel diagram, which we know how to write in the ISL form,

$$A_L(\overline{1}, m, \widehat{P})\frac{1}{P^2}A_R(-\widehat{P}, m{+}1, \cdots, n{-}1, \widehat{n}) = \mathcal{S}(n\ 1\ m)A_R(m', m{+}1, \cdots, n{-}1, n'). \tag{4.2.11}$$

We then build up the full subamplitude $A_L(\overline{1}, 2, \cdots, m, \widehat{P})$ gradually by adding particles between 1 and m. *A priori* it is not guaranteed that $A_L(\overline{1}, 2, \cdots, m, \widehat{P})$ can be constructed in this way. And indeed in the non-supersymmetric case, it was checked in [146] that only few simple amplitudes can be constructed in such a way. From our previous discussion on the relation between ISL and the two-particle-channel BCFW diagram, we have seen that it is very natural to consider ISL for the superamplitudes in $\mathcal{N} = 4$ SYM theory. In fact, supersymmetry provides a huge advantage as we will show in the following sections that one can actually construct full superamplitudes in $\mathcal{N} = 4$ SYM solely by adding particles according to ISL. Let us state our final result here before we proceed further.

We can proceed in the above mentioned way and generate any tree-level super amplitude in $\mathcal{N} = 4$ SYM theory by ISL and this can be schematically written as,

$$A_n = \sum_{i;L,R} (\prod_L \mathcal{S}'_L)(\prod_R \mathcal{S}'_R) A_{\overline{\text{MHV}}}(i', i{+}1, n'), \tag{4.2.12}$$

where summation over i is according to BCFW diagrammatic representation of the amplitudes. The products on $\mathcal{S}_L$ and $\mathcal{S}_R$ and summation on L, R are determined by a set recursion relations (4.3.32) and (4.3.33) which we propose in the subsequent sections to generate the configurations of particles that had to be added on both sides of a BCFW diagram to generate the BCFW diagram. And finally $\mathcal{S}'$, i' and n' are used for the fact that the particles are shifted according to the rules of ISL, namely Eq. (5.1.1) and (4.2.8).

4.2.2 Examples

Before we consider the general procedure for adding particles, let us consider a couple of simple examples to illustrate the idea of ISL. The first case we would like to consider is $\overline{\text{MHV}}$ amplitude. As per the general philosophy we will start with a three-point amplitude and gradually build up the full amplitude by adding particles. Let us consider five-point amplitude first, one way of doing this is following:

- We start by adding the particle 1^+ to $A_{\text{MHV}}(345)$ in order to generate $A_{\text{MHV}}(1345) = \mathcal{S}_+(513)A_{\text{MHV}}(3'45')$, where the shifts are according to (5.1.1). To show this we note that,

$$\begin{aligned} A_{\text{MHV}}(1345) &= \frac{\langle 5\,3\rangle}{\langle 5\,1\rangle\langle 1\,3\rangle}\Big(\frac{\delta^8(\lambda_{3'}\eta_{3'}+\lambda_4\eta_4+\lambda_{5'}\eta_{5'})}{\langle 3'\,4\rangle\langle 4\,5'\rangle\langle 5'\,3'\rangle}\Big) \\ &= \frac{\delta^8(\lambda_1\eta_1+\lambda_3\eta_3+\lambda_4\eta_4+\lambda_5\eta_5)}{\langle 1\,3\rangle\langle 3\,4\rangle\langle 4\,5\rangle\langle 5\,1\rangle}, \end{aligned} \tag{4.2.13}$$

where we simplified the supercharge conserving delta function by Scouten identities.

- Our final goal $A_{\text{NMHV}}(12345)$ can be obtained by further adding 2^- to $A_{\text{MHV}}(1345)$,

$$\begin{aligned} A_{\overline{\text{MHV}}}(12345) &= \mathcal{S}_-(123)A_{\text{MHV}}(1'3'45) \\ &= \frac{\delta^4(\eta_1[23]+\eta_2[31]+\eta_3[12])\delta^8(\sum_i \lambda_i\eta_i 5)}{[1\,2][2\,3][3\,4][4\,5][5\,1]\langle 4\,5\rangle^4}, \end{aligned} \tag{4.2.14}$$

where $1'$ and $3'$ are shifted according to (4.2.8). *We simplified the supercharge conserving delta function by using the fermionic delta function from S_-.*

One can continue the process and add a negative helicity particle to (4.2.14). One particular way we are using here, as the five-point case, is to add 2^- between 1 and 3 to the five-point amplitude $A_{\overline{\text{MHV}}}(13456)$ and we get,[3]

$$A_{\overline{\text{MHV}}}(123456) = \frac{\delta^8(\sum\lambda_i\eta_i)\delta^4(\eta_1[34]+\eta_3[41]+\eta_4[13])\delta^4(\eta_1[23]+\eta_2[31]+\eta_3[12])}{([12][23]\ldots[61])[1\,3]^4\langle 5\,6\rangle^4}. \tag{4.2.15}$$

[3]One of course could add particles in a different way, the answer would be in a different-looking form.

Similarly a compact general formula for n-point $\overline{\text{MHV}}$ amplitudes can be obtained by continuing to add 2^- between 1 and 3,

$$A_{\overline{\text{MHV}}}(1,2,\cdots,n) = \frac{\delta^8(\sum\lambda_i\eta_i)\prod_{i=2}^{n-3}\delta^4(\eta_1[i\,i+1]+\eta_i[i+1\,1]+\eta_{i+1}[1\,i])}{\langle n-1\,n\rangle^4\prod_{i=1}^{n}[i\,i+1]\prod_{i=3}^{n-3}[1\,i]^4}. \tag{4.2.16}$$

Likewise the more familiar Parke-Tarlor formula for MHV amplitude can be built up by adding positive particles.

Another example we like to consider is a particular BCFW diagram for a n-point amplitude with, say, 6-point MHV on one side of the BCFW diagram, namely,

$$A(\bar{1}2345|6\cdots\hat{n}) = A_{\text{MHV}}(\bar{1},2,3,4,5,\widehat{P})\frac{1}{P^2}A_R(-\widehat{P},6,\cdots,\hat{n}), \tag{4.2.17}$$

where we did not specify $A_R(-\widehat{P},6,\cdots,\hat{n})$, in fact it can be anything, as we will discuss in section 4. It is easy to check that this BCFW diagram is equivalent to the following ISL expression,

$$A(\bar{1}2345|6\cdots\hat{n}) = \Big[\mathcal{S}_+(345)\mathcal{S}_+(23'5')\mathcal{S}_+(12'5'')\mathcal{S}_-(n1'5''')\Big]A_R(5'''',\cdots,n'), \tag{4.2.18}$$

where i' means it is shifted once according to the rules (5.1.1) and (4.2.8), i'' means shifted twice, and so on.

4.3 Recursion relation for adding particles

4.3.1 MHV

We have seen a couple of examples of applying ISL to get amplitudes and BCFW diagrams, in this section we will present a systematic way of constructing a BCFW diagram by adding particles one at a time. Let us warm up with the simplest case when the BCFW diagram has a MHV amplitude on one side, see Fig.(4.3). We will state the results first and will explain them shortly.

For $\langle 1\ n]$ BCFW shift, namely Fig.(4.3.a) the way of adding the particles for this case is given as

$$\{1^+, 2^-, 3^+, \cdots, (m-1)^+\}, \tag{4.3.1}$$

the notation means that we add particle 1^+ first, 2^- second, and so on until $(m-1)^+$. Just to simplify the notation, we define it as

$$\widehat{\mathbb{A}}^{(m)}_{\text{MHV}} \equiv \{1^+, 2^-, 3^+, \cdots, (m-1)^+\}, \tag{4.3.2}$$

where $\mathbb{A}$ stands for “Adding particles" and superscript (m) denotes adding all possible particles labeled by i such that $i < m$. We note here that in fact the ordering of the particles $3^+, \cdots, (m-1)^+$ is not important, which is generally true that the ordering of the same helicity particles are not important.

Similarly when we have $A_{\text{MHV}}(\overline{1}, 2, \cdots, i, \widehat{P})$ on one side of a BCFW diagram, namely

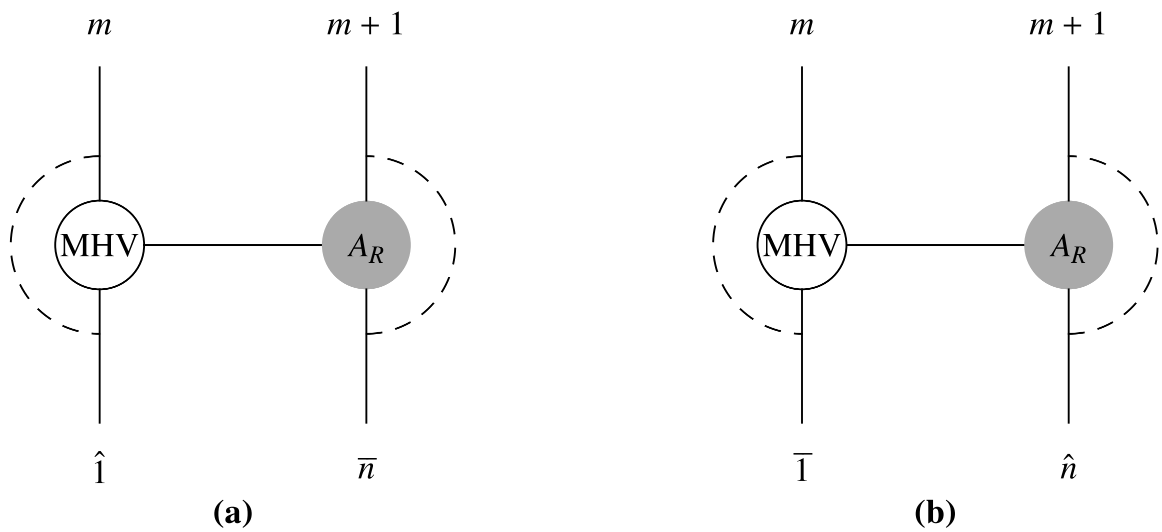

Figure 4.3: **(a):** For the $\langle 1\ n]$ shift we add particles $\{1,\ldots,m-1\}$ on the left side of the first diagram to make it $A_L^{\text{MHV}}(\widehat{1},\ldots,m,\widehat{P})$ while the subamplitude A_R on the right can be of any type.
(b): For the $[1\ n\rangle$ shift we add particles $\{1,\ldots,m-1\}$ on the left side of the first diagram to make it$A_L^{\text{MHV}}(\overline{1},\ldots,m,\widehat{P})$.

for the $[1\ n\rangle$ BCFW shift, see Fig.(4.3.b), we add the particles as

$$\overline{\mathbb{A}}^{(m)}_{\text{MHV}} \equiv \{1^-,2^+,\cdots,(m-1)^+\}. \tag{4.3.3}$$

The above two statements can be understood as follows: let us first consider the $[1\ n\rangle$ shift, by construction we add the particle 1^- first, and by counting the fermionic degrees for a MHV amplitude there must be one and only one negative particle, so the rest of the particles must be positive and hence we are led to (4.3.3).

Similarly for the other case, $A_{\text{MHV}}(\widehat{1},2,\cdots,m,\widehat{P})$, since the first particle now is 1^+, then the next one added must be negative and the remaining should be all positive.

We have proved the results of both cases, $\langle 1\ n]$ shift and $[1\ n\rangle$ shift explicitly by comparing with BCFW recursion relations.

In fact, the BCFW recursion relation in momentum-twistor[4] is already in the ISL form for this simplest case we are considering. The tree-level BCFW recursion relations in momentum-twistor is given as[5]

$$\begin{aligned} M_{n,k}(1,\cdots,n) &= M_{n-1,k}(2,\cdots,n) \\ &+ \sum_{n_R,k_R;j} [j{+}1\ j\ 2\ 1\ n] M_{n_L,k_L}(\widehat{1}_{j+1},\cdots,j,I_{j+1}) M_{n_R,k_R}(I_{j+1},j{+}1,\cdots,n), \end{aligned} \tag{4.3.4}$$

where $n_L + n_R = n + 2, k_L + k_R = k - 1$, and the shifts are given as

$$\widehat{1}_{j+1} = (12)\bigcap(jj{+}1n), I_{j+1} = (jj{+}1)\bigcap(n12). \tag{4.3.5}$$

For the special case we are considering, namely when the amplitude on the left-hand-side is a MHV amplitude, we have $M_{n_L,k_L}(\widehat{1}_{j+1},\cdots,j,I_{j+1}) = 1$, and Eq. (4.3.4) reduces to

$$\begin{aligned} M_{n,k}(1,\cdots,n) &= M_{n-1,k}(2,\cdots,n) \\ &+ \sum_{n_R,k_R;j} [j{+}1\ j\ 2\ 1\ n] M_{n_R,k_R}(I_{j+1},j{+}1,\cdots,n). \end{aligned} \tag{4.3.6}$$

It is quite clear that the first term $M_{n-1,k}(2,\cdots,n)$ can be interpreted as adding a positive particle 1^+, while the second term is corresponding to $\{1^+,2^-,3^+,\cdots,(j-1)^+\}$, which is exactly the same as we described for $\langle 1\ n]$ shift.

---

[4] For a simple review on ISL in momentum-twistor space please see appendix.

[5] For more details about BCFW recursion relations in momentum-twistor and beyond tree-level, please see [28]. For comparison we have done reflection on the original formula, namely $a \to n-a+1$.

When $M_{n_L,k_L}(\widehat{1}_{j+1},\cdots,j,I_{j+1})$ is beyond MHV, the BCFW recursion relations (4.3.4) can not be so simply interpreted as ISL. Instead we will apply our results from MHV case to motivate the recursion relations for adding particles. It allows us to extend this program where our goal is to find a canonical configuration for adding particles to construct one side of the BCFW diagram when that is a general $(m+1)$ point amplitude. In the next couple of sections we motivate the systematic method of achieving our goal for the cases of next-maximally-helicity-violating (NMHV) and next-next-maximally-helicity-violating (NNMHV) amplitudes on one side of BCFW diagrams and finally in the subsequent section we give our general result for the N^{k}MHV case.

4.3.2 NMHV

In this section we consider the case when we have a NMHV amplitude on one side of a BCFW diagram. Let us start with the case when one side of the BCFW diagram is $A_{\rm NMHV}(\overline{1},2,\cdots,m,\widehat{P})$, and we will denote $\overline{\mathbb{A}}^{(m)}_{\rm NMHV}$ as the way of adding particles for this case. To be a NMHV amplitude, m must be greater than 3. When $m=4$, one can easily check that the right way of adding particles is

$$\overline{\mathbb{A}}^{(4)}_{\rm NMHV}=\{1^-,2^+,3^-\}. \tag{4.3.7}$$

To understand the general case, let us first study the relevant $(m+1)$-point NMHV amplitude. The BCFW diagrams contributing to this amplitude are given in Fig.(4.4).

Let us consider the two BCFW diagrams in the box separately. For the first BCFW

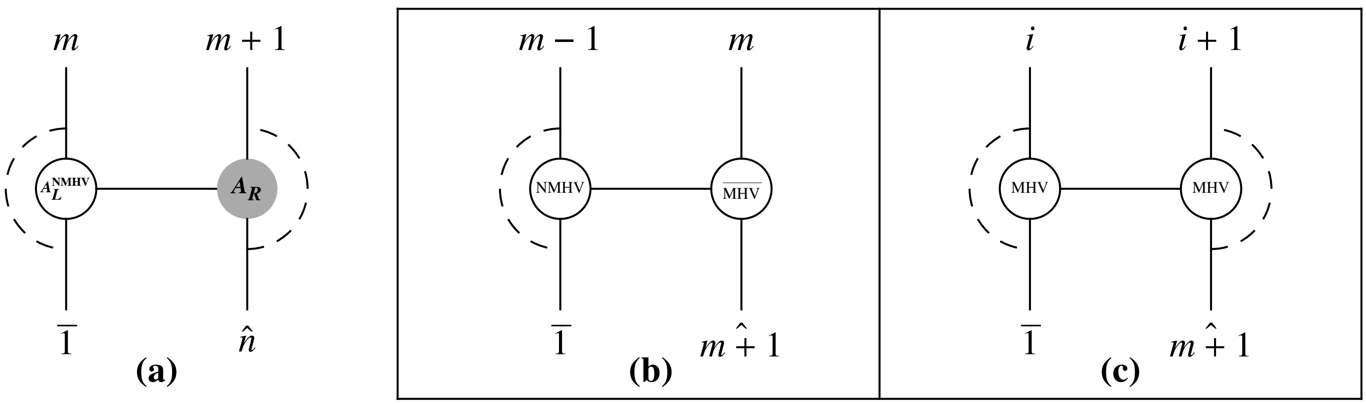

Figure 4.4: **(a):** For the $[1\ n\rangle$ shift we add particles $\{1,\ldots,m-1\}$ on the left side of the this diagram to build up $A_L^{\text{NMHV}}(\overline{1},\ldots,m,\widehat{P})$ while A_R on the right can be of any type. **(b, c):** These are the corresponding BCFW contributions to the $(m+1)$ point subamplitude A_L^{NMHV} in **(a)**.

diagram in the box, Fig.(4.4.b), we have

$$A_{\text{NMHV}}(\overline{1},2,\cdots,m-1,\widehat{P})\frac{1}{P^2}A_{\overline{\text{MHV}}}(-\widehat{P},m,\widehat{m+1}). \tag{4.3.8}$$

We note that the subamplitude $A_{\text{NMHV}}(\overline{1},2,\cdots,m-1,\widehat{P})$ can be viewed as built up by adding particles according to $\overline{\mathbb{A}}^{(m-1)}_{\text{NMHV}}$. So the particles added at the last $(m-2)$ steps for $\overline{\mathbb{A}}^{(m)}_{\text{NMHV}}$ are fully determined for this contribution, namely all particles appeared in $\overline{\mathbb{A}}^{(m-1)}_{\text{NMHV}}$ except 1^-. After those are determined, we are only left with the particles $(m-1)$ and 1. By construction the particle 1^- must be added at the first step, and the particle $(m-1)$ must be positive. Putting all these together the analysis shows that if there is a ISL way of rewriting this BCFW diagram, the way of adding particles for this case is given as

$$\{1^-,(m-1)^+,\overline{\mathbb{A}}^{(m-1)}_{\text{NMHV}}(\cancel{1^-})\}, \tag{4.3.9}$$

where we use $\overline{\mathbb{A}}^{(m-1)}_{\text{NMHV}}(\cancel{1^-})$ to denote all the particles appearing in $\overline{\mathbb{A}}^{(m-1)}_{\text{NMHV}}$ except 1^-.

Then let us consider the other contribution to this amplitude, Fig.(4.4.c),

$$A_{\text{MHV}}(\overline{1},2,\cdots,i,\widehat{P})\frac{1}{P^2}A_{\text{MHV}}(-\widehat{P},i+1,\cdots,\widehat{m+1}). \tag{4.3.10}$$

From previous section we know how to add particles when one side of BCFW diagram is a MHV amplitude. For the MHV amplitude on the left-hand-side, $A_{\text{MHV}}(\overline{1},2,\cdots,i,\widehat{P})$, the corresponding way of adding particles is given by $\overline{\mathbb{A}}^{(i)}_{\text{MHV}}(\cancel{1^-})$; for $A_{\text{MHV}}(-\widehat{P},i+1,\cdots,\widehat{m+1})$, it is given as $\{m^-,(i+2)^+,\cdots,(m-1)^+\}$, however we should note that one cannot add particle m in any step. So after m^- is removed this may be denoted as

$$\mathcal{R}^{i-1}\left[\widehat{\mathbb{A}}^{(m-i)}_{\text{MHV}}(\cancel{1^+,2^-})\right], \tag{4.3.11}$$

where $\mathcal{R}$ is a rotating operation, which does the cyclic shifting, $a\to a+1$ for any a appeared in $\widehat{\mathbb{A}}^{(m-i)}_{\text{MHV}}(\cancel{1^+,2^-})$, and $\mathcal{R}^{i-1}$ mean we rotate the numbers $(i-1)$ times, i.e. $a\to a+i-1$. So from this analysis we learn in what order the particles should be added for the last $(m-3)$ steps and after this is done now we are left with only the particles 1, i and $(i+1)$. The order of their addition can be determined from the knowledge about the case of $m=4$, Eq. (4.3.7), which is simply $\{1^-,i^+,(i+1)^-\}$.

In conclusion, if there is a ISL method of constructing this BCFW diagram, we find that the way of adding particles for this case must be given as

$$\{1^-,i^+,(i+1)^-,\mathcal{R}^{i-1}\left[\widehat{\mathbb{A}}^{(m-i)}_{\text{MHV}}(\cancel{1^+,2^-})\right],\overline{\mathbb{A}}^{(i)}_{\text{MHV}}(\cancel{1^-})\}. \tag{4.3.12}$$

We can combine $\mathcal{R}^{i-1}\left[\widehat{\mathbb{A}}^{(m-i)}_{\text{MHV}}(\cancel{1^+,2^-})\right]$ with $(i+1)^-$ and nicely arrive at $\mathcal{R}^{i-1}\left[\widehat{\mathbb{A}}^{(m-i+1)}_{\text{MHV}}(\cancel{1^+})\right]$. Putting all these together, we reach a recursion relation of adding particles for the case of having a NMHV subamplitude on one side of BCFW diagram

$$\begin{aligned}\overline{\mathbb{A}}^{(m)}_{\text{NMHV}} &= \{1^-,(m-1)^+,\overline{\mathbb{A}}^{(m-1)}_{\text{NMHV}}(1^-)\}\\ &+ \sum_{i=2}^{m-2}\{1^-,i^+,\mathcal{R}^{i-1}\left[\widehat{\mathbb{A}}^{(m-i+1)}_{\text{MHV}}(\cancel{1^+})\right],\overline{A}^{(i)}_{\text{MHV}}(\cancel{1^-})\}. \end{aligned}\tag{4.3.13}$$

With the results from MHV case, it is straightforward to solve this recursion relation and find the general way of adding particles for this case which is given as

$$\begin{aligned}\overline{\mathbb{A}}^{(m)}_{\text{NMHV}} &= \sum_{i=4}^{m-1}\sum_{j=2}^{i-2}\{1^-,(m-1)^+,\cdots,i^+,j^+,(j+1)^-,(j+2)^+,\cdots,(i-1)^+\}\\ &\quad+\sum_{i=2}^{m-2}\{1^-,i^+,(i+1)^-,(i+2)^+,\cdots,(m-1)^+,2^+,\cdots,(i-1)^+\}\\ &= \sum_{i=4}^{m}\sum_{j=2}^{i-2}\{1^-,(m-1)^+,\cdots,i^+,j^+,(j+1)^-,R^+\}, \end{aligned}\tag{4.3.14}$$

where we use R^+ to denote rest of the particles, namely particles except $\{1,(m-1),\cdots,i,j,(j+1)\}$, and they are all positive. There is no need to specify the ordering of these particles in R^+, since the ordering of adding the same helicity particles is not important.

Similarly we can motivate the recursion relations for the other kind of BCFW shift $\langle 1\; n]$, namely the parity flipped version of the previous case, and we will denote it as $\widehat{\mathbb{A}}^{(m)}_{\text{NMHV}}$, see Fig.(4.5). The BCFW diagrams relevant to this $(m+1)$-point NMHV amplitudes are given in Fig.(4.5.b) and Fig.(4.5.c).

Again because of the knowledge of MHV amplitudes, the second case, Fig.(4.5.c),

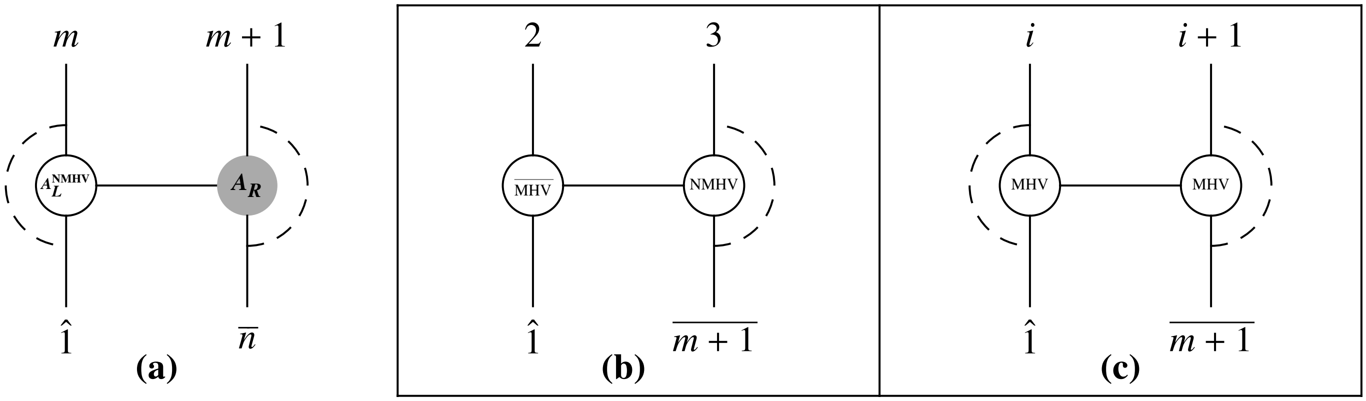

Figure 4.5: **(a):** For the $\langle 1\ n]$ shift we add particles $\{1, \ldots, m-1\}$ on the left side of the first diagram to build up $A_L^{\text{NMHV}}(\widehat{1}, \ldots, m, \overline{P})$ while A_R on the right can be of any type. **(b, c):** These the corresponding BCFW contributions to the $(m+1)$ point subamplitude A_L^{NMHV} from **(a)**.

leads to the following way of adding particles

$$\{1^+, i^-, \mathcal{R}^{i-1}\left[\overline{\mathbb{A}}_{\text{MHV}}^{(m-i+1)}(\cancel{1^-})\right], \widehat{\mathbb{A}}_{\text{MHV}}^{(i)}(\cancel{1^+})\}, \tag{4.3.15}$$

or $\{1^+, i^-, (i+1)^+, (i+2)^+, \cdots, (m-1)^+, 2^-, 3^+, \cdots, (i-1)^+\}$.

As for the contribution from the first diagram, Fig.(4.5.b), let us look at some examples first. For the lowest case, when $m = 5$, from the 5-point NMHV amplitude appeared on the right-hand-side of Fig.(4.5.b), we can easily determine that the last particle added should be 4^-. After this one is fixed, we are left with a $m = 4$ MHV situation, which should have $\{1^+, 2^-, 3^+\}$, so we finally get

$$\{1^+, 2^-, 3^+, 4^-\}, \tag{4.3.16}$$

and we note that the above formula can be nicely rewritten in a suggestive way as,

$$\{1^+, 2^-, \mathcal{R}\left[\overline{\mathbb{A}}^{(4)}_{\text{NMHV}}(\cancel{1^-})\right]\}. \tag{4.3.17}$$

Explicit calculations on higher-point cases show that this pattern preserves. So the result for this case is actually determined by $\overline{\mathbb{A}}^{(m-1)}_{\text{NMHV}}$, and the way of adding particles can be simply summarized as

$$\{1^+, 2^-, \mathcal{R}\left[\overline{\mathbb{A}}^{(m-1)}_{\text{NMHV}}(\cancel{1^-})\right]\}. \tag{4.3.18}$$

This allows us to write a recursion relation of adding particles for this case, which is given as

$$\begin{aligned}\widehat{\mathbb{A}}^{(m)}_{\text{NMHV}} &= \{1^+, 2^-, \mathcal{R}\left[\overline{\mathbb{A}}^{(m-1)}_{\text{NMHV}}(\cancel{1^-})\right]\} \\ &+ \sum_{i=3}^{m-1}\{1^+, i^-, \mathcal{R}^{i-1}\left[\overline{\mathbb{A}}^{(m-i+1)}_{\text{MHV}}(\cancel{1^-})\right], \widehat{\mathbb{A}}^{(i)}_{\text{MHV}}(\cancel{1^+})\}. \end{aligned} \tag{4.3.19}$$

It is also not difficult to solve the recursion relation, and we find the general way of adding particles for this case,

$$\begin{aligned}\widehat{\mathbb{A}}^{(m)}_{\text{NMHV}} &= \sum_{i=3}^{m-1}\{1^+, i^-, (i+1)^+, \cdots, (m-1)^+, 2^-, R_1^+\} \\ &+ \sum_{i=4}^{m-1}\sum_{j=3}^{i-1}\{1^+, 2^-, (m-1)^+, \cdots, (i+1)^+, j^+, (j+1)^-, R_2^+\} \end{aligned} \tag{4.3.20}$$

where R_i^+ is again used to denote particles left over in the corresponding curly brackets.

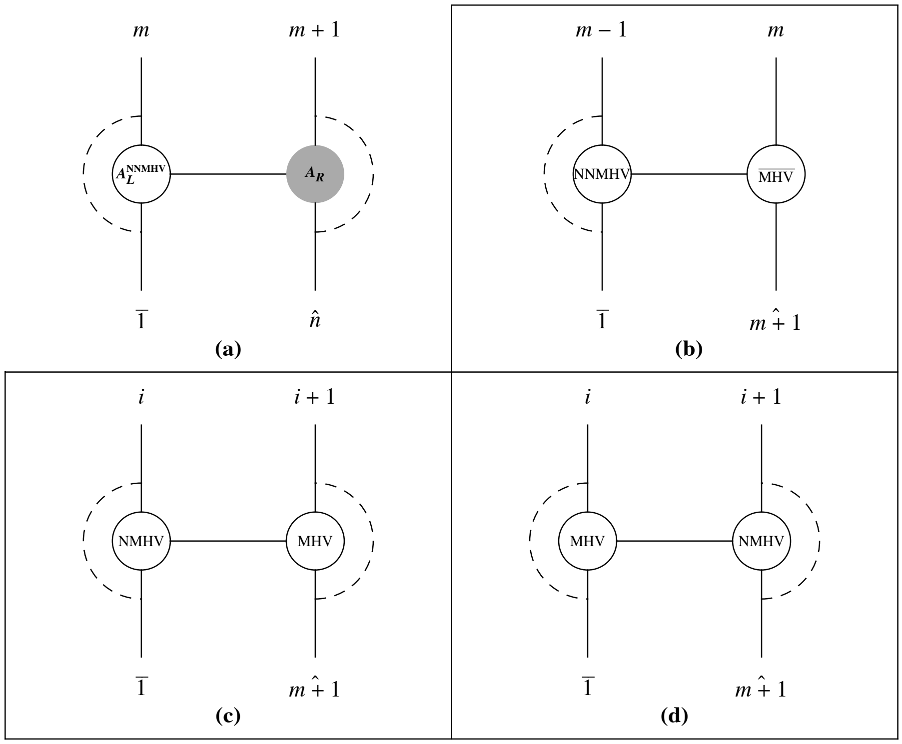

Figure 4.6: **(a):** For the $[1\ n\rangle$ shift we add particles $\{1,\dots,m-1\}$ on the left side of the first diagram to make it $A_L^{\text{NNMHV}}(\overline{1},\dots,m,\widehat{P})$ while the subamplitude A_R on the right can be of any type.
(b, c, d): In these three diagrams inside the box we consider the three different BCFW contributions that are possible for the $(m+1)$ point subamplitude A_L^{NNMHV} from **(a)**.

4.3.3 NNMHV

In this section we will study the case when we have a NNMHV subamplitude on one side of BCFW diagrams, as one more example before generalizing the recursion relations for a general N^{k}MHV case. To understand the ISL for this case, we need to study the corresponding NNMHV amplitude, which are given in the box of Fig.(4.6). We will use the knowledge from previous discussion to determine which particles should be added at certain last steps, consequently it motivates us to obtain the full recursion relations. Let us now study different contributions separately.

For the first BCFW diagram in the box Fig.(4.6.b), namely

$$A_{\rm NNMHV}(\overline{1},2,\cdots,(m-1),\widehat{P})\frac{1}{P^2}A_{\overline{\rm MHV}}(-\widehat{P},m,\widehat{m+1}), \tag{4.3.21}$$

the same as NMHV case, it is quite straightforward to convince oneself that the particles should be added for this case is given as,

$$\{1^-,(m-1)^+,\overline{\mathbb{A}}^{(m-1)}_{\rm NNMHV}(\cancel{1^-})\}. \tag{4.3.22}$$

It is also not difficult to determine how the particles should be added for the second diagram Fig.(4.6.c), which is given as

$$\{1^-,i^+,\mathcal{R}^{i-1}\left[\widehat{\mathbb{A}}^{(m-i+1)}_{\rm MHV}(\cancel{1^+})\right],\overline{\mathbb{A}}^{(i)}_{\rm NMHV}(\cancel{1^-})\}, \tag{4.3.23}$$

where the subamplitude, $A_{\rm NMHV}(\overline{1},\cdots,\widehat{P})$ in this BCFW diagram, contributes $\overline{\mathbb{A}}^{(i)}_{\rm NMHV}(\cancel{1^-})$. As in the case of Eq. (4.3.12) and (4.3.13), the contribution from $A_{\rm MHV}(-\widehat{P},\cdots,\widehat{m+1})$ can be combined with $(i+1)^-$, and finally leads to $\mathcal{R}^{i-1}\left[\widehat{\mathbb{A}}^{(m-i+1)}_{\rm MHV}(\cancel{1^+})\right]$ in the above equation.

Finally let us consider the contribution of the last diagram in the box Fig.(4.6.d). Let us study this case by starting from the simplest case when $m=5$, on the right-hand-side of this BCFW diagram, we have $A_{\rm NMHV}(-\widehat{P},3,4,5,\widehat{6})$. From $\widehat{\mathbb{A}}^{(4)}_{\rm NMHV}$, we understand that this amplitude can be constructed by adding particles $\{6^+,5^-,4^-\}$, which means that the last step of ISL is to add 4^-, as a consequence, if there is a ISL for this BCFW diagram, the particles added before 4^- should be $\{1^-,2^+,3^-\}$. In conclusion for this simplest case we find that the way of adding particles is given as,

$$\{1^-, 2^+, 3^-, 4^-\}, \tag{4.3.24}$$

which can be also be written as

$$\{1^-, 2^+, \mathcal{R}\left[\widehat{\mathbb{A}}^{(4)}_{\rm NMHV}(\not{1}^{+})\right], \overline{\mathbb{A}}^{(2)}_{\rm MHV}(\not{1}^{-})\}, \tag{4.3.25}$$

where $\overline{\mathbb{A}}^{(2)}_{\rm MHV}(\not{1}^{-})$ is of course just empty.

Similar analysis and explicit calculations of higher-point cases show that this pattern, Eq. (4.3.25), can be extended as a general result. As the above formula indicates, for the general case, the contribution from Fig.(4.6.d) leads to the following way of adding particles,

$$\{1^-, i^+, \mathcal{R}^{i-1}\left[\widehat{\mathbb{A}}^{(m-i+1)}_{\rm NMHV}(\not{1}^{+})\right], \overline{\mathbb{A}}^{(i)}_{\rm MHV}(\not{1}^{-})\}. \tag{4.3.26}$$

So gathering all the informtion so far we arrive at a nice recursion relation for this case, which is given as

$$\begin{aligned}\overline{\mathbb{A}}^{(m)}_{\rm NNMHV} &= \{1^-, (m-1)^+, \overline{\mathbb{A}}^{(m-1)}_{\rm NNMHV}(\not{1}^{-})\} \\ &+ \sum_{i=4}^{m-2}\{1^-, i^+, \mathcal{R}^{i-1}\left[\widehat{\mathbb{A}}^{(m-i+1)}_{\rm MHV}(\not{1}^{+})\right], \overline{\mathbb{A}}^{(i)}_{\rm NMHV}(\not{1}^{-})\} \\ &+ \sum_{i=2}^{m-3}\{1^-, i^+, \mathcal{R}^{i-1}\left[\widehat{\mathbb{A}}^{(m-i+1)}_{\rm NMHV}(\not{1}^{+})\right], \overline{\mathbb{A}}^{(i)}_{\rm MHV}(\not{1}^{-})\}.\end{aligned} \tag{4.3.27}$$

Now let us concentrate on the parity inversion of above case, namely the $\langle 1\ n]$ shift, see Fig.(4.7). It is straightforward to determine the last two type BCFW diagrams,

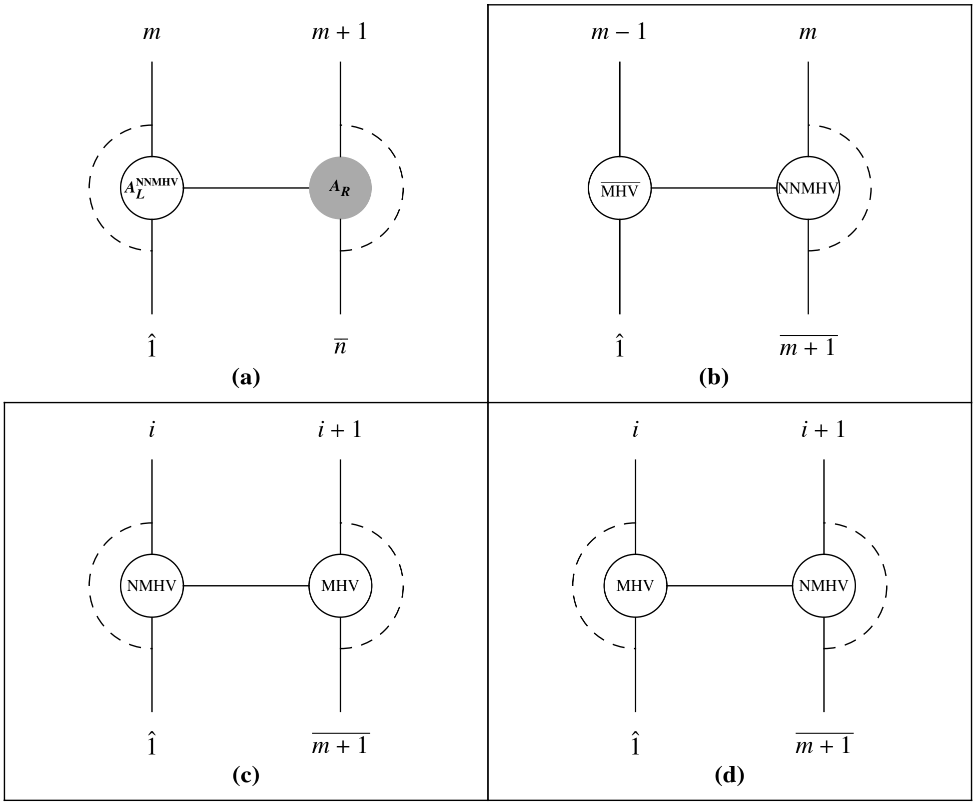

Figure 4.7: **(a):**For the $[1\ n\rangle$ shift we add particles $\{1,\ldots,m-1\}$ on the left side of the first diagram to make it$A_L^{\text{NNMHV}}(\overline{1},\ldots,m,\widehat{P})$ while the subamplitude on the right can be of any type A_R.
(b,c,d): In these three diagrams inside the box we consider the three different BCFW contributions that are possible for the $(m+1)$ point subamplitude A_L^{NNMHV}, from (a)

Fig.(4.7.c) and Fig.(4.7.d), in the box of Fig.(4.7) by the same analysis as the case of $[1\ n\rangle$ shift. The ways of adding particles determined by these two BCFW diagrams are given as the following sum,

$$\begin{aligned} &\sum_{i=4}^{m-1}\{1^+,i^-,\mathcal{R}^{i-1}\left[\overline{\mathbb{A}}_{\text{MHV}}^{(m-i+1)}(\cancel{1})\right],\widehat{\mathbb{A}}_{\text{NMHV}}^{(i)}(\cancel{1})\} \\ +\ &\sum_{i=3}^{m-3}\{1^+,i^-,\mathcal{R}^{i-1}\left[\overline{\mathbb{A}}_{\text{NMHV}}^{(m-i+1)}(\cancel{1})\right],\widehat{\mathbb{A}}_{\text{MHV}}^{(i)}(\cancel{1})\}. \end{aligned} \tag{4.3.28}$$

While for the contribution from Fig.(4.7.b), after examining lots of non-trivial examples, we again observe, as in the case of NMHV amplitudes, that it is determined by lower-point $\overline{\mathbb{A}}^{(m-1)}_{\text{NNMHV}}$ with an action of $\mathcal{R}$, namely

$$\{1^+, 2^-, \mathcal{R}\left[\overline{\mathbb{A}}^{(m-1)}_{\text{NNMHV}}(\cancel{1})\right]\}. \tag{4.3.29}$$

In summary that the final recursion relation of adding particles for this case is given as

$$\begin{aligned}
\widehat{\mathbb{A}}^{(m)}_{\text{NNMHV}} &= \{1^+, 2^-, \mathcal{R}\left[\overline{\mathbb{A}}^{(m-1)}_{\text{NNMHV}}(\cancel{1})\right]\} \qquad (4.3.30)\\
&+ \sum_{i=4}^{m-1}\{1^+, i^-, \mathcal{R}^{i-1}\left[\overline{\mathbb{A}}^{(m-i+1)}_{\text{MHV}}(\cancel{1})\right], \widehat{\mathbb{A}}^{(i)}_{\text{NMHV}}(\cancel{1})\}\\
&+ \sum_{i=3}^{m-3}\{1^+, i^-, \mathcal{R}^{i-1}\left[\overline{\mathbb{A}}^{(m-i+1)}_{\text{NMHV}}(\cancel{1})\right], \widehat{\mathbb{A}}^{(i)}_{\text{MHV}}(\cancel{1})\}.
\end{aligned}$$

4.3.4 N^{k}MHV

In this section we will generalize the above recursion relations for the previously studied special cases to any kind of BCFW diagram of $\mathcal{N} = 4$ super amplitudes. In this case we want to determine how to add particles when we have a BCFW diagram with $A_{\text{N}^k\text{MHV}}(\overline{1}, 2, \cdots, \widehat{P})$ (and $A_{\text{N}^k\text{MHV}}(\widehat{1}, 2, \cdots, \widehat{P})$ for $\langle 1\ n]$ shift) on one side of the BCFW diagram.

The way to determine the ISL for this case, namely the $[1\ n\rangle$ shift, is to analyse the corresponding N^{k}MHV amplitude, which is given by Fig.(4.8.a). By considering $A_{\text{N}^{l-1}\text{MHV}}(\overline{1}, 2, \cdots, i, \widehat{P})$ and $A_{\text{N}^{k-l}\text{MHV}}(-\widehat{P}, (i+1), \cdots, m, \widehat{m+1})$ separately and carrying out a similar analysis as the simpler cases of previous sections, it is not difficult

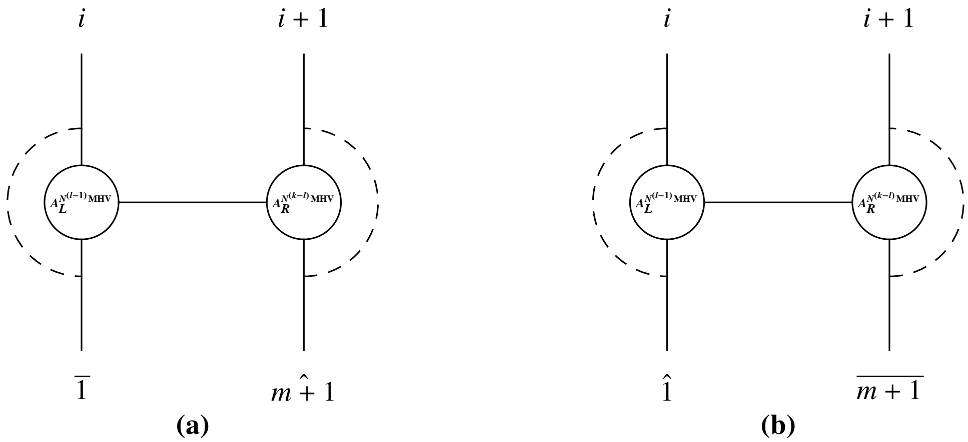

Figure 4.8: **(a):** Contribution to a $(m+1)$point N^kMHV amplitude for $[1\ m+1\rangle$ shift. **(b):**Contribution to a $(m+1)$point N^kMHV amplitude for $\langle 1\ m+1]$ shift.

to find that the way of adding particles for this typical BCFW diagram is given as,

$$\{1^-, i^+, \mathcal{R}^{i-1}\left[\widehat{\mathbb{A}}^{(m-i+1)}_{\mathrm{N}^{l-1}\mathrm{MHV}}(\cancel{1^+})\right], \overline{\mathbb{A}}^{(i)}_{\mathrm{N}^{k-l}\mathrm{MHV}}(\cancel{1^-})\}, \tag{4.3.31}$$

which is a nice generalization of the special simpler examples we considered earlier. The final recursion relation is also straightforward to write down, which is given as

$$\begin{aligned}
\overline{\mathbb{A}}^{(m)}_{\mathrm{N}^k\mathrm{MHV}} &= \{1^-, (m-1)^+, \overline{\mathbb{A}}^{(m-1)}_{\mathrm{N}^k\mathrm{MHV}}(\cancel{1^-})\} \\
&+ \sum_{l=1}^{k} \sum_{\substack{i=l+2 \\ (2\,\mathrm{for}\,l=1)}}^{m-k+l-2} \{1^-, i^+, \mathcal{R}^{i-1}\left[\widehat{\mathbb{A}}^{(m-i+1)}_{\mathrm{N}^{k-l}\mathrm{MHV}}(\cancel{1^+})\right], \overline{\mathbb{A}}^{(i)}_{\mathrm{N}^{l-1}\mathrm{MHV}}(\cancel{1^-})\}.
\end{aligned} \tag{4.3.32}$$

Similarly for the case of $\langle 1\ n]$ shift, Fig.(4.8.b), the recursion relation is given as,

$$\begin{aligned}
\widehat{\mathbb{A}}^{(m)}_{\mathrm{N}^k\mathrm{MHV}} &= \{1^+, 2^-, \mathcal{R}\left[\overline{\mathbb{A}}^{(m-1)}_{\mathrm{N}^k\mathrm{MHV}}(\cancel{1^-})\right]\} \\
&+ \sum_{l=1}^{k} \sum_{i=l+2}^{\substack{(m-k+l-1\,\mathrm{for}\,l=k) \\ m-k+l-2}} \{1^+, i^-, \mathcal{R}^{i-1}\left[\overline{\mathbb{A}}^{(m-i+1)}_{\mathrm{N}^{k-l}\mathrm{MHV}}(\cancel{1^-})\right], \widehat{\mathbb{A}}^{(i)}_{\mathrm{N}^{l-1}\mathrm{MHV}}(\cancel{1^+})\}.
\end{aligned} \tag{4.3.33}$$

We would like to make a few comments on the above general recursion relations before we move on. We note that, as in the case of simpler examples of NMHV and NNMHV cases, the recursion relations are in fact coupled, namely $\overline{\mathbb{A}}^{(m)}$ and $\widehat{\mathbb{A}}^{(m)}$ are determined recursively by each other. This fact is of course very natural since each BCFW diagram is made up of two subamplitudes (in left and right), which can be constructed by $\overline{\mathbb{A}}^{(m)}$ and $\widehat{\mathbb{A}}^{(m)}$ separately. Although the pattern is quite intriguing, we were not able to prove this general recursion relation. However lots of non-trivial examples have been checked and we find that the amplitudes constructed from our recursion relations agree with those obtained by BCFW. In Appendix.B we present one such non-trivial examples and even more complicated cases had been worked out and matched with the BCFW results numerically. Further it is easy to convince oneself that $[1\ n\rangle$ shift and $\langle 1\ n]$ shift should be related to each other by parity conjugation even though our recursion relations do not have manifest parity symmetry. This is indeed true and we find that

$$\overline{\mathbb{A}}^{(m)}_{\mathrm{N}^k\mathrm{MHV}} = \mathcal{P}\Big[\widehat{\mathbb{A}}^{(m)}_{\mathrm{N}^{m-k-3}\mathrm{MHV}}\Big], \tag{4.3.34}$$

where $\mathcal{P}$ denotes the parity conjugation, namely it flips the signs of the particles $i^+ \leftrightarrow i^-$. This fact serves as a strong consistency check on our recursion relations.

4.3.5 Amplitudes from ISL

We would like to conclude this section by summarising the prescription for constructing any BCFW diagram in $\mathcal{N} = 4$ SYM, for instance let us consider a typical BCFW term given as

$$A_L(\overline{1},2,\cdots,i,\widehat{P})\frac{1}{P^2}A_R(-\widehat{P},i{+}1,\cdots,\widehat{n}). \tag{4.3.35}$$

One can start with a three-point amplitude $A_{\overline{\text{MHV}}}(i,i{+}1,n)$. By construction the first particle to be added is 1^-, which is added between i and n.[6] We then keep adding particles between 1 and i according to the recursion relations of $\overline{\mathbb{A}}^{(i)}$ to fill $A_L(\overline{1},2,\cdots,i,\widehat{P})$ in the BCFW diagram, and separately $A_R(-\widehat{P},i{+}1,\cdots,\widehat{n})$ can be filled by adding particles between $(i{+}1)$ and n by applying the recursion relation of $\widehat{\mathbb{A}}^{(n-i)}$ with the simple replacement of $k\to n-k+1$ for the elements in $\widehat{\mathbb{A}}^{(n-i)}$.

So in this way, any tree-level super amplitude in $\mathcal{N}=4$ SYM theory can be schematically written in an ISL form,

$$A_n=\sum_{i;L,R}(\prod_L \mathcal{S}'_L)(\prod_R \mathcal{S}'_R)A_{\overline{\text{MHV}}}(i',i{+}1,n'), \tag{4.3.36}$$

where summation over i is according to BCFW diagrammatic representation of the amplitudes, while products on $\mathcal{S}_L$ and $\mathcal{S}_R$ and summation on L,R are determined by the recursion relation (4.3.32) and (4.3.33), finally $\mathcal{S}'$, i' and n' are used for the fact that the particles are shifted according to the rules of ISL. Here we like to stress that it is fairly easy to write down the actual amplitudes according to Eq. (4.3.36). In particular in the language of momentum-twistor, according to Eq. (C.1.1) adding a positive particle is fairly straightforward, in fact it does not change the form of the lower-point amplitude at all. For adding a negative particle we just need to multiply the lower-point amplitude with a R-invariant by Eq. (C.1.2), with some proper shifts

[6]Or we could start with $A_{\text{MHV}}(1,i,i{+}1)$, and the first particle to be added now is n^+, between $(i{+}1)$ and 1.

on the corresponding particles, in Appendix B a non-trivial example is presented as we had also mentioned earlier.

4.4 BCFW shifts from ISL

From the previous sections we have seen that we can construct any BCFW diagram by adding particles according to ISL, where the canonical configuration for adding the required particles is given by the proposed recursion relations in (4.3.32) and (4.3.33). Now let us stress the fact that once we have determined the canonical configuration to build a given BCFW diagram of our interest we use (5.1.1) and (4.2.8) for shifting momenta and fermionic coordinates at every step of adding a particle. For instance let us go back to the example we considered in section 2, i.e. (4.2.17) and we recall here that

$$A(\bar{1}2345|6,\cdots,\widehat{n}) = \Big[\mathcal{S}_{+}(345)\mathcal{S}_{+}(23'5')\mathcal{S}_{+}(12'5'')\mathcal{S}_{-}(n1'5''')\Big]A_{R}(5'''',\cdots,n'). \tag{4.4.1}$$

If the BCFW and ISL form of $A(\bar{1},2,3,4,5|6,\cdots,\widehat{n})$ have to match, as we had claimed, then the following equality between the BCFW and ISL quantities need to be satisfied, namely,

$$\widehat{P} = 5'''', \qquad \widehat{n} = n', \quad \text{and} \qquad \bar{1} = 1'. \tag{4.4.2}$$

Using (5.1.1) and (4.2.8), it can be easily shown that for this particular example the above equality holds. So here we see the very important fact that for adding particle from one side of a BCFW diagram, say for example here the left, the ISL shifts only affect those particles in the right subamplitude A_R which are adjacent to the A_L. In this case they are 5 and n. So the ISL configuration obtained for one side is blind to any configuration of particles on the other side and we will see this feature also being true for more general BCFW diagram. For those cases too, a similar equality between the BCFW and ISL expressions holds, as we will prove shortly. Let us first state the form of this equivalence. Let us consider the case where we can construct a BCFW diagram by ISL given in the following form,

$$A_L(\overline{1}, 2, \cdots, i, \widehat{P})\frac{1}{P^2}A_R(-\widehat{P}, (i{+}1), \cdots, \widehat{n}) = \sum(\prod \mathcal{S}')A_R(i_s, (i{+}1), \cdots, (n{-}1), n_s),$$

where the summation and products are determined by the proposed recursion relations, and here we use the subscript s to denote the final shifted momenta obtained from ISL. The soft-factors are of course shifted too, which we denote as $\mathcal{S}'$. The conclusion is that the following equalities between the ISL and BCFW shifted quantities hold,

$$i_s = \widehat{P}, \quad 1_s = \overline{1}, \quad n_s = \widehat{n}, \tag{4.4.3}$$

where the equality implies that both the bosonic momenta as well as the corresponding fermionic coordinate η's satisfy the equality.

To be more precise, let us consider the shift of type $[1\ n\rangle$, the result for the other kind of shift $\langle 1\ n]$ can be obtained by parity conjugate. For this case, we first add

1^- to $A_R(i, i{+}1, \cdots, n)$ and particles i and n are shifted as follows

$$
\begin{aligned}
i &\rightarrow i+\frac{[1n]}{[in]}\lambda_1\tilde{\lambda}_i=(1+i)+\frac{s_{1i}}{\langle 1|i|n]}\lambda_1\tilde{\lambda}_n, \\
n &\rightarrow n+\frac{s_{1i}}{\langle 1|i|n]}\lambda_1\tilde{\lambda}_n,
\end{aligned} \tag{4.4.4}
$$

where $s_{ij} \equiv (p_i + p_j)^2$ is the Mandelstam variable. From the recursion relation, (4.3.32) and (4.3.33), we observe that whenever a negative particle, j^-, is added to a lower-point amplitude there is always a positive particle, i^+ already in front of it, being added at an earlier stage. When we say i is in front of j it is in the sense that these particles are cyclically ordered and hence $i < j$. This implies that λ_1 in above equation will not be shifted, since it can only be shifted by a negative particle, which is added next to 1. The above conclusion precisely agrees with BCFW shifts for $[1\ n\rangle$ case, where only $\tilde{\lambda}_1$ and λ_n are shifted.

By the construction ISL preserves momentum conservation, so it is straightforward to see that Eq. (4.4.4) will lead to the following equation when we finish adding all the particles,

$$
\begin{aligned}
i_s &= (1+2+\cdots+i)+\frac{s_{12\cdots i}}{\langle 1|2+\cdots+i|n]}\lambda_1\tilde{\lambda}_n=\widehat{P}, \\
n_s &= n+\frac{s_{12\cdots i}}{\langle 1|2+\cdots+i|n]}\lambda_1\tilde{\lambda}_n=\widehat{n},
\end{aligned} \tag{4.4.5}
$$

and we note that these are of course just the BCFW shifts for $\widehat{P}$ and $\widehat{n}$.

As for the fermionic coordinates, both η_i and η_n do not get shifted due to addition of the particle 1^-, and η_n will never be shifted by further addition of particles. So we see that there is no shift on η_n, which agrees also with the BCFW scenario.

To determine the remaining shifted particles we can simply use the conservation laws, since the action of ISL keeps momenta and supercharge conserved. So by momentum conservation we get

$$1_s = -\left(2+3+\cdots+(i-1)\right)+i_s = 1+\frac{s_{12\cdots i}}{\langle 1|2+\cdots+i|n]}\lambda_1\tilde{\lambda}_n. \tag{4.4.6}$$

The ISL shifts on η_{i_s} can be similarly obtained by applying supercharge conservation,

$$\lambda_{1s}\eta_{1_s}+\lambda_2\eta_2+\cdots+\lambda_{ns}\eta_n = \lambda_1\eta_1+\lambda_2\eta_2+\cdots+\lambda_n\eta_n \tag{4.4.7}$$

which gives us,

$$\eta_{1_s} = \eta_1 - \frac{\langle \widehat{n}n\rangle}{\langle 1n\rangle}\eta_n = \eta_1 - \frac{s_{12\cdots i}}{\langle 1|2+\cdots+i|n]}\eta_n. \tag{4.4.8}$$

Both (4.4.6) and (4.4.8) agree with the results from BCFW shift of $[1\ n\rangle$.

We now summarize the conclusion from the above discussion. Here we observed that when we add the particles from one side (say A_L) of the BCFW diagram it affects only those two particles from the other side (say A_R) which are adjacent to this subdiagram (A_L). Moreover the effect of the successive ISL shifts on these two adjacent particles are exactly equivalent to the appropriate BCFW shifts, which ensures that the amplitudes constructed by ISL agree with BCFW recursion relation. Furthermore, no other knowledge about the other side of the BCFW diagram is needed, which would turn out to be very important for the application of our discussion to form factors in the the following section.

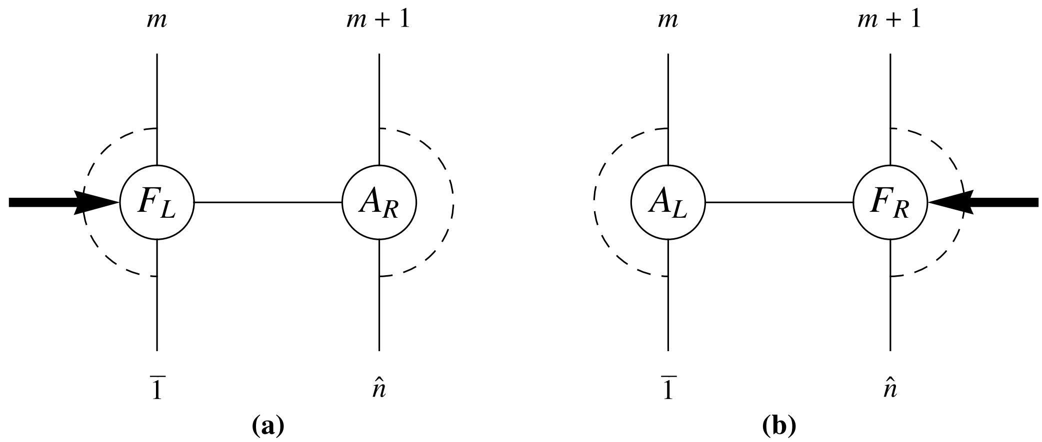

Figure 4.9: **(a,b):** The two possible BCFW diagrams for the $[1\ n\rangle$ shift where F is the form factor and A is the amplitude.

4.5 Constructing form factors

In this section, we will study another interesting object in $\mathcal{N} = 4$ SYM, the form factors. We would like to apply the ISL we have developed for the amplitude to form factor as well. The object has been extensively studied in various aspects [149, 150, 151, 152, 153, 154]. Before going to the discussion of ISL for form factor, let us give a lightning review on form factors. We will closely follow the reference [151].[7]

The form factors are the matrix elements of a gauge-invariant, composite operator between the vacuum and some external scattering states,

$$F(q; 1, 2, \cdots, n) = \langle 1, 2, \cdots, n|\mathcal{O}(q)|0\rangle, \tag{4.5.1}$$

where $\langle 1, 2, \cdots, n|$ are the external states, $|0\rangle$ is the vacuum, and $\mathcal{O}(q)$ is a gauge

[7]For more details on form factors please see previously mentioned references.

invariant operator carrying momentum q; by momenta conservation we have the sum of the momenta of external particles $\sum_{i=1}^{n} p_i = q$, and q is not null, namely $q^2 \neq 0$. In $\mathcal{N} = 4$ SYM, one can consider supersymmetric form factors by supersymmetrizing the external states as well as the operator. Here we can consider the full stress-tensor $\mathcal{T}(x, \theta^+, \theta^-)$ or we also allow considering the chiral part of the stress-tensor $\mathcal{T}(x, \theta^+) = \mathcal{T}(x, \theta^+, \theta^- = 0)$,[8] which we will do here. After Fourier transformation, the supersymmetrized form factor can be written as

$$F(q, \gamma^+; 1, 2, \cdots, n) = \langle 1, 2, \cdots, n | \mathcal{T}(q, \gamma^+) | 0 \rangle, \tag{4.5.2}$$

where γ^+ is corresponding to the Fourier transformation of the fermionic valuable θ_+. One can compute this object by various methods, including the well-known MHV rules and BCFW recursion relation. The supersymmetric BCFW recursion relations for form factor is simply given as

$$\begin{aligned} F(q, \gamma^+; 1, 2, \cdots, n) &= \sum_i \Big[\int d^4\eta F(q, \gamma^+; \bar{1}, 2, \cdots, m, \widehat{P}) A(-\widehat{P}, (m{+}1), \cdots, \widehat{n}) \\ &+ \int d^4\eta A(\bar{1}, 2, \cdots, m, \widehat{P}) F(q, \gamma^+; -\widehat{P}, (m{+}1), \cdots, \widehat{n}) \Big], \end{aligned} \tag{4.5.3}$$

with the same usual supersymmetric BCFW shifts, see (4.2.1) and (4.2.2). The BCFW diagram is given in Fig.(4.9).

For the case of MHV, it is straightforward to find the solution that form factor for

[8] We have used harmonic superspace, and the form of $\mathcal{T}$ is not that important for our discussion, for the expression of $\mathcal{T}$ and details on harmonic superspace see for instance [155, 156]

this simple case is given as,

$$F_{\rm MHV}(q,\gamma^+;1,2,\cdots,n)=\frac{\delta^4(\sum_{i=1}^n\lambda_i\tilde\lambda_i-q)\delta^4(\sum_{i=1}^n\lambda_i\eta_i^-)\delta^4(\sum_{i=1}^n\lambda_i\eta_i^+-\gamma^+)}{\langle 12\rangle\langle 23\rangle\cdots\langle n1\rangle}\tag{4.5.4}$$

As one can note that except the conservation delta-functions, the above formula is exactly the same as the famous Parke-Taylor formula for the scattering amplitudes. And indeed form factors resemble many properties of amplitudes, in particular one important property which is relevant to our discussion is that form factors have exactly the same soft limit by taking external on-shell particles to be soft as the amplitudes do.[9]

We observe that one side of the BCFW recursion of form factors is always given by an amplitude as shown in Eq. (4.5.3). As we discussed in previous section that if we add particles from one-side of a BCFW diagram, it is immaterial what is the type of object on the other side of the BCFW diagram, so it is quite clear that form factors can also be fully constructed by ISL. The idea of ISL we described in previous sections for the scattering amplitudes can apply to form factors directly without any essential modification. The way of adding particles for form factors is precisely the same as in the case of scattering amplitudes, except that now we need to add particles from both sides of BCFW diagrams, which is not a problem at all because we have derived recursion relations for adding particles with two type of BCFW shifts, namely $\bar{1}$ and $\hat{1}$. So for adding particles from left-hand-side of BCFW diagrams of the form factor, it is exactly the same as the amplitudes. But now we also have to add particles from the other side with the following simple replacement rule, $i\to n+1-i$. From the above discussion, we find that schematically the BCFW

[9] One can also take the operator $\mathcal{O}$ to be soft, see the discussion in [152, 151]

recursion relation of form factors, Eq. (4.5.3) can be written in a ISL form,

$$\begin{aligned} F(q,\gamma^+;1,2,\cdots,n) &= \sum_{m;L,R}\Big[(\prod_R \mathcal{S}'_R)F(q,\gamma^+;1',2,\cdots,m,(m{+}1)') \\ &+ (\prod_L \mathcal{S}'_L)F(q,\gamma^+;m',(m+1),\cdots,n{-}1,n')\Big]. \end{aligned} \tag{4.5.5}$$

Let us consider a simple example to illustrate the above formula (4.5.5). As case of amplitudes, we consider maximally non-MHV (MNMHV) form factor, which was considered in [157, 151]. It is a form factor with the self-dual field strength $\mathrm{Tr}(F_{\mathrm{SD}}^2)$ and all negative helicity gluons states,

$$F_{\mathrm{MNMHV}}(q;1,\cdots,n) = \langle 1\cdots n|\mathrm{Tr}(F_{\mathrm{SD}}^2)|0\rangle|_{\mathrm{MNMHV}}, \tag{4.5.6}$$

and the result of this special form factor is given as

$$F_{\mathrm{MNMHV}}(q;1,\cdots,n) = \delta^4(\sum_{i=1}^n \lambda_i\tilde\lambda_i - q)\frac{q^4}{[12]\cdots[n1]}\eta_1^4\cdots\eta_n^4. \tag{4.5.7}$$

There is only a two-particle channel BCFW diagram for this case, so it is easy to see that it can be written as an ISL form,

$$F_{\mathrm{MNMHV}}(q;1,2,\cdots,n) = \mathcal{S}_-(n\ 1\ 2)F_{\mathrm{MNMHV}}(q;2',3,\cdots,n'). \tag{4.5.8}$$

It is easy to check that the formula (4.5.6) indeed satisfies the above recursion relation, Eq. (4.5.8). Alternatively one can start with a two-point MNMHV (it is just MHV for this special case) form factor and then keep adding negative particles to arrive at (4.5.6).

4.6 Conclusion

In this paper we had shown that any tree-level superamplitudes as well as supersymmetric form factors in $\mathcal{N} = 4$ SYM can be constructed by ISL. With guidance from BCFW recursion relations and detailed study of nontrivial examples, we are able to obtain a set of recursion relations, which give us the configuration for adding particles in order to construct any BCFW diagram in $\mathcal{N} = 4$ SYM. Consequently, these recursion relations allow us to generate any tree-level superamplitudes and form factors by ISL method. It is a fascinating insight that for $\mathcal{N} = 4$ SYM theory, the restrictions imposed due to soft limit is sufficient to determine the full scattering amplitudes, at least at tree-level. We note that scattering amplitudes constructed by ISL make both Yangian symmetry and soft-limit manifest. The application of ISL method to form factors indicates that there may also exist hidden symmetry in form factors, given that similarity has been noticed between form factors and the scattering amplitudes in $\mathcal{N} = 4$ SYM.

So convincingly the ISL method provides a new way of uncovering the deep mathematical structure of scattering amplitudes in $\mathcal{N} = 4$ SYM. The idea of ISL has been a extremely useful tool for constructing Grassmannian formalism for $\mathcal{N} = 4$ SYM, while in this paper we provide another intriguing use of it. And the picture we developed, of adding particles to lower-point amplitudes for generating higher-point amplitudes, seems to be intrinsically geometrical, which may be closely related to the Polytopes picture for the scattering amplitudes [106]. Moreover, as we had shown in the paper, ISL method may also be relevant as another useful tool for carrying out efficient computations in $\mathcal{N} = 4$ SYM theory, both for the scattering amplitudes and form factors.

It would be of great interest to extend this idea for the scattering amplitudes to other theories and also beyond tree-level and leading singularities. Some interesting attempt has been made for $\mathcal{N} = 8$ super gravity, where most of the progress so far had been for the simplest MHV case. The authors of [146] were able to write the fist non-MHV amplitude, six-point NMHV gravity amplitude in a ISL form, however the form seems quite complicated to be amenable for further generalization to higher-point cases. One important difficulty for applying ISL method to gravity amplitudes is that there is no color-ordering. One naive guess would be to apply the ISL to the ordered subamplitudes, where the BCFW recursion relations for ordered subamplitudes have the same structure as those of Yang-Mills amplitudes [158], but we leave these interesting questions to be addressed in future.

Chapter 5

Gravity Tree amplitudes using Bonus Relations

5.1 Introduction

In this thesis so far we have been discussing anout the structure of amplitudes in $\mathcal{N} = 4$ super Yang–Mills theory (SYM), which has remarkable simplicities obscured by the usual local formulation and Feynman-diagram calculations. On the other hand, Arkani-Hamed *et al.* have proposed the idea that $\mathcal{N} = 8$ supergravity (SUGRA) may be the quantum field theory with the simplest amplitudes [14], and there is strong evidence for it: recently there have been intensive studies on both the hidden symmetries (e.g. $E_{7(7)}$ symmetry, see [159, 160, 161, 162]), and the ultraviolet behavior of the theory (see [163, 164, 165, 166, 167, 35, 168, 169, 170] and references therein).

However, we do not need to go beyond the tree level to see the simplicity. As shown in [14], gravity tree amplitudes satisfy non-trivial relations, or "bonus relations", which are absent in SYM color-ordered amplitudes. These bonus relations have been applied to MHV amplitudes in [171] to show the equivalence of various MHV formulae in the literature [172, 173, 174, 175, 176], especially to simplify formulae with $(n-2)!$ permutations to those with $(n-3)!$ permutations. The full strength of these relations, however, can only be demonstrated when applied to general, non-MHV amplitudes, and the purpose of the present note is to use bonus relations to simplify explicit formulae of SUGRA tree amplitudes, which are obtained by solving BCFW recursion relations. Before proceeding, let us elaborate on BCFW recursion relations and bonus relations of SUGRA amplitudes.

Supersymmetric BCFW recursion relations [56, 55] hold in both SYM and SUGRA because their amplitudes vanish when two supermomenta are taken to infinity in a complex superdirection [55, 14]. More specifically, under the supersymmetric BCFW shifts of momenta and $SU(\mathcal{N})$ Grassmannian variables,

$$\begin{aligned} \lambda_{\widehat{1}}(z) &= \lambda_1 + z\lambda_n, \\ \widetilde{\lambda}_{\overline{n}}(z) &= \widetilde{\lambda}_n - z\widetilde{\lambda}_1, \\ \eta_{\widehat{n}}(z) &= \eta_n - z\eta_1, \end{aligned} \tag{5.1.1}$$

SYM and SUGRA amplitudes have at least $1/z$ falloff at large z, thus the contour integral $\oint \frac{dz}{z} M(z)$ can be rewritten as a sum over residues without boundary contributions,

$$M_n = \sum_{L,R} \int d^{4\mathcal{N}}\eta M_L(\widehat{1}, L, \{-\widehat{P}(z_P), \eta\}) \frac{1}{P^2} M_R(\{\widehat{P}(z_P), \eta\}, R, \overline{n}), \tag{5.1.2}$$

where the poles $z = z_P$ are determined by putting the internal momenta $\widehat{P}(z_P) = \sum_{i\in L} P_i + P_{\widehat{1}}$ on shell. By solving the recursion relations, explicit formulae for up to N^3MHV amplitudes, and an algorithm to calculate all tree amplitudes in SUGRA was proposed in [158]. The result can be written as a summation over $(n-2)!$ "ordered gravity subamplitudes" with different permutations of particles $2, \ldots, n-1$. In contrast to SYM color-ordered amplitudes, the SUGRA amplitudes actually have a faster, $1/z^2$, falloff and the contour integral $\oint dz M(z)$ gives the bonus relations,

$$0 = \sum_{L,R} \int d^8\eta M_L(\widehat{1}, L, \{-\widehat{P}(z_P), \eta\}) \frac{z_P}{P^2} M_R(\{\widehat{P}(z_P), \eta\}, R, \overline{n}). \tag{5.1.3}$$

Similar to the MHV case [171], we shall see that these relations can further simplify the explicit formulae for non-MHV amplitudes by reducing the $(n-2)!$-permutation sum to a new $(n-3)!$-permutation one.

Another important method that has been widely used to calculate gravity tree amplitudes are Kawai-Lewellen-Tye (KLT) relations, first derived in string theory [39] which express (super)gravity tree amplitudes as sums of products of two copies of (super)Yang–Mills amplitudes in the field-theory limit. Recently KLT relations have been proved in gravity [177, 178] and in SUGRA [179] using BCFW recursion relations, without resorting to string theory. While the well-known KLT relations have a form of $(n-3)!$ permutations [180] (see also [178]), in the proof it is natural to use the newly proposed $(n-2)!$ form suitable for BCFW recursion relations [177], and a direct link between these two forms has been derived in [181]. In a related approach, the so-called square relations between gravity and Yang-Mills amplitudes, which can be viewed as a reformulation of KLT relations, have been proposed and proved in [33]. These relations also possess a freedom of going from $(n-2)!$-permutation form to the simpler $(n-3)!$ form, which, similar to the freedom in KLT relations, reflects the Bern-Carrasco-Johansson (BCJ) relations between Yang-Mills amplitudes [33]. For SUGRA amplitudes, the advantage of having solved BCFW relations to some extent will enable us to go beyond this implicit freedom following from BCJ relations, and show the simplification of gravity amplitudes directly in their explicit forms.

This chapter is organized as following. In section 5.2 we briefly review tree amplitudes in SUGRA and their bonus relations, especially the simplification of MHV amplitudes when using these relations. Then we apply these relations to some examples beyond MHV amplitudes, including the NMHV and N^{2}MHV amplitudes, and prove these simplified formulae in section 5.3. The generalization to all tree-level SUGRA amplitudes are presented in section 5.4.

5.2 A brief review of tree amplitudes in SUGRA and bonus relations

5.2.1 Tree Amplitudes in SUGRA from BCFW Recursion Relations

By solving Eq. (5.1.2), all color-ordered SYM tree amplitudes have been obtained and can be written schematically as [148],

$$A_n(1,...,n) = A^{\mathrm{MHV}}(1,\ldots,n)\sum_\alpha R_\alpha(1,\ldots,n), \tag{5.2.1}$$

where

$$A^{\mathrm{MHV}}(1,\ldots,n) = \frac{\delta^8(\sum_i \lambda_i \eta_i)}{\langle 12\rangle\langle 23\rangle\cdots\langle n1\rangle} \tag{5.2.2}$$

is the MHV superamplitudes, and R_α are the so-called dual superconformal invariants, which, for N^{k}MHV amplitudes, are products of k basic invariants of the form,

$$R_{n;a_1b_1;a_2b_2;\ldots;a_rb_r;ab} = \frac{\langle a a-1\rangle\langle b b-1\rangle\ \delta^{(4)}(\langle\xi|x_{b_ra}x_{ab}|\theta_{bb_r}\rangle + \langle\xi|x_{b_rb}x_{ba}|\theta_{ab_r}\rangle)}{x_{ab}^2\langle\xi|x_{b_ra}x_{ab}|b\rangle\langle\xi|x_{b_ra}x_{ab}|b-1\rangle\langle\xi|x_{b_rb}x_{ba}|a\rangle\langle\xi|x_{b_rb}x_{ba}|a-1\rangle}\,, \tag{5.2.3}$$

where the chiral spinor ξ is given by

$$\langle\xi| = \langle n|x_{na_1}x_{a_1b_1}x_{b_1a_2}x_{a_2b_2}\ldots x_{a_rb_r}\,, \tag{5.2.4}$$

and dual (super)coordinates are defined as

$$x_{ij} = p_i + p_{i+1} + \cdots + p_{j-1}\,,$$
$$\theta_{ij} = \lambda_i \eta_i + \cdots + \lambda_{j-1}\eta_{j-1}\,. \tag{5.2.5}$$

There is only one invariant $R = 1$ for MHV case, while we have a sum of $R_{n;a_1b_1}$ with $1 < a_1 < b_1 < n$ for NMHV case. Furthermore, for N^{2}MHV case we have $R_{n;a_1b_1}R^{b_1a_1}_{n;a_1b_1,a_2b_2}$ with $1 < a_1 < a_2 < b_2 \le b_1 < n$ and $R_{n;a_1b_1}R^{a_1b_1}_{n;a_2b_2}$ with $1 < a_1 < b_1 \le a_2 < b_2 < n$, where superscripts denote boundary modifications of these invariants [148].

Generally the summation variables α, and boundary modifications, can be represented by a rooted tree diagram [148, 158] (see Fig. 5.2.1(a) and Fig. 5.2.1(b)). For N^{k}MHV amplitudes, there are $C_k = \frac{(2k)!}{k!(k+1)!}$ (Catalan number) types of terms labeled by α's corresponding to a path from the root to the k-th level in Fig. 5.2.1(a), and each type can be written as a list of k pairs of labels with a particular order between them, $\alpha \equiv \{n; a_1, b_1; \ldots ; a_k, b_k\}$. Not only does the summation over α include all types of terms, but it also sums over all possible $1 < a_i, b_i < n$ in the corresponding order.

In [158], solving Eq. (5.1.2) for SUGRA is simplified by using ordered gravity subamplitude $M(1, \ldots , n)$, which satisfy the ordered BCFW recursion relations similar to Yang-Mills theory,

$$M(1,\ldots,n) \equiv \sum_{i=3}^{n-1} \int \frac{d^8\eta}{P^2} M(\widehat{1}, 2, \ldots , i-1, \widehat{P}) M(-\widehat{P}, i, \ldots , n-1, \overline{n})\,, \tag{5.2.6}$$

and the sum of $(n-2)!$ permutations of ordered gravity subamplitudes gives the full

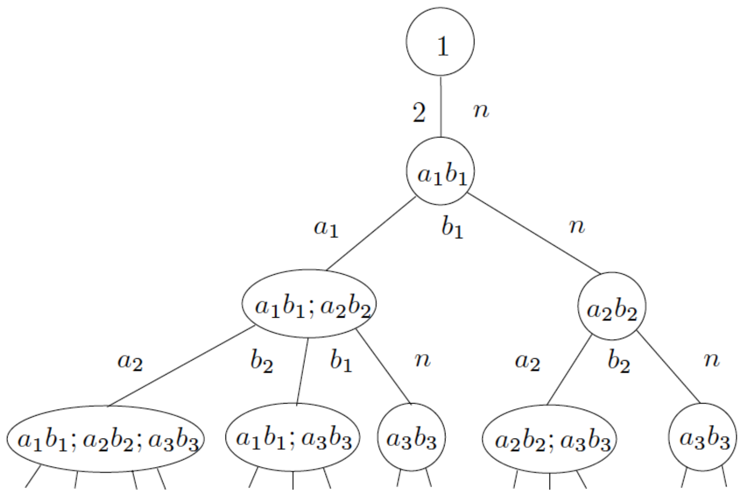

(a) A rooted tree diagram for tree-level SYM amplitudes. The figure is the same as the tree diagram presented in [158].

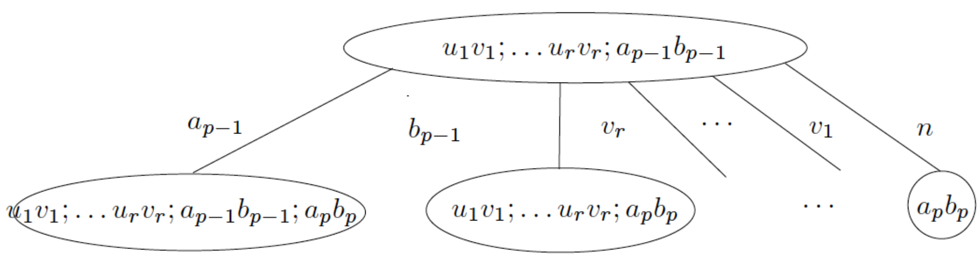

(b) The rule for going from line $p-1$ to line p (for $p > 1$) in Fig. 5.2.1. For every vertex in line $p-1$ of the form given at the top of the diagram, there are $r+2$ vertices in the lower line (line p). The labels in these vertices start with $u_1v_1; \dots u_rv_r; a_{p-1}b_{p-1}; a_pb_p$ and they get sequentially shorter, with each step to the right removing the pair of labels adjacent to the last pair a_p, b_p until only the last pair is left. The summation limits between each line are also derived from the labels of the vertex above. The left superscripts which appear on the associated R-invariants start with $u_1v_1 \dots u_rv_rb_{p-1}a_{p-1}$ for the left-most vertex. The next vertex to the right has the superscript $u_1v_1 \dots u_rv_ra_{p-1}b_{p-1}$, i.e. the same as the first but with the final pair in alphabetical order. The next vertex has the superscript $u_1v_1 \dots u_rv_r$ and thereafter the pairs are sequentially deleted from the right.

Figure 5.1: Rooted tree diagram for tree-level SYM amplitudes

amplitude,

$$\mathcal{M}_n = \sum_{\mathcal{P}(2,3,\ldots,n-1)} M(1,\ldots,n). \tag{5.2.7}$$

A solution for $M(1,\ldots,n)$ is obtained in [158],

$$M(1,...,n) = [A^{\rm MHV}(1,\ldots,n)]^2 \sum_\alpha G_\alpha R_\alpha^2(1,\ldots,n), \tag{5.2.8}$$

where the invariants R_α are exactly the same as those in SYM (including boundary modifications), namely products of basic invariants (5.2.3), with the same set of summation variables α as given in Fig. 5.2.1(a) and Fig. 5.2.1(b), and the 'dressing factors', G_α, are independent of the Grassmannian variables η_i, and they break dual conformal invariance of the SYM solution. These factors have been calculated explicitly for up to N^{3}MHV amplitudes, for example MHV case,

$$G^{\rm MHV}(1,\ldots,n) = x_{13}^2 \prod_{s=2}^{n-3} \frac{\langle s|x_{s,s+2}x_{s+2,n}|n\rangle}{\langle sn\rangle}\,, \tag{5.2.9}$$

and there is an algorithm to calculate them in general cases, but we do not need their expressions in this note. In addition, tree-level amplitudes of n-graviton scattering can be obtained from SUGRA superamplitudes (5.2.7), by choosing fermionic coordinates $\eta = 0$ for positive-helicity gravitons, and integrating over $d^8\eta$ for negative-helicity ones. Details of the solution can be found in [158].

Therefore, SUGRA tree amplitude can be written as a summation of $(n-2)!$ ordered gravity subamplitudes, and each of them has a structure similar to SYM ordered amplitude. In the following we shall use bonus relations to reduce this form to a simpler, $(n-3)!$ form, and first we recall the simplest MHV case.

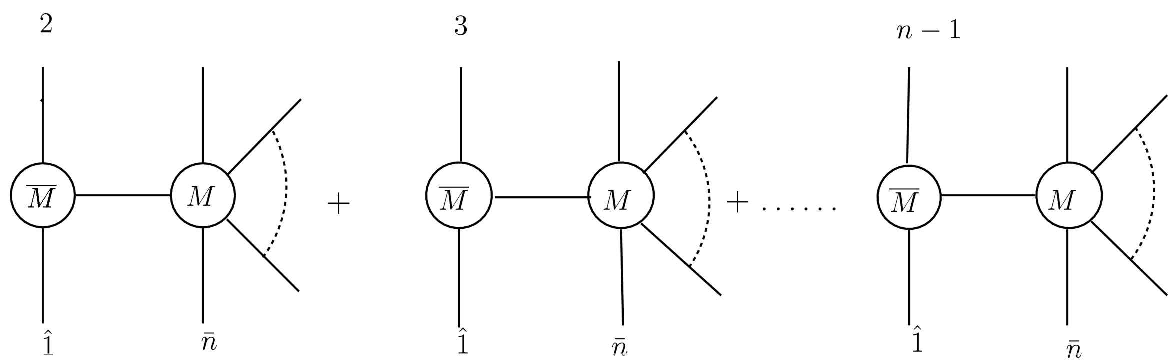

Figure 5.2: All factorizations contributing to (5.2.11) for the MHV amplitude.

5.2.2 Applying Bonus Relations to MHV Amplitudes

Applying bonus relation to MHV SUGRA tree-level amplitudes was well understood in [171]. From Eq. (5.2.9), we have the MHV amplitudes as a summation of $(n-2)!$ terms,

$$\mathcal{M}_n^{\text{MHV}} = G^{\text{MHV}}(1,\ldots n)[A^{\text{MHV}}(1,\ldots,n)]^2 + \mathcal{P}(2,3,\ldots,n-1). \tag{5.2.10}$$

From Fig. 5.2, we see that there are $(n-2)$ BCFW factorizations and thus the formula can be expressed as,

$$\mathcal{M}_n^{\text{MHV}} = M_2 + M_3 + \ldots + M_{n-1}, \tag{5.2.11}$$

where each M_i is a BCFW term from $\overline{\text{MHV}}(\widehat{1}, i, \widehat{P}(z_i)) \times \text{MHV}_{\text{n}-1}$ with $z_i = -\frac{\langle 1i\rangle}{\langle ni\rangle}$. Now since the amplitude has $1/z^2$ fall off, we have a bonus relation which is simple in the MHV case,

$$0 = z_2 M_2 + z_3 M_3 + \ldots + z_{n-1} M_{n-1}. \tag{5.2.12}$$

Using this relation, we can express the last diagram M_{n-1} in terms of the other $n-3$ diagrams, and a simple manipulation gives us a $(n-3)!$-term formula,

$$\begin{aligned}\mathcal{M}_n^{\text{MHV}} &= B^{\text{MHV}} G^{\text{MHV}}(1,2,\ldots,n)[A^{\text{MHV}}(1,2,\ldots,n)]^2 \\ &\quad + \mathcal{P}(2,3,\ldots,n-2).\end{aligned} \tag{5.2.13}$$

where we have defined the MHV bonus coefficient $B^{\text{MHV}} = \frac{\langle 1\ n\rangle\langle n-1\ n-2\rangle}{\langle 1\ n-1\rangle\langle n\ n-2\rangle}$. Beyond MHV, we have many more types of BCFW diagrams with complicated structures and the application of bonus relations becomes trickier. In the next section, we shall work out the NMHV and N^{2}MHV cases, and then move on to general amplitudes in section 4.

5.3 Applying Bonus Relations to Non-MHV Gravity Tree Amplitudes

5.3.1 General Strategy

Before moving on to examples, we first explain the general strategy for applying bonus relations to non-MHV gravity tree amplitudes. For a N^{k}MHV amplitude, inhomogeneous contributions of the form N^{p}MHV $\times$ N^{q}MHV are needed ($p+q+1 = k$)[1]. Naively one would like to use "bonus-simplified"[2] lower-point amplitudes for

[1]We follow the notations of reference [148] to call the contributions from diagrams of type Fig. 5.3(a) or Fig. 5.3(b) as inhomogeneous contributions, while those from Fig. 5.3(c) as homogeneous ones.

[2]Here "bonus-simplified" means that these lower-point amplitudes used in the BCFW diagrams are simplified by using bonus relations.

both M_L and M_R in Eq. (5.1.2), but this is not compatible with the fact that we can only delete one diagram (not two) by applying the bonus relations (5.1.3), if we want to preserve the structure of ordered BCFW recursion relations.

To keep the advantages of the ordered BCFW recursion relations, which are crucial to solve for all tree-level amplitudes, instead we shall apply bonus relations selectively. The idea is illustrated in Fig. 5.3. Similar to the MHV case, we shall delete Fig. 5.3(d) by using bonus relations (5.1.3). To compute the inhomogeneous parts of the amplitudes, we shall use the bonus-simplified amplitude only on one side of a BCFW diagram, namely the lower-point amplitude with the leg $(n-1)$ in it, as indicated in Fig. 5.3(a) and Fig. 5.3(b). In this way, the amplitude splits into two types, one type coming from the diagrams of the form as in Fig. 5.3(d), which has the leg $(n-1)$ adjacent to the leg n and will be called the normal, or type I contributions, and the other one coming from those having the form as in Fig. 5.3(b), which has the leg $(n-1)$ exchanged with another leg (b_1-1), and will be called the exchanged, or type II contributions,

$$\mathcal{M}_n = \left[A_n^{\text{MHV}}\right]^2 \Big(\sum_\alpha B_\alpha^{(1,m_1)} G_\alpha R_\alpha^2 + \sum_\beta B_\beta^{(2,m_2)} [G_\beta R_\beta^2 (b_1 - 1 \leftrightarrow n-1)] \Big) + \mathcal{P}(2,3,\ldots,n-2), \tag{5.3.1}$$

where $(b_1-1 \leftrightarrow n-1)$ denotes the exchanges of momenta $(p_{b_1-1} \leftrightarrow p_{n-1})$ as well as the fermionic coordinates $(\eta_{b_1-1} \leftrightarrow \eta_{n-1})$, and we have used square bracket to indicate that the exchanges act only on the expression inside the bracket. The superscript (i, m_i) in $B_\alpha^{(i,m_i)}$ is used to show the type of this contribution, which will become clear in the examples.

Thus we have seen that, by using bonus relations, any amplitude can be written as a

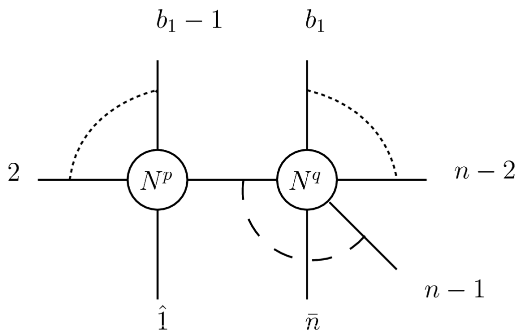

(a) Inhomogeneous diagram type I

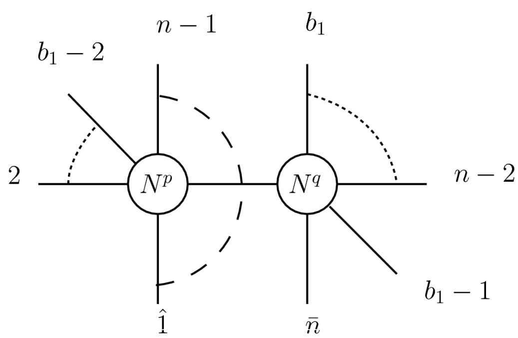

(b) Inhomogeneous diagram type II

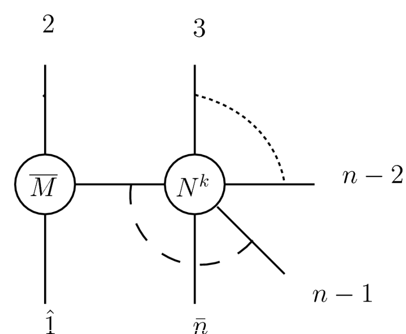

(c) Homogeneous diagram

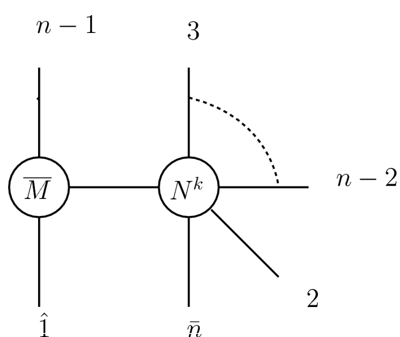

(d) Diagram deleted by bonus relations

Figure 5.3: Different types of diagrams for a general N^{k}MHV amplitude, where $k = p + q + 1$. We use a dashed line $- - --$ connecting three legs to denote a bonus-simplified lower-point amplitude, in which these three legs are kept fixed. For lower-point amplitudes without dashed lines, we use the usual $(n-2)!$ form.

summation of $(n-3)!$ permutations with the coefficients $B_{\alpha}^{(i,m_i)}$, which will be called bonus coefficients. In this section, we shall calculate all bonus coefficients for NMHV and N^2MHV cases, and generalize the pattern observed in these examples to general N^kMHV amplitudes in the next section. Once bonus coefficients are calculated, we obtain explicitly all simplified SUGRA tree amplitudes.

5.3.2 NMHV Amplitudes

Here we use bonus relations to simplify the $(n-2)!$ form of NMHV amplitudes. First we state the general simplified form of NMHV amplitudes, and then prove it by induction. To be concise, we abbreviate the combinations

$$\{n; a_1 b_1\} \equiv G_{n;a_1b_1}\Big[R_{n;a_1b_1} A^{\mathrm{MHV}}(1,2,\ldots,n)\Big]^2 \tag{5.3.2}$$

and similar notations will be used in the following sections.

As mentioned above generally, we delete the contributions corresponding to Fig. 5.3(d) by using the bonus relation (5.1.3). It is straightforward to compute the inhomogeneous contributions from the two MHV $\times$ MHV diagrams, Fig. 5.4(a) and Fig. 5.4(b). Firstly, let us consider the contribution from Fig. 5.4(a), which corresponds to terms with $a_1 = 2$, and we have

$$M_1 = B^{(1)}_{n;2b_1}\{n; 2b_1\}, \quad \text{with} \;\; 4 \leq b_1 \leq n-1, \tag{5.3.3}$$

where $B^{(1)}_{n;2b_1}$ are the special cases of the general bonus coefficients $B^{(1)}_{n;a_1b_1}$. We have used the superscript (1) to indicate that this is the contribution coming from type-I

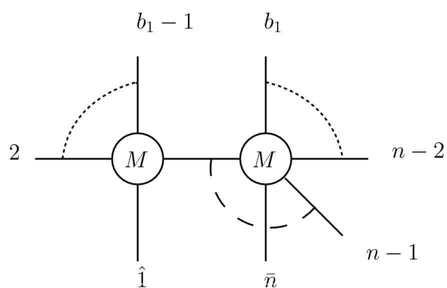

(a) Inhomogeneous diagram type I

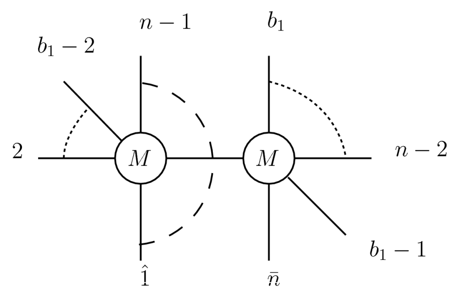

(b) Inhomogeneous diagram type II

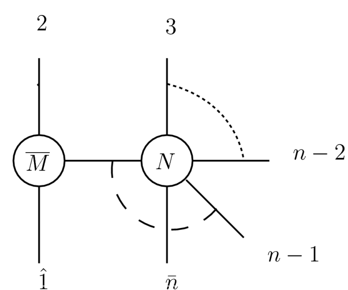

(c) Homogeneous diagram

Figure 5.4: Diagrams for NMHV amplitudes.

diagram, and similar notations will be used below.

When $b_1 \neq n-1$, the bonus coefficients are given by,

$$B^{(1)}_{n;a_1b_1} = B^{\rm MHV}\frac{\langle n-1|x_{b_1a_1}x_{b_1n}|n\rangle}{\langle n-1|x_{b_1a_1}x_{a_1n}|n\rangle}. \tag{5.3.4}$$

Here we note that we can get the above coefficients from the previous ones, namely the bonus coefficients of MHV amplitude, multiplied by the factor $\frac{\langle n-1|x_{b_1a_1}x_{b_1n}|n\rangle}{\langle n-1|x_{b_1a_1}x_{a_1n}|n\rangle}$. It is a general feature of this type of coefficients for N^{k}MHV case, which are given by N^{k-1}MHV coefficients multiplied by the same factor, as we will see explicitly again in the N^{2}MHV case.

However when $b_1 = n-1$, no bonus relation can be used for the right-hand-side 3-point MHV amplitude in Fig. 5.4(a), and we find

$$B^{(1)}_{n;a_1n-1} = \frac{\langle 1\ n\rangle}{\langle 1\ n-1\rangle}\frac{\langle n-1|x_{n-1a_1}|n-1]}{\langle n|x_{na_1}|n-1]}. \tag{5.3.5}$$

For the exchanged diagrams, Fig. 5.4(b), the contribution can be similarly written as

$$M_2 = B^{(2)}_{n;2b_1}[\{n;2a_1\}(b_1-1\leftrightarrow n-1)], \quad \text{with} \ \ 4\leq b_1 \leq n-1, \tag{5.3.6}$$

where the bonus coefficients $B^{(2)}_{n;a_1b_1}$ are given by

$$B^{(2)}_{n;a_1b_1} = \frac{\langle 1\ n\rangle}{\langle 1\ n-1\rangle}\frac{\langle n-1\ b_1-2\rangle(x'_{a_1b_1})^2}{\langle n|x_{na_1}x'_{a_1b_1}|b_1-2\rangle}, \tag{5.3.7}$$

and we have defined $x'_{a_ib_i}$ as,

$$\begin{aligned} x'_{a_ib_i} &\equiv x_{a_ib_i-1} + x_{n-1n} \\ &= x_{a_ib_i}(p_{b_i-1} \leftrightarrow p_{n-1}). \end{aligned} \tag{5.3.8}$$

All the above calculations do not include the boundary case $a_1 = n-3, b_1 = n-1$, which needs special treatment. This boundary case is special because it recursively reduces to the special 5-point NMHV ($\overline{\text{MHV}}$) amplitude. It does not have the diagram with the type of $\overline{\text{MHV}}_3\times$ NMHV, and one has to treat it separately. We apply the bonus relations to this case in the following way: we use Eq. (5.1.3) to delete the contribution from Fig. 5.5(a), and compute Fig. 5.5(b), and we find

$$\mathcal{M}_5 = -\frac{[24][34][51]}{[23][45][41]}\Big[\{5;24\}(3\leftrightarrow 4)\Big] + \mathcal{P}(2,3). \tag{5.3.9}$$

By plugging the above 5-point result in Fig. 5.5(c), we get the boundary term of the 6-point NMHV amplitude

$$M_6^{(\text{boundary})} = \frac{\langle 16\rangle\langle 25\rangle[35][45]x_{36}^2}{\langle 15\rangle[34]\langle 2|1+6|5]\langle 6|1+2|5]}\Big[\{6;35\}(4\leftrightarrow 5)\Big]. \tag{5.3.10}$$

A generic form for the boundary term of the n-point NMHV amplitudes can be obtained as a straightforward generalization of (5.3.9) and (5.3.10),

$$M_n^{(\text{boundary})} = B^{(\text{boundary})}_{n;n-3\ n-1}\Big[\{n;n-3\ n-1\}(n-2\leftrightarrow n-1)\Big], \tag{5.3.11}$$

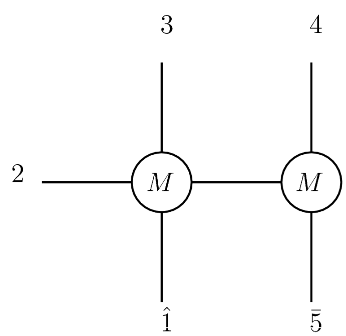

(a) 5-point diagram deleted by bonus relation

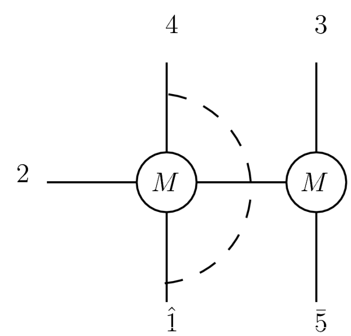

(b) 5-point diagram

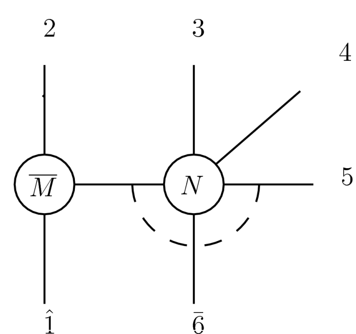

(c) 6-point diagram calculating the boundary contribution

Figure 5.5: Diagrams for 5-point NMHV amplitude and the boundary term of 6-point NMHV amplitude. Fig. 5.5(a) and Fig. 5.5(b) are used to calculate the bonus-simplified 5-point right-hand-side amplitude of Fig. 5.5(c).

where $B^{\text{(boundary)}}_{n;n-3\ n-1}$ is given by,

$$B^{\text{(boundary)}}_{n;n-3\ n-1} = \frac{\langle 1n\rangle\langle n-4\ n-1\rangle[n-3\ n-1][n-2\ n-1]x^2_{n-3n}}{\langle 1\ n-1\rangle[n-3\ n-2]\langle n-4|x_{n-3\ n-1}|n-1]\langle n|x_{n-1\ n-3}|n-1]}. \tag{5.3.12}$$

Putting everything together, we obtain the general formula for NMHV amplitude and as promised, the amplitude indeed can be written as a sum of $(n-3)!$ permutations

$$\begin{aligned}\mathcal{M}^{\text{NMHV}}_n \;&=\; \sum_{a_1=2}^{n-4}\sum_{b_1=a_1+2}^{n-1}\Big(B^{(1)}_{n;a_1b_1}\{n;a_1b_1\} + B^{(2)}_{n;a_1b_1}[\{n;a_1b_1\}(b_1-1\leftrightarrow n-1)]\Big) + M^{\text{(boundary)}}_n \\ &\quad +\mathcal{P}(2,3,\ldots,n-2).\end{aligned} \tag{5.3.13}$$

Proof by Induction

Here we shall give an inductive proof for the simplified NMHV formula. For $a_1 = 2$, as we explained above, the formula follows directly from Fig. 5.4(a) and Fig. 5.4(b). Therefore we shall focus on the cases when $a_1 \geq 3$, which correspond to the homogeneous contributions from Fig. 5.4(c). We shall prove that the formula satisfies the BCFW recursion relations.

First note that we have deleted one diagram of the form $\mathrm{MHV_L}(\widehat{1}, \mathrm{n}-1, \widehat{\mathrm{P}}) \times \mathrm{MHV_R}$ by using bonus relations, this results in a multiplicative prefactor for the overall amplitude, which is given by,

$$(1 - \frac{z_2}{z_{n-1}}) = \frac{\langle 1n\rangle\langle n-1\ 2\rangle}{\langle n2\rangle\langle 1n-1\rangle}. \tag{5.3.14}$$

Let us consider the bonus coefficient $B^{(1)}_{n;a_1b_1}$, other coefficients $B^{(2)}_{n;a_1b_1}$ and $B^{\text{(boundary)}}_{n;n-3\ n-1}$

can be treated similarly. By plugging formula (5.3.4) into the $(n-1)$-point amplitude $M(-\widehat{P}, 3, 4, \ldots, n-1, \overline{n})$ in Fig. 5.4(c), it is straightforward to check that the second piece of $B^{(1)}_{n;a_1b_1}$, $\frac{\langle n-1|x_{b_1a_1}x_{b_1n}|n\rangle}{\langle n-1|x_{b_1a_1}x_{a_1n}|n\rangle}$, is transformed back to itself under the recursion relations.

For the first piece $B^{\rm MHV} = \frac{\langle n-1\ n-2\rangle\langle 1\ n\rangle}{\langle n\ n-2\rangle\langle 1\ n-1\rangle}$ of $B^{(1)}_{n;a_1b_1}$, which is the MHV bonus coefficient, the proof is essentially the same as in the MHV case. Taking into account the factor in (5.3.14) coming from bonus relations, we have

$$\frac{\langle n-1\ n-2\rangle\langle \widehat{p}\ n\rangle}{\langle n\ n-2\rangle\langle \widehat{p}\ n-1\rangle} \times \frac{\langle 1\ n\rangle\langle n-1\ 2\rangle}{\langle 1\ n-1\rangle\langle n\ 2\rangle} = \frac{\langle n-1\ n-2\rangle\langle 1\ n\rangle}{\langle n\ n-2\rangle\langle 1\ n-1\rangle}. \tag{5.3.15}$$

Thus the contribution with $B^{(1)}_{n;a_1b_1}$ indeed satisfies the recursion relations.

Finally we should remark that we have used the fact that $\{n; a_1b_1\}$ by themselves satisfy the ordered BCFW recursion relations during the whole proof.

5.3.3 N^{2}MHV amplitudes

In this subsection we consider N^{2}MHV amplitudes as one more example to show the general features of bonus-simplified gravity amplitudes. Similar to NMHV case, let us denote the ordered gravity solutions in the following way

$$\begin{aligned} H^{(1)}_{n;a_1b_1,a_2b_2}\Big[R_{n;a_1b_1}R^{b_1a_1}_{n;a_1b_1,a_2b_2}A^{\rm MHV}(1,2,\ldots,n)\Big]^2 &\equiv \ \{n; a_1b_1, a_2b_2\}_1, \\ H^{(2)}_{n;a_1b_1,a_2b_2}\Big[R_{n;a_1b_1}R^{a_1b_1}_{n;a_2b_2}A^{\rm MHV}(1,2,\ldots,n)\Big]^2 &\equiv \ \{n; a_1b_1, a_2b_2\}_2. \end{aligned}$$

There are four relevant types of diagrams (and a boundary case) which contribute to the general N^{2}MHV amplitudes. The general structure of N^{2}MHV is given in

Fig. 5.6 and the corresponding contributions from each of the four diagrams can be calculated separately.

First we consider the contributions from the diagrams in Fig. 5.6(b), which are of the form MHV× NMHV. We use bonus-simplified amplitude for the right-hand-side NMHV amplitude and we obtain[3],

$$\begin{aligned} M_{\mathrm{I}} &= \sum_{2\le a_1,b_1\le n-1}\sum_{b_1\le a_2,b_2<n}\Big(B^{(1,1)}_{n;a_1b_1;a_2b_2}\{n;a_1b_1;a_2b_2\}_2 \\ &\quad + B^{(1,2)}_{n;a_1b_1;a_2b_2}[\{n;a_1b_1;a_2b_2\}_2(b_2-1\leftrightarrow n-1)]\Big) \\ &\quad + \sum_{2\le a_1,b_1\le n-1} B^{(1,\text{boundary})}_{n;a_1b_1;n-3n-1}[\{n;a_1b_1;n-3n-1\}_2(n-2\leftrightarrow n-1)], \end{aligned} \tag{5.3.16}$$

where in the first sum $a_2\le n-4$ because of the range of summation of the first term in Eq. (5.3.13). Here the bonus coefficients are given by

$$\begin{aligned} B^{(1,1)}_{n;a_1b_1;a_2b_2} &= \frac{\langle 1n\rangle\langle n-1\ n-2\rangle\langle n-1|x_{a_2b_2}x_{b_2n}|n\rangle}{\langle 1n-1\rangle\langle n\ n-2\rangle\langle n-1|x_{a_2b_2}x_{a_2n}|n\rangle}\frac{\langle n-1|x_{a_1b_1}x_{b_1n}|n\rangle}{\langle n-1|x_{a_1b_1}x_{a_1n}|n\rangle} \\ B^{(1,1)}_{n;a_1b_1;a_2b_2} &= \frac{\langle 1n\rangle\langle n-1|x_{n-1a_2}|n-1]}{\langle 1n-1\rangle\langle n|x_{na_2}|n-1]}\frac{\langle n-1|x_{a_1b_1}x_{b_1n}|n\rangle}{\langle n-1|x_{a_1b_1}x_{a_1n}|n\rangle}\quad (b_2=n-1) \\ B^{(1,2)}_{n;a_1b_1;a_2b_2} &= \frac{\langle 1n\rangle\langle n-1\ b_2-2\rangle(x'_{a_2b_2})^2}{\langle 1n-1\rangle\langle n|x_{na_2}x'_{a_2b_2}|b_2-2\rangle}\frac{\langle n-1|x_{a_1b_1}x_{b_1n}|n\rangle}{\langle n-1|x_{a_1b_1}x_{a_1n}|n\rangle} \\ B^{(1,\text{boundary})}_{n;a_1b_1;n-3n-1} &= B^{(\text{boundary})}_{n;n-3\ n-1}\frac{\langle n-1|x_{a_1b_1}x_{b_1n}|n\rangle}{\langle n-1|x_{a_1b_1}x_{a_1n}|n\rangle}, \end{aligned} \tag{5.3.17}$$

where the last term $B^{(1,\text{boundary})}_{n;a_1b_1;n-3n-1}$ comes from Eq. (5.3.12). Again the superscripts are used to show the types of the contributions. For instance, in the superscript $(1,1)$ of $B^{(1,1)}_{n;a_1b_1;a_2b_2}$, the first "1" means that it is the type-I contribution, while the second "1" implies that it is descendant from the NMHV case. A generalization to

[3]Here and in the following calculations we have included the corresponding homogeneous terms, for the case we consider the contributions are from Fig. 5.6(a)

the N^{k}MHV case will be $B^{(m)}_{n;a_1b_1;\ldots;a_kb_k}$, where m is a string composed of three kinds of labels, "1" "2" and "boundary".

As we have mentioned in the NMHV case, and we want to stress it here again that the bonus coefficients of Fig. 5.6(b) are simply given as the previous ones, namely the coefficients of NMHV amplitudes, with replacements $(a_1 \to a_2, b_1 \to b_2)$ and multiplied by the same factor $\frac{\langle n-1|x_{a_1b_1}x_{b_1n}|n\rangle}{\langle n-1|x_{a_1b_1}x_{a_1n}|n\rangle}$.

Next, we calculate the contributions from the diagrams in Fig. 5.6(c) which are of the form NMHV$\times$ MHV and we get

$$\begin{aligned} M_{\rm II} = &\sum_{2\leq a_1,b_1\leq n-1}\ \sum_{a_1\leq a_2,b_2<b_1} \Big(B^{(2,1)}_{n;a_1b_1;a_2b_2}\{n;a_1b_1;a_2b_2\}_1(n-1\leftrightarrow b_1-1) \\ &+ B^{(2,2)}_{n;a_1b_1;a_2b_2}[\{n;a_1b_1;a_2b_2\}_1(b_2-1\leftrightarrow b_1-1)]\Big) \\ &+ \sum_{2\leq a_1\leq n-3} B^{(2,\text{boundary})}_{n;a_1n-1;n-4n-2}[\{n;a_1n-1;n-3n-1\}_1(n-2\leftrightarrow n-1)]. \end{aligned} \tag{5.3.18}$$

In the above sum we do not include the boundary case $(a_1,b_1,a_2,b_2) = (n-4, n-1, n-4, n-2)$, which we shall study separately. The coefficients are given by

$$\begin{aligned} B^{(2,1)}_{n;a_1b_1;a_2b_2} &= \frac{\langle 1n\rangle\langle n-1\ b_1-2\rangle\langle n-1|x_{b_2a_2}x'_{b_2b_1}x'_{a_1b_1}x_{a_1n}|n\rangle(x'_{a_1b_1})^2}{\langle 1n-1\rangle\langle b_1-2|x'_{a_1b_1}x_{a_1n}|n\rangle\langle n-1|x_{b_2a_2}x'_{a_2b_1}x'_{a_1b_1}x_{a_1n}|n\rangle} \\ B^{(2,1)}_{n;a_1b_1;a_2b_2} &= \frac{\langle 1n\rangle\langle n-1|x_{n-1a_2}|n-1](x'_{a_1b_1})^2}{\langle 1n-1\rangle\langle n|x_{na_1}x'_{a_1b_1}x'_{b_1a_2}|n-1]} \quad (b_2=n-2) \\ B^{(2,2)}_{n;a_1b_1;a_2b_2} &= \frac{\langle 1n\rangle\langle n-1\ b_2-2\rangle(x'_{a_2b_2})^2(x'_{a_1b_1})^2}{\langle 1n-1\rangle\langle n|x_{na_1}x'_{a_1b_1}x'_{b_1a_2}x'_{a_2b_2}|b_2-2\rangle} \\ B^{(2,\text{boundary})}_{n;a_1b_1;n-4n-2} &= \frac{\langle 1n\rangle\langle b_1-4\ n-1\rangle[b_1-3\ n-1][b_1-2\ n-1](x'_{b_1-3b_1})^2(x'_{a_1b_1})^2}{\langle 1\ n-1\rangle[b_1-3\ b_1-2]\langle b_1-4|x_{b_1-4\ b_1-1}|n-1]\langle n|x_{na_1}x'_{a_1b_1}x_{b_1-1b_1-3}|n-1]}. \end{aligned} \tag{5.3.19}$$

By comparing the results with those of NMHV, now we are ready to see the patterns. For this type of diagrams Fig. 5.6(c), the bonus coefficients can be obtained from

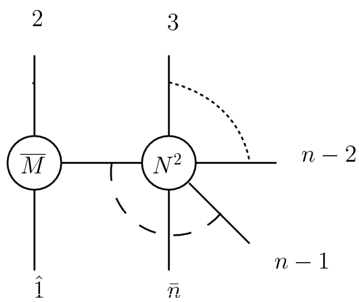

(a) Homogeneous diagram

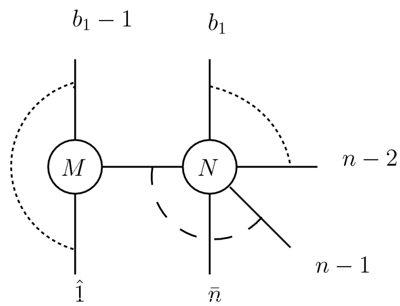

(b) Inhomogeneous diagram type I

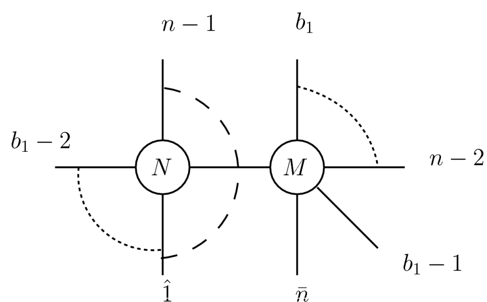

(c) Inhomogeneous diagram type II

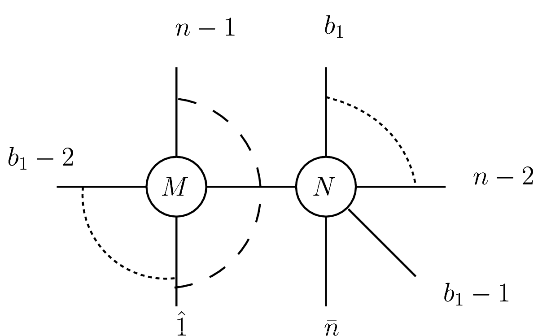

(d) Inhomogeneous diagram type II

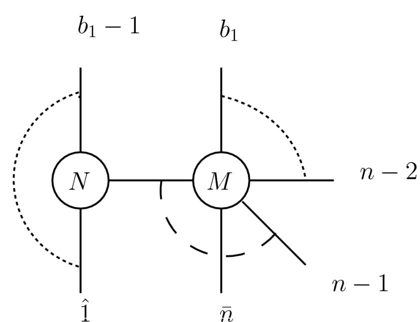

(e) Inhomogeneous diagram type I

Figure 5.6: Diagrams for N^2MHV amplitudes.

the results of NMHV by doing the following replacements on the indices of region momenta x's: $n \to b_1, a_1 \to a_2, b_1 \to b_2$, and $x \to x'$ when x has the index n with it. Furthermore one should apply the changes on $\langle n|$ as well as $\langle n-i|$, which read $\langle n| \to \langle n|x_{na_1}x'_{a_1b_1}$, and $\langle n-i|(\text{or } [n-i|) \to \langle b_1-i|(\text{or } [b_1-i|)$ for $i>1$. Finally we multiply the obtained answers by a factor $(x'_{a_1b_1})^2$.

The bonus coefficients of the contributions from other diagrams are actually the same as those of the NMHV case. For the sake of completeness, let us write down these contributions: for the contribution from Fig. 5.6(d), we have

$$M_{\text{III}} = \sum_{2\le a_1,b_1\le n-1}\sum_{b_1\le a_2,b_2<n} B^{(2)}_{n;a_1b_1;a_2b_2}[\{n;a_1b_1;a_2b_2\}_2(b_1-1\leftrightarrow n-1)], \tag{5.3.20}$$

where the bonus coefficients $B^{(2)}_{n;a_1b_1;a_2b_2}$ are given by Eq. (5.3.7); for the other contributions coming from Fig. 5.6(e), we get

$$M_{\text{IV}} = \sum_{2\le a_1,b_1\le n-1}\sum_{a_1\le a_2,b_2<b_1} B^{(1)}_{n;a_1b_1;a_2b_2}\{n;a_1b_1;a_2b_2\}_1, \tag{5.3.21}$$

and similarly the coefficients are given by Eq. (5.3.4) and Eq. (5.3.5).

Again as in the case of Eq. (5.3.18), this formula does not include the boundary case, $\{n;a_1b_1;a_2b_2\}_1 = \{n;n-4n-1;n-4n-2\}_1$, which should be considered separately, as we shall do below.

Similar to 5-point NMHV amplitude, the 6-point N^{2}MHV amplitude is special which only receives contributions from diagrams of NMHV $\times$ MHV type and we must treat it separately. We can delete Fig. 5.7(a) by bonus relations, and the contribution

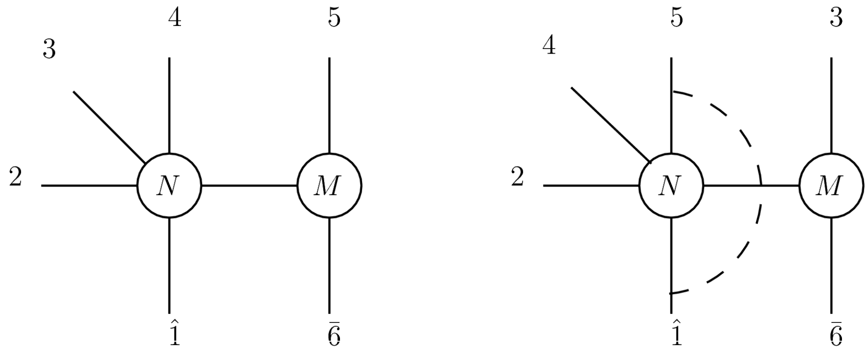

(a) 6-point diagram deleted by bonus relations

(b) 6-point diagram

Figure 5.7: Diagrams for 6-point N^{2}MHV amplitude.

from Fig. 5.7(b) gives,

$$\mathcal{M}_6 = -\frac{[16][25][45]}{[15][24][56]}[\{6; 25, 24\}_1(3 \leftrightarrow 5)] + \mathcal{P}(2, 3, 4). \tag{5.3.22}$$

As the NMHV case (5.3.11), 6-point N^{2}MHV amplitude (5.3.22) can also be similarly generalized, and we obtain the boundary term of the full n-point N^{2}MHV amplitudes,

$$M_n^{(\text{boundary})} = B^{(\text{boundary})}_{n;n-4\ n-1;n-4\ n-2}[\{n; n-4\ n-1; n-4\ n-2\}_1(n-3 \leftrightarrow n-2)], \tag{5.3.23}$$

where the bonus coefficients are given as

$$B^{(\text{boundary})}_{n;n-4\ n-1;n-4\ n-2} = \frac{\langle 1n\rangle\langle n-5\ n-1\rangle[n-4\ n-1][n-2\ n-1]x^2_{n-4n}}{\langle 1n-1\rangle[n-4\ n-2]\langle n-5|x_{n-4\ n-1}|n-1]\langle n|x_{n-1\ n-4}|n-1]} \tag{5.3.24}$$

Therefore we have calculated all the contributions for N^{2}MHV amplitudes and as in the NMHV case, it can also be written as a sum of $(n-3)!$ permutations,

$$\mathcal{M}_n^{\mathrm{N}^2\mathrm{MHV}} = M_{\mathrm{I}} + M_{\mathrm{II}} + M_{\mathrm{III}} + M_{\mathrm{IV}} + M_n^{(\text{boundary})} + \mathcal{P}(2,3,\ldots,n-2). \quad (5.3.25)$$

The result can be proved very similarly by induction as in the NMHV case.

5.4 Generalization to all gravity tree amplitudes

Now we have all the ingredients for generalizing our results and stating the patterns for all tree-level gravity amplitudes. Our way of using bonus relations gives the simplified tree-level N^{k}MHV superamplitude as a sum of $(n-3)!$ permutations, and each of them contains normal and exchanged contributions,

$$\mathcal{M}_n^{\mathrm{N}^k\mathrm{MHV}} = \left[A_n^{\mathrm{MHV}}\right]^2 \Big(\sum_{\alpha} B_\alpha^{(1,m_1)} G_\alpha R_\alpha^2 + \sum_{\beta} B_\beta^{(2,m_2)} [G_\beta R_\beta^2 (b_1{-}1 \leftrightarrow n{-}1)]\Big) + \mathcal{P}(2,3,\ldots,n{-}2). \quad (5.4.1)$$

In both contributions, by reducing the homogeneous term recursively, we have k types of terms from k BCFW channels, N^{p}MHV $\times$ N^{q}MHV, for $p+q+1=k$ with $0 \le p, q < k$. As we have stressed repeatedly, to respect the ordered structure, we have only used bonus relations on one lower-point amplitude, namely the right-hand-side N^{q}MHV for normal contribution, and the left-hand-side N^{p}MHV for exchanged contribution.

Before presenting all the bonus coefficients for general tree amplitudes, we pause to show by induction that bonus relations roughly reduce the number of terms from $(n-2)!$ in the original solution to $(k+1)(n-3)!$ in the simplified one. To get the previous counting we note that in the N^{p}MHV$\times$ N^{q}MHV channel of the normal contribution, by applying bonus relations to the N^{q}MHV lower-point amplitude we can reduce the number of terms from $(n-2)!/k$ to $(q+1)(n-3)!/k$. Taking into account all channels gives us $(1+2+\ldots+k)(n-3)!/k$ terms, with the same number from the exchanged contribution, thus the simplified form has only $(k+1)(n-3)!$ terms. By parity, one only needs N^{k}MHV amplitudes with $n > 2k+2$ legs and thus the bonus relations can be used to delete at least half of the terms in tree amplitudes. The simplification becomes more significant when $n \gg k$.

Now we generalize the pattern found in the NMHV and N^{2}MHV cases to write down all the bonus coefficients for general tree amplitudes. As we have learned from the examples, once the bonus coefficients of N^{k-1}MHV amplitudes are calculated, then for the N^{k}MHV amplitudes, one only needs to compute two types of new contributions for N^{k}MHV amplitudes, namely the normal contribution from MHV $\times$ N^{k-1}MHV channel ($q = k-1$) and the exchanged contribution from N^{k-1}MHV $\times$ MHV channel ($p = k-1$) (see Fig. 5.8). All other bonus coefficients $B^{(m)}_{\alpha}$ of N^{p}MHV $\times$ N^{q}MHV with $q < k-1$ and $p < k-1$, are the same as those computed previously, namely the results from N^{k-1}MHV amplitudes. Since the summation variables of N^{k}MHV amplitude can be obtained by adding a pair of new labels a_k, b_k to the previous one, α', $\alpha = \{\alpha'; a_k, b_k\}$, the result can be written as

$$B^{(m)}_{\alpha} \;=\; B^{(m)}_{\alpha'}, \tag{5.4.2}$$

for both normal contributions with $q < k-1$ and exchanged ones with $p < k-1$.

Thus we only need to calculate two new contributions from Fig. 5.8(a) and Fig. 5.8(b).

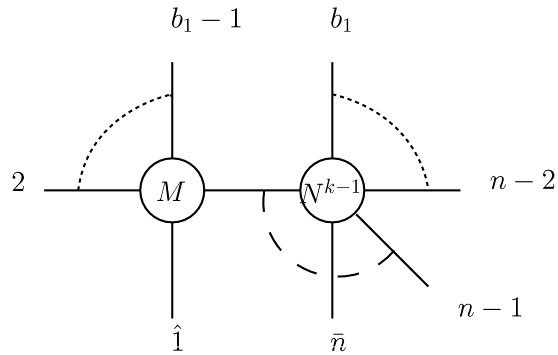

(a) MHV $\times$ N^{k-1}MHV

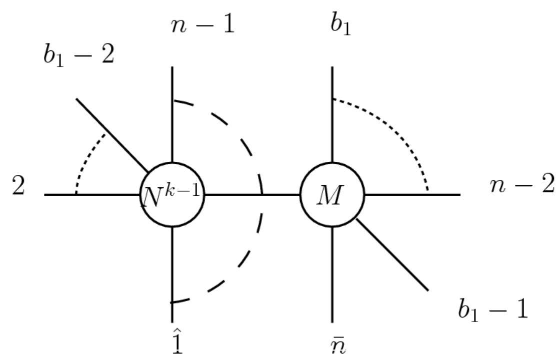

(b) N^{k-1}MHV $\times$ MHV

Figure 5.8: Two relevant diagrams for computing new bonus coefficients for n-point N^{k}MHV amplitude. The rest of the bonus coefficients can be obtained recursively from the N^{k-1}MHV case.

It is straightforward to confirm that all the observations we have made for the cases of NMHV and N^{2}MHV can be directly generalized to all tree-level amplitudes. We shall first state the rules and then justify them. Firstly, just like Eq. (5.3.4) and Eq. (5.3.17) for NMHV and N^{2}MHV cases, the bonus coefficients of Fig. 5.8(a), $B_{\alpha}^{(1,m_1)}$, can be similarly obtained by the replacements on the indices of the region momenta x's, $a_i \to a_{i+1}, b_i \to b_{i+1}$, for $B_{\alpha'}^{(m_1)}$ of N^{k-1}MHV amplitudes, then multiplying with a simple common factor of the form $\frac{\langle n-1|x_{a_1b_1}x_{b_1n}|n\rangle}{\langle n-1|x_{a_1b_1}x_{a_1n}|n\rangle}$, which are the same for all tree-level amplitudes,

$$B^{(1,m_1)}_{\alpha} = \frac{\langle n-1|x_{a_1b_1}x_{b_1n}|n\rangle}{\langle n-1|x_{a_1b_1}x_{a_1n}|n\rangle} B^{(m_1)}_{\alpha'}(a_i \to a_{i+1}, b_i \to b_{i+1}). \tag{5.4.3}$$

Secondly, the bonus coefficients for the new exchanged contributions Fig. 5.8(b), $B^{(2,m_2)}_{\beta}$, can be obtained by taking $B^{(m_2)}_{\beta'}$ of N^{k-1}MHV amplitudes, and performing the following replacements on the indices of region momenta x's, namely $n \to b_1, a_i \to a_{i+1}, b_i \to b_{i+1}$, and $x \to x'$ when x has index n with it. And for the spinors, we have $\langle n| \to \langle n|x_{na_1}x'_{a_1b_1}$ as well as $|n-i\rangle$(or $|n-i]$) $\to |b_1-i\rangle$(or $|b_1-i]$) for $i > 1$. In addition, the obtained answers are further multiplied by a factor $(x'_{a_1b_1})^2$,

$$B^{(2,m_2)}_{\beta} \quad = \quad (x'_{a_1b_1})^2 B^{(m_2)}_{\beta'}, \tag{5.4.4}$$

where the arguments of $B^{(m_2)}_{\beta'}$ should be changed under the rules we described above.

All these rules can be understood in a simple way. For the rules of the normal contributions, the common factor is obtained in the following way,

$$(1-\frac{z_i}{z_{n-1}})\frac{\langle n1\rangle}{\langle n-11\rangle} \to (1-\frac{z_i}{z_{n-1}})\frac{\langle n\widehat{P}\rangle}{\langle n-1\widehat{P}\rangle} \to \frac{\langle n-1|x_{a_1b_1}x_{b_1n}|n\rangle}{\langle n-1|x_{a_1b_1}x_{a_1n}|n\rangle}, \tag{5.4.5}$$

where $(1-\frac{z_i}{z_{n-1}})$ comes from the fact that we delete one diagram using bonus relations, and $\frac{\langle n1\rangle}{\langle n-11\rangle}$ is a factor that always appears in every bonus coefficient.

While for the rules of the exchanged contributions, we find that the factor $(x'_{a_1b_1})^2$

appears because

$$\langle n1\rangle \to \langle \widehat{P}\widehat{1}\rangle \to [\widehat{P}\widehat{1}]\langle \widehat{P}\widehat{1}\rangle \to (x'_{a_1b_1})^2, \tag{5.4.6}$$

and $\langle n|$ changes in the following way under the recursion relations,

$$\langle n| \to \langle \widehat{P}| \to \langle n1\rangle[1\widehat{P}]\langle \widehat{P}| \to \langle n|x_{na_1}x'_{a_1b_1}. \tag{5.4.7}$$

Besides, the transformation rule of $x_{n\gamma_i}$ follows as

$$x_{n\gamma_i} \to x_{\widehat{P}\gamma_{i+1}} \to x'_{b_1\gamma_{i+1}}, \tag{5.4.8}$$

where γ can be a or b and we have used the fact that $p_{\widehat{P}} = p_{b_1}+\cdots+p_{n-2}+p_{b_1-1}+p_{\widehat{n}}$. So in this way, we have a complete understanding of the rules we have proposed.

Finally, as shown in the examples a boundary contribution has to be considered separately because the special case $(k+4)$-point N^{k}MHV amplitude only has diagrams of N^{k-1}MHV $\times$ MHV type. For this special contribution, it is straightforward to obtain a general form,

$$M_n^{(\text{boundary})} = B_{\beta_0}^{(\text{boundary})}\Big[\Big(A_n^{\text{MHV}}\Big)^2 G_{\beta_0}R_{\beta_0}^2(n-k-1 \leftrightarrow n-1)\Big], \tag{5.4.9}$$

where $\beta_0 = \{n; n-k-2\ n-1; n-k-2\ n-2; \ldots; n-k-2\ n-k\}$, and the coefficients can be written as

$$B_{\beta_0}^{(\text{boundary})} = \frac{\langle 1n\rangle\langle n-k-3\ n-1\rangle[n-k-2\ n-1][n-k\ n-1]x^2_{n-k-2\ n}}{\langle 1n-1\rangle[n-k-2\ n-2]\langle n-k-3|x_{n-k-3\ n-1}|n-1]\langle n|x_{n-1\ n-k-2}|n-1]} \tag{5.4.10}$$

Therefore, we have found a set of explicit rules to write down all the bonus coefficients for all tree amplitude in $\mathcal{N} = 8$ supergravity.

5.5 Conclusion and outlook

In this note, we simplified tree-level amplitudes in $\mathcal{N} = 8$ SUGRA, from the BCFW form with a sum of $(n-2)!$ permutations to a new form as a sum of $(n-3)!$ permutations. This is achieved by using the bonus relations, which are relations between tree amplitudes in theories without color ordering. In contrast to the MHV case, a naive use of the bonus relations ruins the structure of the non-MHV ordered tree-level solution, thus we proposed an improved application of the relations, which respects the ordered structure. The key point here is to apply the bonus relations to only one of two lower-point amplitudes in any BCFW diagram, which indeed brings SUGRA amplitudes to a simplified form having a $(n-3)!$-permutation sum with some bonus coefficients. To illustrate the method, we have explicitly calculated simplified amplitudes for the NMHV and N^2MHV cases. We have also argued that the pattern generalizes to N^kMHV cases, and presented a simple way for writing down the bonus coefficients of all amplitudes, thus one can recursively obtain the simplified form for general SUGRA tree amplitudes.

The simplification is based on an explicit solution from BCFW recursion relations of SUGRA tree amplitudes of [158], which is in spirit similar to but in details different from KLT relations. From a computational point of view, any gravity amplitude obtained from $(n-3)!$ (or the newly proposed $(n-2)!$) form of KLT relations is a sum of $(n-3)!^2$ (or $(n-2)!^2$) terms; at least in the special case of $\mathcal{N} = 8$ SUGRA, an explicit solution with only $(n-2)!$ terms was found in [158], which is a significant simplification[4]. Furthermore, in this note we have used the bonus relations to reduce it to a sum with only $(k+1)(n-3)!$ terms. Further simplifications of gravity tree amplitudes are certainly worth investigating.

Apart from the computational advantages, the simplification is also conceptually interesting. The relations between gravity and gauge theories have been reexamined from various perspectives recently [33, 177, 178]. A common feature, of these "gravity"="gauge theory"^{2} methods, is the freedom of rewriting $(n-2)!$ forms of gravity tree amplitudes as $(n-3)!$ forms, essentially by using BCJ relations on the gauge theory side. Our result confirms this freedom at an explicit level by directly using it to simplify SUGRA amplitudes, which also suggests that bonus relations may be regarded as explicit gravity relations induced by Yang-Mills BCJ relations. It may be fruitful to understand the exact connections between our method, general forms of KLT relations, and the square relations. In particular, it would be nice to go beyond SUGRA and see if similar simplifications occur generally, given that both BCFW recursion relations and bonus relations are valid in more general gravity theories.

Bonus relations and simplifications we obtained at tree level can also have implications for loop amplitudes. Through the generalized unitarity-cut method, our new form of tree amplitudes can be used in calculations of loop amplitudes. In addition, the square relations have been conjectured to hold at loop level [40], thus we may expect similar simplifications directly for the SUGRA loop amplitudes.

[4] It would be nice to see if one can derive the explicit $(n-2)!$ form (similarly our simplified $(n-3)!$ form) from $(n-2)!$ (similarly $(n-3)!$) KLT relations. For the simplest MHV case, both have been derived in [181].

Appendix A

Appendix for Chapter 2

A.1 Useful integrals

Here we list some formulas, which have been extensively used in this paper. For more details about these formulas, see [182, 81].

X integral formula

$$\int_0^{+\infty} \prod_i \left(\frac{\mathrm{d}t_i}{t_i} t^{\alpha_i}\right) \int_{AdS} \mathrm{d}X \, e^{2T\cdot X} = \pi^h \Gamma\left(\frac{\sum_i \alpha_i - 2h}{2}\right) \int_0^{+\infty} \prod_i \left(\frac{\mathrm{d}t_i}{t_i} t^{\alpha_i}\right) e^{T^2}, \tag{A.1.1}$$

where $T = \sum_i t_i P_i$.

Q_i integral formula

$$\int_0^{+\infty} \frac{\mathrm{d}s}{s}\frac{\mathrm{d}\bar{s}}{\bar{s}} s^{h+c} s^{h-c} \int_{\partial AdS} \mathrm{d}Q\, e^{2T\cdot Q} = 2\pi^h \int_0^{+\infty} \frac{\mathrm{d}s}{s}\frac{\mathrm{d}\bar{s}}{\bar{s}} s^{h+c} s^{h-c} e^{T^2}, \tag{A.1.2}$$

where $T = (sX + \bar{s}Y)$.

t integral formula

This is also called the Symanzik star integration formula where we consider a set of n points in Euclidean space x_i and their differences $x_i - x_j$. In the embedding formalism we have $P_{ij} \equiv -2P_i \cdot P_j = (x_i - x_j)^2$. Then Symanzik's formula is:

$$\int_0^{+\infty} \left(\prod_{i=1}^{n} \frac{\mathrm{d}t_i}{t_i} t^{\Delta_i}\right) e^{-(\sum\limits_{1\leq i<j\leq n} t_i t_j P_{ij})} = \frac{\pi^h/2}{(2\pi i)^{\frac{1}{2}n(n-3)}} \int \mathrm{d}\delta_{ij} \prod_{1\leq i<j\leq n} \Gamma(\delta_{ij})\,(P_{ij})^{-\delta_{ij}} \tag{A.1.3}$$

where the integration is over $n(n-3)/2$ variables and the integration paths are chosen parallel to the imaginary axis, with real parts such that the real parts of the arguments of the gamma functions are positive.

A.2 Example: 9-points in ϕ^3 theory

In order to illustrate the general strategy of isolating the maximal vertex in any arbitrary Witten diagram, as discussed in section 3.3, here we will study a specific example, that of a 9-point Witten diagram in ϕ^3 theory and we will write down the results as a special case of (2.3.35) and (2.3.36). We have the Q variables labeled as $Q_{1'}, Q_{2'}, Q_{3'}, Q_1, Q_2, Q_3$ and then we will integrate them out in that particular order.

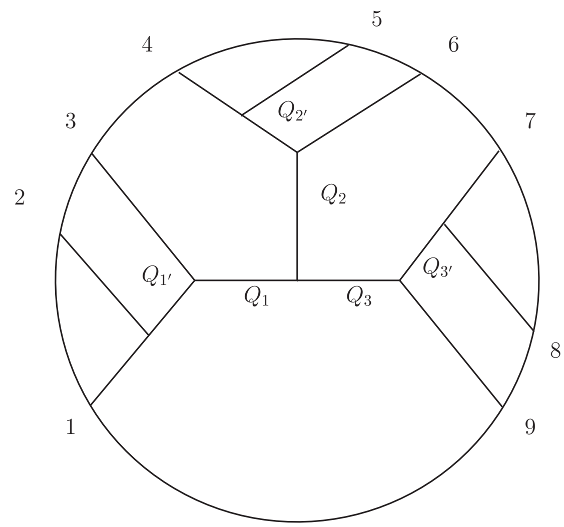

Figure A.1: A vertex with all off-shell legs in 9-point amplitude in ϕ^3 theory

We note here that only the variables Q_1, Q_2, Q_3 are relevant for the vertex under consideration. After doing all the Q integrals we will get the exponent as before given by (2.3.33),

$$E_{Q_3} = \sum_{i=1}^{3} (\mathcal{D}_{i'})^2 + \sum_{l=1}^{3} \left(\overline{s}_l \mathcal{Y}_{l-1}^Z + s_l \mathcal{B}_l^Z \right)^2, \tag{A.2.1}$$

where the term in the first bracket is given by

$$\begin{aligned} \mathcal{D}_{1'} &= P_3 t_3 \overline{s}_{1'} + s_{1'} \left(P_1 t_1 + P_2 t_2 \right), \\ \mathcal{D}_{2'} &= P_6 t_6 \overline{s}_{2'} + s_{2'} \left(P_4 t_4 + P_5 t_5 \right), \\ \mathcal{D}_{3'} &= P_9 t_9 \overline{s}_{3'} + s_{3'} \left(P_7 t_7 + P_8 t_8 \right), \end{aligned} \tag{A.2.2}$$

and these terms do not contain any of the variables relevant to the vertex we are interested in and hence we will not consider them further. Now let us focus on the term inside the second bracket where the relevant functions $\mathcal{B}^Z$ and $\mathcal{Y}^Z$, defined by (2.3.34), are given by,

$$\begin{aligned}
\mathcal{B}^Z_1 &= \mathcal{D}_{1'}\overline{s}_{1'} + P_3 t_3,\\
\mathcal{B}^Z_2 &= \mathcal{D}_{2'}\overline{s}_{2'} + P_6 t_6,\\
\mathcal{B}^Z_3 &= \mathcal{D}_{3'}\overline{s}_{3'} + P_9 t_9
\end{aligned} \tag{A.2.3}$$

and

$$\begin{aligned}
\mathcal{Y}^Z_0 &= 0,\\
\mathcal{Y}^Z_1 &= s_1\mathcal{B}^Z_1\overline{s}_1,\\
\mathcal{Y}^Z_2 &= s_2\mathcal{B}^Z_2\left(\overline{s}_1^2+1\right)\overline{s}_2 + s_1\mathcal{B}^Z_1\overline{s}_1\left(\left(\overline{s}_1^2+1\right)\overline{s}_2^2+1\right).
\end{aligned} \tag{A.2.4}$$

The next step is to expand the second term of E_{Q_3} like before and after doing all the t_i integrals we get the form of the integrand as in (2.3.35),

$$\mathcal{M}(k_j) = \int ds\mathcal{V}(s)\int\prod_{j=1}^{3}\frac{ds_j}{s_j}\frac{d\overline{s}_j}{\overline{s}_j}\, s_j^{h+c_j+a_j}\overline{s}_j^{h-c_j+a_j}g_j^{-b_j}\prod_{j=1}^{3}H_j(s_j^2F_j,s), \tag{A.2.5}$$

where g and F are defined by (2.3.14) and (2.3.17) and a_j, b_j are defined by (2.3.21) and (2.3.22) respectively. Moreover, the part which is irrelevant to the maximal vertex is given by

$$\begin{aligned}
\mathcal{V}(s) &= \prod_{j=1'}^{3'}\frac{ds_j}{s_j}s_j^{h+c_j+a'_j}\overline{s}_j^{h-c_j+a'_j}\left(\overline{s}_{1'}^2+1\right)^{-k_3(k_1+k_2+k_3)}\\
&\times\left(\overline{s}_{2'}^2+1\right)^{-k_6(k_4+k_5+k_6)}\left(\overline{s}_{3'}^2+1\right)^{-k_9(k_7+k_8+k_9)},
\end{aligned} \tag{A.2.6}$$

where,

$$\begin{aligned} a'_{1'} &= -(k_1+k_2)^2, \\ a'_{2'} &= -(k_4+k_5)^2, \\ a'_{3'} &= -(k_7+k_8)^2. \end{aligned} \tag{A.2.7}$$

The complicated H function which would eventually give the terms relevant for the vertex, is given by,

$$\begin{aligned} H_1(s_1^2F_1, s) &= \left(F_1 s_1^2 \left(\overline{s}_{1'}^2 + 1\right) + 1\right)^{(k_1+k_2)k_3} \left(s_{1'}^2 \left(F_1 s_1^2 \overline{s}_{1'}^2 + 1\right) + 1\right)^{k_1 k_2}, \\ H_2(s_2^2F_2, s) &= \left(F_2 s_2^2 \left(\overline{s}_{2'}^2 + 1\right) + 1\right)^{(k_4+k_5)k_6} \left(s_{2'}^2 \left(F_2 s_2^2 \overline{s}_{2'}^2 + 1\right) + 1\right)^{k_4 k_5}, \\ H_3(s_3^2F_3, s) &= \left(F_3 s_3^2 \left(\overline{s}_{3'}^2 + 1\right) + 1\right)^{(k_7+k_8)k_9} \left(s_{3'}^2 \left(F_3 s_3^2 \overline{s}_{3'}^2 + 1\right) + 1\right)^{k_7 k_8} \end{aligned} \tag{A.2.8}$$

Now, as before, we can use the the transformation

$$s_i^2 \to \frac{s_i^2}{F_i} \tag{A.2.9}$$

and we will get the required form of the $\overline{s}$ integral part as in (2.3.36), to be

$$\mathcal{M}(k_i)\Big|_{\overline{s}} = \int \prod_{i=1}^{3} \frac{d\overline{s}_i}{\overline{s}_i} \, \overline{s}_i^{h-c_i+a_i} g_i^{-b_i} F_i^{\frac{-h+c_i+a_i}{2}}. \tag{A.2.10}$$

From (A.2.8) we also see that after the rescaling of s_i^2's we are left with a term of the form ,

$$\begin{aligned}
\mathcal{V}'(s) &= \left(s_1^2\left(\overline{s}_{1'}^2+1\right)+1\right)^{(k_1+k_2)k_3}\left(s_{1'}^2\left(s_1^2\overline{s}_{1'}^2+1\right)+1\right)^{k_1k_2} \\
&\times \left(s_2^2\left(\overline{s}_{2'}^2+1\right)+1\right)^{(k_4+k_5)k_6}\left(s_{2'}^2\left(s_2^2\overline{s}_{2'}^2+1\right)+1\right)^{k_4k_5} \\
&\times \left(s_3^2\left(\overline{s}_{3'}^2+1\right)+1\right)^{(k_7+k_8)k_9}\left(s_{3'}^2\left(s_3^2\overline{s}_{3'}^2+1\right)+1\right)^{k_7k_8}, \qquad \text{(A.2.11)}
\end{aligned}$$

which we note is independent of the $\overline{s}$ variables related to the maximal vertex and hence irrelevant.

Appendix B

Appendix for Chapter 3

B.1 Details on the double box computation

A list of 9 multiplicatively independent cross-ratios required to describe conformally invariant functions of six point is given by the following set:

$$u_1 = \frac{x_{14}^2 x_{23}^2}{x_{13}^2 x_{24}^2}, \quad u_2 = \frac{x_{15}^2 x_{24}^2}{x_{14}^2 x_{25}^2}, \quad u_3 = \frac{x_{16}^2 x_{25}^2}{x_{15}^2 x_{26}^2}, \quad u_4 = \frac{x_{25}^2 x_{34}^2}{x_{24}^2 x_{35}^2},$$
$$u_5 = \frac{x_{26}^2 x_{35}^2}{x_{25}^2 x_{36}^2}, \quad u_6 = \frac{x_{12}^2 x_{36}^2}{x_{13}^2 x_{26}^2}, \quad u_7 = \frac{x_{36}^2 x_{45}^2}{x_{35}^2 x_{46}^2}, \quad u_8 = \frac{x_{13}^2 x_{46}^2}{x_{14}^2 x_{36}^2}, \quad u_9 = \frac{x_{14}^2 x_{56}^2}{x_{15}^2 x_{46}^2}. \tag{B.1.1}$$

In order to carry out the computation for the $d = 6$ hexagon in $2d$ kinematics we can first restrict the general kinematics of (B.1.1) to a four-dimensional subspace parameterized by 12 momentum twistors [183]. Subsequently, we can further restrict the $4d$ momentum twistors to a subspace of $2d$ kinematics which can be very simply parameterized using 6 independent cross-ratios, as a generalization of the parameterization used in [116, 100, 118]:

$$
\begin{aligned}
Z_1 &= \begin{pmatrix} 0 \\ 0 \\ i\sqrt{2}\chi_2^+ \\ \frac{i(1-\chi_2^+)}{\sqrt{2}} \end{pmatrix}, \quad Z_2 = \begin{pmatrix} i\sqrt{2}\chi_3^- \\ \frac{i(1-\chi_3^-)}{\sqrt{2}} \\ 0 \\ 0 \end{pmatrix}, \quad Z_3 = \begin{pmatrix} 0 \\ 0 \\ i\sqrt{2}\chi_3^+ \\ \frac{i(1-\chi_3^+)}{\sqrt{2}} \end{pmatrix}, \quad Z_4 = \begin{pmatrix} i\sqrt{2}\chi_1^- \\ \frac{i(1-\chi_1^-)}{\sqrt{2}} \\ 0 \\ 0 \end{pmatrix}. \\
Z_5 &= \begin{pmatrix} 0 \\ 0 \\ i\sqrt{2}\chi_1^+ \\ \frac{i(1-\chi_1^+)}{\sqrt{2}} \end{pmatrix}, \quad Z_6 = \begin{pmatrix} 0 \\ \frac{i}{\sqrt{2}} \\ 0 \\ 0 \end{pmatrix}, \quad Z_7 = \begin{pmatrix} 0 \\ 0 \\ i\sqrt{2} \\ -i\sqrt{2} \end{pmatrix}, \quad Z_8 = \begin{pmatrix} -i\sqrt{2} \\ \frac{i}{\sqrt{2}} \\ 0 \\ 0 \end{pmatrix}, \\
Z_9 &= \begin{pmatrix} 0 \\ 0 \\ i\sqrt{2} \\ -i\sqrt{2} \end{pmatrix}, \quad Z_{10} = \begin{pmatrix} -i\sqrt{2} \\ \frac{i}{\sqrt{2}} \\ 0 \\ 0 \end{pmatrix}, \quad Z_{11} = \begin{pmatrix} 0 \\ 0 \\ 0 \\ \frac{i}{\sqrt{2}} \end{pmatrix}, \quad Z_{12} = \begin{pmatrix} i\sqrt{2}\chi_2^- \\ \frac{i(1-\chi_2^-)}{\sqrt{2}} \\ 0 \\ 0 \end{pmatrix}
\end{aligned}
\tag{B.1.2}
$$

In terms of these variables one may compute the $x_{ij}^2 = \det(Z_{2i-1}Z_{2i}Z_{2j-1}Z_{2j})$, so that the 9 cross-ratios (B.1.1) are given by

$$\begin{aligned}
u_1 &= \frac{\chi_1{}^- (\chi_3{}^- + 1) (\chi_1{}^+ - \chi_3{}^+)}{(\chi_1{}^- + 1) \chi_3{}^- (\chi_1{}^+ - \chi_2{}^+)}, \\
u_2 &= \frac{(\chi_1{}^- + 1) (\chi_2{}^+ + 1)}{(\chi_3{}^- + 1) (\chi_3{}^+ + 1)}, \\
u_3 &= \frac{(\chi_2{}^- - \chi_3{}^-) \chi_2{}^+ (\chi_3{}^+ + 1)}{(\chi_2{}^- - \chi_1{}^-) (\chi_2{}^+ + 1) \chi_3{}^+}, \\
u_4 &= \frac{\chi_3{}^+ + 1}{\chi_1{}^+\chi_1{}^- + \chi_1{}^- + \chi_1{}^+ + 1}, \\
u_5 &= \frac{(\chi_2{}^- - \chi_1{}^-) (\chi_1{}^+ + 1) \chi_3{}^+}{\chi_2{}^-\chi_1{}^+ (\chi_3{}^+ + 1)}, \\
u_6 &= \frac{\chi_2{}^- (\chi_1{}^- - \chi_3{}^-) \chi_1{}^+ (\chi_2{}^+ - \chi_3{}^+)}{(\chi_2{}^- - \chi_1{}^-) \chi_3{}^- (\chi_1{}^+ - \chi_2{}^+) \chi_3{}^+}, \\
u_7 &= \frac{\chi_2{}^-\chi_1{}^+}{(\chi_2{}^- + 1) (\chi_1{}^+ + 1)}, \\
u_8 &= \frac{(\chi_2{}^- + 1) \chi_3{}^- (\chi_1{}^+ - \chi_2{}^+)}{\chi_2{}^- (\chi_3{}^- + 1) \chi_1{}^+}, \\
u_9 &= \frac{\chi_3{}^- + 1}{\chi_2{}^+\chi_2{}^- + \chi_2{}^- + \chi_2{}^+ + 1}.
\end{aligned} \tag{B.1.3}$$

B.2 Details on the triple box computation

B.2.1 Cross-ratios for eight-point functions

A list of 20 multiplicatively independent cross-ratios required to describe conformally invariant functions of eight points is given by the following set:

$$\begin{aligned}
u_1 &= \frac{x_{15}^2 x_{24}^2}{x_{14}^2 x_{25}^2}, \quad u_2 = \frac{x_{16}^2 x_{25}^2}{x_{15}^2 x_{26}^2}, \quad u_3 = \frac{x_{17}^2 x_{26}^2}{x_{16}^2 x_{27}^2}, \quad u_4 = \frac{x_{26}^2 x_{35}^2}{x_{25}^2 x_{36}^2}, \\
u_5 &= \frac{x_{27}^2 x_{36}^2}{x_{26}^2 x_{37}^2}, \quad u_6 = \frac{x_{28}^2 x_{37}^2}{x_{27}^2 x_{38}^2}, \quad u_7 = \frac{x_{37}^2 x_{46}^2}{x_{36}^2 x_{47}^2}, \quad u_8 = \frac{x_{38}^2 x_{47}^2}{x_{37}^2 x_{48}^2}, \\
u_9 &= \frac{x_{13}^2 x_{48}^2}{x_{14}^2 x_{38}^2}, \quad u_{10} = \frac{x_{48}^2 x_{57}^2}{x_{47}^2 x_{58}^2}, \quad u_{11} = \frac{x_{14}^2 x_{58}^2}{x_{15}^2 x_{48}^2}, \quad u_{12} = \frac{x_{15}^2 x_{68}^2}{x_{16}^2 x_{58}^2}, \\
u_{13} &= \frac{x_{13}^2 x_{28}^2}{x_{12}^2 x_{38}^2}, \quad u_{14} = \frac{x_{13}^2 x_{24}^2}{x_{14}^2 x_{23}^2}, \quad u_{15} = \frac{x_{24}^2 x_{35}^2}{x_{25}^2 x_{34}^2}, \quad u_{16} = \frac{x_{35}^2 x_{46}^2}{x_{36}^2 x_{45}^2}, \\
u_{17} &= \frac{x_{46}^2 x_{57}^2}{x_{47}^2 x_{56}^2}, \quad u_{18} = \frac{x_{57}^2 x_{68}^2}{x_{58}^2 x_{67}^2}, \quad u_{19} = \frac{x_{17}^2 x_{68}^2}{x_{16}^2 x_{78}^2}, \quad u_{20} = \frac{x_{17}^2 x_{28}^2}{x_{18}^2 x_{27}^2}.
\end{aligned} \tag{B.2.1}$$

As in the previous section for the double box computation in $2d$ kinematics we can use the momentum twistor parameterization of the above cross-ratios in terms of 16 momentum twistors in a four-dimensional subspace, which are again expressed in a $2d$ subspace parameterized by 10 cross-ratios. The momentum twistor representation is given by,

$$
\begin{aligned}
Z_1 &= \begin{pmatrix} 0 \\ 0 \\ i\sqrt{2} \\ -i\sqrt{2} \end{pmatrix}, \quad Z_2 = \begin{pmatrix} -i\sqrt{2} \\ \frac{i}{\sqrt{2}} \\ 0 \\ 0 \end{pmatrix}, \quad Z_3 = \begin{pmatrix} 0 \\ 0 \\ 0 \\ \frac{i}{\sqrt{2}} \end{pmatrix}, \quad Z_4 = \begin{pmatrix} i\sqrt{2}\chi_1^- \\ \frac{i(1-\chi_1^-)}{\sqrt{2}} \\ 0 \\ 0 \end{pmatrix}, \\
Z_5 &= \begin{pmatrix} 0 \\ 0 \\ i\sqrt{2}\chi_1^+ \\ \frac{i(1-\chi_1^+)}{\sqrt{2}} \end{pmatrix}, \quad Z_6 = \begin{pmatrix} 0 \\ \frac{i}{\sqrt{2}} \\ 0 \\ 0 \end{pmatrix}, \quad Z_7 = \begin{pmatrix} 0 \\ 0 \\ i\sqrt{2} \\ -i\sqrt{2} \end{pmatrix}, \quad Z_8 = \begin{pmatrix} -i\sqrt{2} \\ \frac{i}{\sqrt{2}} \\ 0 \\ 0 \end{pmatrix}, \\
Z_9 &= \begin{pmatrix} 0 \\ 0 \\ i\sqrt{2}\chi_2^+ \\ \frac{i(1-\chi_2^+)}{\sqrt{2}} \end{pmatrix}, \quad Z_{10} = \begin{pmatrix} i\sqrt{2}\chi_2^- \\ \frac{i(1-\chi_2^-)}{\sqrt{2}} \\ 0 \\ 0 \end{pmatrix}, \quad Z_{11} = \begin{pmatrix} 0 \\ 0 \\ i\sqrt{2}\chi_3^+ \\ \frac{i(1-\chi_3^+)}{\sqrt{2}} \end{pmatrix}, \quad Z_{12} = \begin{pmatrix} i\sqrt{2}\chi_3^- \\ \frac{i(1-\chi_3^-)}{\sqrt{2}} \\ 0 \\ 0 \end{pmatrix}, \\
Z_{13} &= \begin{pmatrix} 0 \\ 0 \\ i\sqrt{2}\chi_4^+ \\ \frac{i(1-\chi_4^+)}{\sqrt{2}} \end{pmatrix}, \quad Z_{14} = \begin{pmatrix} i\sqrt{2}\chi_4^- \\ \frac{i(1-\chi_4^-)}{\sqrt{2}} \\ 0 \\ 0 \end{pmatrix}, \quad Z_{15} = \begin{pmatrix} 0 \\ 0 \\ i\sqrt{2}\chi_5^+ \\ \frac{i(1-\chi_5^+)}{\sqrt{2}} \end{pmatrix}, \quad Z_{16} = \begin{pmatrix} i\sqrt{2}\chi_5^- \\ \frac{i(1-\chi_5^-)}{\sqrt{2}} \\ 0 \\ 0 \end{pmatrix}
\end{aligned}
\tag{B.2.2}
$$

In terms of (B.2.2) the 20 cross-ratios then take the values

$$
\begin{aligned}
u_1 &= \frac{(\chi_1{}^- + 1)\,(\chi_2{}^+ + 1)}{(\chi_1{}^- - \chi_2{}^-)\,\chi_2{}^+}, \quad u_2\frac{(\chi_1{}^- - \chi_2{}^-)\,\chi_2{}^+\,(\chi_3{}^+ + 1)}{(\chi_1{}^- - \chi_3{}^-)\,(\chi_2{}^+ + 1)\,\chi_3{}^+}, \\
u_3 &= \frac{(\chi_1{}^- - \chi_3{}^-)\,\chi_3{}^+\,(\chi_4{}^+ + 1)}{(\chi_1{}^- - \chi_4{}^-)\,(\chi_3{}^+ + 1)\,\chi_4{}^+}, \quad u_4 = \frac{\chi_2{}^-\,(\chi_1{}^- - \chi_3{}^-)\,(\chi_1{}^+ - \chi_2{}^+)\,\chi_3{}^+}{(\chi_1{}^- - \chi_2{}^-)\,\chi_3{}^-\chi_2{}^+\,(\chi_1{}^+ - \chi_3{}^+)}, \\
u_5 &= \frac{\chi_3{}^-\,(\chi_1{}^- - \chi_4{}^-)\,(\chi_1{}^+ - \chi_3{}^+)\,\chi_4{}^+}{(\chi_1{}^- - \chi_3{}^-)\,\chi_4{}^-\chi_3{}^+\,(\chi_1{}^+ - \chi_4{}^+)}, \quad u_6 = \frac{\chi_4{}^-\,(\chi_1{}^- - \chi_5{}^-)\,(\chi_1{}^+ - \chi_4{}^+)\,\chi_5{}^+}{(\chi_1{}^- - \chi_4{}^-)\,\chi_5{}^-\chi_4{}^+\,(\chi_1{}^+ - \chi_5{}^+)}, \\
u_7 &= \frac{(\chi_3{}^- + 1)\,\chi_4{}^-\,(\chi_1{}^+ - \chi_4{}^+)}{\chi_3{}^-\,(\chi_4{}^- + 1)\,(\chi_1{}^+ - \chi_3{}^+)}, \quad u_8 = \frac{(\chi_4{}^- + 1)\,\chi_5{}^-\,(\chi_1{}^+ - \chi_5{}^+)}{\chi_4{}^-\,(\chi_5{}^- + 1)\,(\chi_1{}^+ - \chi_4{}^+)}, \\
u_9 &= \frac{(\chi_5{}^- + 1)\,(\chi_1{}^+ + 1)}{\chi_5{}^-\,(\chi_1{}^+ - \chi_5{}^+)}, \quad u_{10} = \frac{(\chi_2{}^- - \chi_4{}^-)\,(\chi_5{}^- + 1)\,(\chi_2{}^+ - \chi_4{}^+)}{(\chi_4{}^- + 1)\,(\chi_2{}^- - \chi_5{}^-)\,(\chi_2{}^+ - \chi_5{}^+)}, \\
u_{11} &= -\frac{(\chi_2{}^- - \chi_5{}^-)\,(\chi_2{}^+ - \chi_5{}^+)}{(\chi_5{}^- + 1)\,(\chi_2{}^+ + 1)}, \quad u_{12} = \frac{(\chi_3{}^- - \chi_5{}^-)\,(\chi_2{}^+ + 1)\,(\chi_3{}^+ - \chi_5{}^+)}{(\chi_2{}^- - \chi_5{}^-)\,(\chi_3{}^+ + 1)\,(\chi_2{}^+ - \chi_5{}^+)}, \\
u_{13} &= \frac{(\chi_1{}^- - \chi_5{}^-)\,(\chi_1{}^+ + 1)\,\chi_5{}^+}{\chi_5{}^-\,(\chi_1{}^+ - \chi_5{}^+)}, \quad u_{14} = \frac{(\chi_1{}^- + 1)\,(\chi_1{}^+ + 1)}{\chi_1{}^-\chi_1{}^+}, \\
u_{15} &= \frac{(\chi_1{}^- + 1)\,\chi_2{}^-\,(\chi_1{}^+ - \chi_2{}^+)}{(\chi_1{}^- - \chi_2{}^-)\,\chi_2{}^+}, \quad u_{16} = \frac{\chi_2{}^-\,(\chi_3{}^- + 1)\,(\chi_1{}^+ - \chi_2{}^+)}{(\chi_2{}^- + 1)\,\chi_3{}^-\,(\chi_1{}^+ - \chi_3{}^+)}, \\
u_{17} &= \frac{(\chi_3{}^- + 1)\,(\chi_2{}^- - \chi_4{}^-)\,(\chi_2{}^+ - \chi_4{}^+)}{(\chi_2{}^- - \chi_3{}^-)\,(\chi_4{}^- + 1)\,(\chi_2{}^+ - \chi_3{}^+)}, \quad u_{18} = \frac{(\chi_2{}^- - \chi_4{}^-)\,(\chi_3{}^- - \chi_5{}^-)\,(\chi_2{}^+ - \chi_4{}^+)\,(\chi_3{}^+ - \chi_5{}^+)}{(\chi_3{}^- - \chi_4{}^-)\,(\chi_2{}^- - \chi_5{}^-)\,(\chi_3{}^+ - \chi_4{}^+)\,(\chi_2{}^+ - \chi_5{}^+)} \\
u_{19} &= -\frac{(\chi_3{}^- - \chi_5{}^-)\,(\chi_4{}^+ + 1)\,(\chi_3{}^+ - \chi_5{}^+)}{(\chi_3{}^- - \chi_4{}^-)\,(\chi_2{}^- - \chi_5{}^-)\,(\chi_3{}^+ - \chi_4{}^+)\,(\chi_2{}^+ - \chi_5{}^+)}, \quad u_{20} = \frac{(\chi_1{}^- - \chi_5{}^-)\,(\chi_4{}^+ + 1)\,\chi_5{}^+}{(\chi_1{}^- - \chi_4{}^-)\,\chi_4{}^+\,(\chi_5{}^+ + 1)}. \text{(B.2.3}
\end{aligned}
$$

B.2.2 A Γ-function parameterization

Upon expressing the δ_{ij} in terms of 20 independent variables c_i according to the labeling of the 20 cross-ratios in the previous subsection, the product $\prod_{i<j}^{8}\Gamma(\delta_{ij})$

appearing in (3.5.8) becomes

$$\begin{aligned}\prod_{i<j}^{8}\Gamma(\delta_{ij}) \;=\;& \Gamma\left(c_2-c_3-c_4+c_5+1\right)\Gamma\left(c_5-c_6-c_7+c_8+1\right)\Gamma\left(c_8-c_9-c_{10}+c_{11}+1\right)\\ & \Gamma\left(-c_1+c_2+c_{11}-c_{12}+1\right)\Gamma\left(c_{13}\right)\Gamma\left(c_6-c_8+c_9+c_{13}\right)\Gamma\left(-c_9-c_{13}-c_{14}\right)\\ & \Gamma\left(c_{14}\right)\Gamma\left(c_1+c_9-c_{11}+c_{14}\right)\Gamma\left(-c_1-c_{14}-c_{15}\right)\Gamma\left(c_{15}\right)\Gamma\left(c_1-c_2+c_4+c_{15}\right)\\ & \Gamma\left(-c_4-c_{15}-c_{16}\right)\Gamma\left(c_{16}\right)\Gamma\left(c_4-c_5+c_7+c_{16}\right)\Gamma\left(-c_7-c_{16}-c_{17}\right)\Gamma\left(c_{17}\right)\\ & \Gamma\left(c_7-c_8+c_{10}+c_{17}\right)\Gamma\left(-c_{10}-c_{17}-c_{18}\right)\Gamma\left(c_{18}\right)\Gamma\left(c_{10}-c_{11}+c_{12}+c_{18}\right)\\ & \Gamma\left(-c_{12}-c_{18}-c_{19}\right)\Gamma\left(c_{19}\right)\Gamma\left(-c_2+c_3+c_{12}+c_{19}\right)\Gamma\left(-c_6-c_{13}-c_{20}\right)\\ & \Gamma\left(-c_3-c_{19}-c_{20}\right)\Gamma\left(c_{20}\right)\Gamma\left(c_3-c_5+c_6+c_{20}\right). \qquad \text{(B.2.4)}\end{aligned}$$

Appendix C

Appendix for Chapter 4

C.1 ISL in Momentum Twistor

It is often more convenient to consider ISL in momentum twistor. In [28] the authors provide a general prescription for constructing an n-point Yangian invariant, $Y_{n,k}$ by adding a particle to the $n-1$ point Yangian invariant. We will give a brief review of their ideas here.[1] Building Yangian invariants can be done in two ways, either it is k preserving operation as in

$$Y'_{n,k}(\mathcal{Z}_1, \ldots, \mathcal{Z}_{n-1}, \mathcal{Z}_n) = Y_{n-1,k}(\mathcal{Z}_1, \ldots \mathcal{Z}_{n-1}), \tag{C.1.1}$$

or both k and n increasing operation as in

$$Y'_{n,k}(\ldots, \mathcal{Z}_{n-1}, \mathcal{Z}_n, \mathcal{Z}_1, \ldots) = [n-2\ n-1\ n\ 1\ 2] Y_{n-1,k-1}(\ldots, \widehat{\mathcal{Z}_{n-1}}, \widehat{\mathcal{Z}_1}, \ldots). \tag{C.1.2}$$

[1] See [28, 184] for more details.

We can see that the first case is pretty straightforward as it does not change the functional form of the Yangian invariants. For the second type, the lower point invariant have their super momentum twistors adjacent to the added particle, i.e. the n_{th} particle, deformed by the following shifts,

$$\begin{aligned}\widehat{\mathcal{Z}_1} &= \mathcal{Z}_1\langle 2\ n-2\ n-1\ n\rangle + \mathcal{Z}_2\langle n-2\ n-1\ n\ 1\rangle;\\ \widehat{\mathcal{Z}_{n-1}} &= \mathcal{Z}_{n-2}\langle n-1\ n\ 1\ 2\rangle + \mathcal{Z}_{n-1}\langle n\ 1\ 2\ n-2\rangle,\end{aligned}\tag{C.1.3}$$

and we have the R-invariant defined as

$$[a\ b\ c\ d\ e] = \frac{\delta^{0|4}(\eta_a\langle b\ c\ d\ e\rangle + \text{cyclic})}{\langle a\ b\ c\ d\rangle\langle b\ c\ d\ e\rangle\langle c\ d\ e\ a\rangle\langle d\ e\ a\ b\rangle\langle e\ a\ b\ c\rangle}.\tag{C.1.4}$$

Translate to the language of usual spinor formalism the first case (C.1.1) is corresponding to adding a positive particle in section 2, while the second one (C.1.2) is corresponding to adding a negative particle.

C.2 Example of the ISL recursion relations

Here we consider one concrete example of how a BCFW diagram can be built up from three-point amplitude by the recursion relation. The BCFW diagram is of the form

$$A_{\mathrm{NMHV}}(\overline{1},2,3,4,5,\widehat{P}) \times A_{\mathrm{NMHV}}(-\widehat{P},6,7,8,9,\widehat{10}),\tag{C.2.1}$$

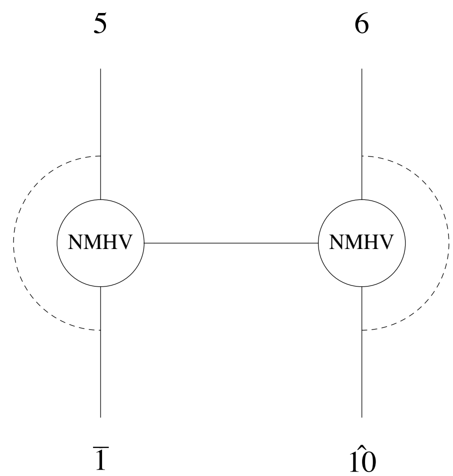

Figure C.1: A particular BCFW diagram occuring in 10 point N^3MHV amplitude

and we will study this in the language of momentum-twistor, which is more compact. According to our prescription (4.3.36) we will start with $A_{\overline{\mathrm{MHV}}}(5,6,10)$ and by adding 1^-, we get $A_{\mathrm{MHV}}(1,5,6,10)=1$ in the language of momentum-twistor. According to the recursion relations, we can gradually add particles between 1 and 5, as well as 6 and 10, the final results are listed below,

$$
\begin{aligned}
\{1^-,4^+,2^+,3^-\}_L\,\{9^-,8^+,7^-\}_R &\equiv [9\;8\;\mathbf{7}\;6\;5][1\;10\;\mathbf{9}\;6\;5][1\;2\;\mathbf{3}\;4\;5]\\
\{1^-,2^+,3^-,4^+\}_L\,\{9^-,8^+,7^-\}_R &\equiv [9\;8\;\mathbf{7}\;6\;5][1\;10\;\mathbf{9}\;6\;5][1\;2\;\mathbf{3}\;5\;\hat{\hat{6}}]\\
\{1^-,3^+,4^-,2^+\}_L\,\{9^-,8^+,7^-\}_R &\equiv [9\;8\;\mathbf{7}\;6\;5][1\;10\;\mathbf{9}\;6\;5][1\;3\;\mathbf{4}\;5\;\hat{\hat{6}}]\\
\{1^-,4^+,2^+,3^-\}_L\,\{9^-,8^+,7^-\}_R &\equiv [1\;10\;\mathbf{9}\;8\;7][1\;\widehat{10}\;\hat{\mathbf{8}}\;6\;5][1\;2\;\mathbf{3}\;4\;5]\\
\{1^-,2^+,3^-,4^+\}_L\,\{8^-,7^+,9^-\}_R &\equiv [1\;10\;\mathbf{9}\;8\;7][1\;\widehat{10}\;\hat{\mathbf{8}}\;6\;5][1\;2\;\mathbf{3}\;5\;\hat{\hat{6}}]\\
\{1^-,3^+,4^-,2^+\}_L\,\{7^-,9^-,8^+\}_R &\equiv [1\;10\;\mathbf{9}\;8\;7][1\;\widehat{10}\;\hat{\mathbf{8}}\;6\;5][1\;3\;\mathbf{4}\;5\;\hat{\hat{6}}]\\
\{1^-,4^+,2^+,3^-\}_L\,\{9^-,8^+,7^-\}_R &\equiv [1\;10\;\mathbf{9}\;7\;6][1\;\widehat{10}\;\hat{\mathbf{7}}\;6\;5][1\;2\;\mathbf{3}\;4\;5]\\
\{1^-,2^+,3^-,4^+\}_L\,\{8^-,7^+,9^-\}_R &\equiv [1\;10\;\mathbf{9}\;7\;6][1\;\widehat{10}\;\hat{\mathbf{7}}\;6\;5][1\;2\;\mathbf{3}\;5\;\hat{\hat{6}}]\\
\{1^-,3^+,4^-,2^+\}_L\,\{7^-,9^-,8^+\}_R &\equiv [1\;10\;\mathbf{9}\;7\;6][1\;\widehat{10}\;\hat{\mathbf{7}}\;6\;5][1\;3\;\mathbf{4}\;5\;\hat{\hat{6}}],
\end{aligned}
\tag{C.2.2}
$$

where the left-hand-side denotes the way of adding particles (both from left and right of the BCFW diagram) to the three-point amplitude $A_{\overline{\text{MHV}}}(5,6,10)$, while the right-hand-side means the answer in terms of R-invariant, and hats denote the shifts according to Eq. (C.1.3). We have also checked much more complicated examples.

C.3 Two-particle channel BCFW and ISL in gravity

One can also generalize the discussion in section 2 for Yang-Mills amplitudes to the gravity amplitudes [146]. In gravity the three-point $\overline{\text{MHV}}$ amplitude is given as

$$M_L(1,2,\widehat{P}) = \frac{\delta^8(\eta_1[2\widehat{P}] + \eta_2[\widehat{P}1] - \eta_{\widehat{P}}[12])}{[12]^2[2\widehat{P}]^2[\widehat{P}1]^2}, \tag{C.3.1}$$

and the corresponding soft factor is defined as following,

$$\mathcal{G}_+(n\ 1\ 2) \equiv M_L(1,2,\widehat{P})\frac{1}{s_{12}} = \frac{\langle n2\rangle^2[21]}{\langle n1\rangle^2\langle 12\rangle} = \mathcal{S}_+^2(n\ 1\ 2)s_{12}, \tag{C.3.2}$$

with the same shifts on particles 2 and n as Eq. (5.1.1).

Since there is a bonus relation between gravity amplitudes[14, 171, 47], the above soft factor can be further simplified. For instance for a MHV amplitude, under the shift Eq. (4.2.1), we have BCFW recursion relation and the bonus relation,

$$\begin{aligned} M_2 + M_3 + \cdots + M_{n-1} &= M, \\ z_2M_2 + z_3M_3 + \cdots + z_{n-1}M_{n-1} &= 0, \end{aligned} \tag{C.3.3}$$

which allows us to remove M_{n-1} in the whole amplitude M and get an extra bonus factor [171]

$$B_{n-1} = 1 - \frac{\langle 1i\rangle\langle nn-1\rangle}{\langle ni\rangle\langle 1n-1\rangle} = \frac{\langle 1n\rangle\langle in-1\rangle}{\langle ni\rangle\langle 1n-1\rangle}, \tag{C.3.4}$$

multiply this bonus factor with soft factor $\mathcal{G}(n, 1, i)$ in (C.3.2), we arrive at more familiar result

$$\mathcal{G}_B(n\ 1\ i) = \frac{\langle ni\rangle\langle in-1\rangle[i1]}{\langle n1\rangle\langle 1i\rangle\langle 1n-1\rangle}, \tag{C.3.5}$$

which is the soft factor used in [180, 140], and the corresponding ISL recursion relation from this soft factor is the same as the one appeared in [144], which was originally obtained from $\mathcal{N} = 7$ BCFW. [185] Similar consideration can be done for negative graviton.

Bibliography

[1] S. J. Parke and T. Taylor, "An Amplitude for n Gluon Scattering," *Phys.Rev.Lett.* **56** (1986) 2459.

[2] F. A. Berends and W. Giele, "The Six Gluon Process as an Example of Weyl-Van Der Waerden Spinor Calculus," *Nucl.Phys.* **B294** (1987) 700.

[3] F. A. Berends and W. Giele, "Recursive Calculations for Processes with n Gluons," *Nucl.Phys.* **B306** (1988) 759.

[4] M. L. Mangano, S. J. Parke, and Z. Xu, "Duality and Multi - Gluon Scattering," *Nucl.Phys.* **B298** (1988) 653.

[5] S. J. Parke and T. Taylor, "Perturbative QCD Utilizing Extended Supersymmetry," *Phys.Lett.* **B157** (1985) 81.

[6] M. T. Grisaru, H. Pendleton, and P. van Nieuwenhuizen, "Supergravity and the S Matrix," *Phys.Rev.* **D15** (1977) 996.

[7] M. T. Grisaru and H. Pendleton, "Some Properties of Scattering Amplitudes in Supersymmetric Theories," *Nucl.Phys.* **B124** (1977) 81.

[8] Z. Kunszt, "Combined Use of the Calkul Method and N=1 Supersymmetry to Calculate QCD Six Parton Processes," *Nucl.Phys.* **B271** (1986) 333.

[9] E. Witten, "Perturbative gauge theory as a string theory in twistor space," *Commun.Math.Phys.* **252** (2004) 189–258, `arXiv:hep-th/0312171 [hep-th]`.

[10] R. Roiban, M. Spradlin, and A. Volovich, "On the tree level S matrix of Yang-Mills theory," *Phys.Rev.* **D70** (2004) 026009, `arXiv:hep-th/0403190 [hep-th]`.

[11] F. Cachazo, P. Svrcek, and E. Witten, "MHV vertices and tree amplitudes in gauge theory," *JHEP* **0409** (2004) 006, `arXiv:hep-th/0403047 [hep-th]`.

[12] R. Britto, F. Cachazo, and B. Feng, "New recursion relations for tree amplitudes of gluons," *Nucl.Phys.* **B715** (2005) 499–522, `arXiv:hep-th/0412308 [hep-th]`.

[13] R. Britto, F. Cachazo, B. Feng, and E. Witten, "Direct proof of tree-level recursion relation in Yang-Mills theory," *Phys.Rev.Lett.* **94** (2005) 181602, `arXiv:hep-th/0501052 [hep-th]`.

[14] N. Arkani-Hamed, F. Cachazo, and J. Kaplan, "What is the Simplest Quantum Field Theory?," *JHEP* **1009** (2010) 016, `arXiv:0808.1446 [hep-th]`.

[15] Z. Bern, L. J. Dixon, and D. A. Kosower, "Unitarity based techniques for one loop calculations in QCD," *Nucl.Phys.Proc.Suppl.* **51C** (1996) 243–249, `arXiv:hep-ph/9606378 [hep-ph]`.

[16] C. Anastasiou, Z. Bern, L. J. Dixon, and D. Kosower, "Planar amplitudes in maximally supersymmetric Yang-Mills theory," *Phys.Rev.Lett.* **91** (2003) 251602, `arXiv:hep-th/0309040 [hep-th]`.

[17] Z. Bern, L. J. Dixon, and V. A. Smirnov, "Iteration of planar amplitudes in maximally supersymmetric Yang-Mills theory at three loops and beyond," *Phys.Rev.* **D72** (2005) 085001, `arXiv:hep-th/0505205 [hep-th]`.

[18] J. Drummond, J. Henn, G. Korchemsky, and E. Sokatchev, "Generalized unitarity for N=4 super-amplitudes," *Nucl.Phys.* **B869** (2013) 452–492, `arXiv:0808.0491 [hep-th]`.

[19] J. Drummond, J. Henn, G. Korchemsky, and E. Sokatchev, "Dual superconformal symmetry of scattering amplitudes in N=4 super-Yang-Mills theory," *Nucl.Phys.* **B828** (2010) 317–374, `arXiv:0807.1095 [hep-th]`.

[20] L. F. Alday and J. M. Maldacena, "Gluon scattering amplitudes at strong coupling," *JHEP* **0706** (2007) 064, `arXiv:0705.0303 [hep-th]`.

[21] J. Drummond, J. Henn, G. Korchemsky, and E. Sokatchev, "Hexagon Wilson loop = six-gluon MHV amplitude," *Nucl.Phys.* **B815** (2009) 142–173, `arXiv:0803.1466 [hep-th]`.

[22] N. Beisert, R. Ricci, A. A. Tseytlin, and M. Wolf, "Dual Superconformal Symmetry from AdS(5) x S**5 Superstring Integrability," *Phys.Rev.* **D78** (2008) 126004, `arXiv:0807.3228 [hep-th]`.

[23] N. Berkovits and J. Maldacena, "Fermionic T-Duality, Dual Superconformal Symmetry, and the Amplitude/Wilson Loop Connection," *JHEP* **0809** (2008) 062, `arXiv:0807.3196 [hep-th]`.

[24] B. Eden, G. P. Korchemsky, and E. Sokatchev, "From correlation functions to scattering amplitudes," *JHEP* **1112** (2011) 002, `arXiv:1007.3246 [hep-th]`.

[25] L. F. Alday, B. Eden, G. P. Korchemsky, J. Maldacena, and E. Sokatchev, "From correlation functions to Wilson loops," *JHEP* **1109** (2011) 123, `arXiv:1007.3243 [hep-th]`.

[26] B. Eden, G. P. Korchemsky, and E. Sokatchev, "More on the duality correlators/amplitudes," *Phys.Lett.* **B709** (2012) 247–253, `arXiv:1009.2488 [hep-th]`.

[27] N. Arkani-Hamed, F. Cachazo, C. Cheung, and J. Kaplan, "A Duality For The S Matrix," *JHEP* **1003** (2010) 020, `arXiv:0907.5418 [hep-th]`.

[28] N. Arkani-Hamed, J. L. Bourjaily, F. Cachazo, S. Caron-Huot, and J. Trnka, "The All-Loop Integrand For Scattering Amplitudes in Planar N=4 SYM," *JHEP* **1101** (2011) 041, `arXiv:1008.2958 [hep-th]`.

[29] N. Arkani-Hamed, F. Cachazo, and C. Cheung, "The Grassmannian Origin Of Dual Superconformal Invariance," *JHEP* **1003** (2010) 036, `arXiv:0909.0483 [hep-th]`.

[30] L. Mason and D. Skinner, "Dual Superconformal Invariance, Momentum Twistors and Grassmannians," *JHEP* **0911** (2009) 045, `arXiv:0909.0250 [hep-th]`.

[31] N. Arkani-Hamed, J. L. Bourjaily, F. Cachazo, A. B. Goncharov, A. Postnikov, *et al.*, "Scattering Amplitudes and the Positive Grassmannian," `arXiv:1212.5605 [hep-th]`.

[32] A. B. Goncharov, M. Spradlin, C. Vergu, and A. Volovich, "Classical Polylogarithms for Amplitudes and Wilson Loops," *Phys.Rev.Lett.* **105** (2010) 151605, `arXiv:1006.5703 [hep-th]`.

[33] Z. Bern, J. Carrasco, and H. Johansson, "New Relations for Gauge-Theory Amplitudes," *Phys.Rev.* **D78** (2008) 085011, `arXiv:0805.3993 [hep-ph]`.

[34] G. Bossard, P. Howe, and K. Stelle, "A Note on the UV behaviour of maximally supersymmetric Yang-Mills theories," *Phys.Lett.* **B682** (2009) 137–142, `arXiv:0908.3883 [hep-th]`.

[35] H. Elvang, D. Z. Freedman, and M. Kiermaier, "A simple approach to counterterms in N=8 supergravity," *JHEP* **1011** (2010) 016, `arXiv:1003.5018 [hep-th]`.

[36] R. Kallosh and P. Ramond, "Light-by-Light Scattering Effect in Light-Cone Supergraphs," `arXiv:1006.4684 [hep-th]`.

[37] J. Bjornsson and M. B. Green, "5 loops in 24/5 dimensions," *JHEP* **1008** (2010) 132, `arXiv:1004.2692 [hep-th]`.

[38] P. Vanhove, "The Critical ultraviolet behaviour of N=8 supergravity amplitudes," `arXiv:1004.1392 [hep-th]`.

[39] H. Kawai, D. Lewellen, and S. Tye, "A Relation Between Tree Amplitudes of Closed and Open Strings," *Nucl.Phys.* **B269** (1986) 1.

[40] Z. Bern, J. J. M. Carrasco, and H. Johansson, "Perturbative Quantum Gravity as a Double Copy of Gauge Theory," *Phys.Rev.Lett.* **105** (2010) 061602, `arXiv:1004.0476 [hep-th]`.

[41] M. F. Paulos, "Towards Feynman rules for Mellin amplitudes," *JHEP* **1110** (2011) 074, `arXiv:1107.1504 [hep-th]`.

[42] A. L. Fitzpatrick, J. Kaplan, J. Penedones, S. Raju, and B. C. van Rees, "A Natural Language for AdS/CFT Correlators," *JHEP* **1111** (2011) 095, arXiv:1107.1499 [hep-th].

[43] D. Nandan, A. Volovich, and C. Wen, "On Feynman Rules for Mellin Amplitudes in AdS/CFT," *JHEP* **1205** (2012) 129, arXiv:1112.0305 [hep-th].

[44] M. F. Paulos, M. Spradlin, and A. Volovich, "Mellin Amplitudes for Dual Conformal Integrals," *JHEP* **1208** (2012) 072, arXiv:1203.6362 [hep-th].

[45] N. Arkani-Hamed, "http://www.ippp.dur.ac.uk/workshops/09/amplitudes/„" in *talk at Amplitudes 09*. 2009.

[46] D. Nandan and C. Wen, "Generating All Tree Amplitudes in N=4 SYM by Inverse Soft Limit," *JHEP* **1208** (2012) 040, arXiv:1204.4841 [hep-th].

[47] S. He, D. Nandan, and C. Wen, "Note on Bonus Relations for N=8 Supergravity Tree Amplitudes," *JHEP* **1102** (2011) 005, arXiv:1011.4287 [hep-th].

[48] M. L. Mangano, "The Color Structure of Gluon Emission," *Nucl.Phys.* **B309** (1988) 461.

[49] Z. Bern and D. A. Kosower, "Color decomposition of one loop amplitudes in gauge theories," *Nucl.Phys.* **B362** (1991) 389–448.

[50] L. J. Dixon, "Calculating scattering amplitudes efficiently," arXiv:hep-ph/9601359 [hep-ph].

[51] R. Penrose and M. A. MacCallum, "Twistor theory: An Approach to the quantization of fields and space-time," *Phys.Rept.* **6** (1972) 241–316.

[52] R. Penrose, "A BRIEF INTRODUCTION TO TWISTORS," *Surveys High Energ.Phys.* **1** (1980) 267–288.

[53] A. Hodges, "The Box Integrals in Momentum-Twistor Geometry," arXiv:1004.3323 [hep-th].

[54] V. Nair, "A CURRENT ALGEBRA FOR SOME GAUGE THEORY AMPLITUDES," *Phys.Lett.* **B214** (1988) 215.

[55] N. Arkani-Hamed and J. Kaplan, "On Tree Amplitudes in Gauge Theory and Gravity," *JHEP* **0804** (2008) 076, `arXiv:0801.2385 [hep-th]`.

[56] A. Brandhuber, P. Heslop, and G. Travaglini, "A Note on dual superconformal symmetry of the N=4 super Yang-Mills S-matrix," *Phys.Rev.* **D78** (2008) 125005, `arXiv:0807.4097 [hep-th]`.

[57] J. M. Maldacena, "The Large N limit of superconformal field theories and supergravity," *Adv.Theor.Math.Phys.* **2** (1998) 231–252, `arXiv:hep-th/9711200 [hep-th]`.

[58] G. Mack, "D-dimensional Conformal Field Theories with anomalous dimensions as Dual Resonance Models," *Bulg.J.Phys.* **36** (2009) 214–226, `arXiv:0909.1024 [hep-th]`.

[59] G. Mack, "D-independent representation of Conformal Field Theories in D dimensions via transformation to auxiliary Dual Resonance Models. Scalar amplitudes," `arXiv:0907.2407 [hep-th]`.

[60] P. A. Dirac, "Wave equations in conformal space," *Annals Math.* **37** (1936) 429–442.

[61] S. Weinberg, "Six-dimensional Methods for Four-dimensional Conformal Field Theories," *Phys.Rev.* **D82** (2010) 045031, `arXiv:1006.3480 [hep-th]`.

[62] E. Witten, "Anti-de Sitter space and holography," *Adv.Theor.Math.Phys.* **2** (1998) 253–291, `arXiv:hep-th/9802150 [hep-th]`.

[63] S. Gubser, I. R. Klebanov, and A. M. Polyakov, "Gauge theory correlators from noncritical string theory," *Phys.Lett.* **B428** (1998) 105–114, `arXiv:hep-th/9802109 [hep-th]`.

[64] H. Liu and A. A. Tseytlin, "On four point functions in the CFT / AdS correspondence," *Phys.Rev.* **D59** (1999) 086002, `arXiv:hep-th/9807097 [hep-th]`.

[65] H. Liu, "Scattering in anti-de Sitter space and operator product expansion," *Phys.Rev.* **D60** (1999) 106005, arXiv:hep-th/9811152 [hep-th].

[66] E. D'Hoker and D. Z. Freedman, "General scalar exchange in AdS(d+1)," *Nucl.Phys.* **B550** (1999) 261–288, arXiv:hep-th/9811257 [hep-th].

[67] D. Z. Freedman, S. D. Mathur, A. Matusis, and L. Rastelli, "Comments on 4 point functions in the CFT / AdS correspondence," *Phys.Lett.* **B452** (1999) 61–68, arXiv:hep-th/9808006 [hep-th].

[68] D. Z. Freedman, S. D. Mathur, A. Matusis, and L. Rastelli, "Correlation functions in the CFT(d) / AdS(d+1) correspondence," *Nucl.Phys.* **B546** (1999) 96–118, arXiv:hep-th/9804058 [hep-th].

[69] E. D'Hoker, D. Z. Freedman, S. D. Mathur, A. Matusis, and L. Rastelli, "Graviton exchange and complete four point functions in the AdS / CFT correspondence," *Nucl.Phys.* **B562** (1999) 353–394, arXiv:hep-th/9903196 [hep-th].

[70] G. Arutyunov and S. Frolov, "Four point functions of lowest weight CPOs in N=4 SYM(4) in supergravity approximation," *Phys.Rev.* **D62** (2000) 064016, arXiv:hep-th/0002170 [hep-th].

[71] G. Arutyunov, F. Dolan, H. Osborn, and E. Sokatchev, "Correlation functions and massive Kaluza-Klein modes in the AdS / CFT correspondence," *Nucl.Phys.* **B665** (2003) 273–324, arXiv:hep-th/0212116 [hep-th].

[72] G. Arutyunov and E. Sokatchev, "On a large N degeneracy in N=4 SYM and the AdS / CFT correspondence," *Nucl.Phys.* **B663** (2003) 163–196, arXiv:hep-th/0301058 [hep-th].

[73] L. Berdichevsky and P. Naaijkens, "Four-point functions of different-weight operators in the AdS/CFT correspondence," *JHEP* **0801** (2008) 071, arXiv:0709.1365 [hep-th].

[74] L. I. Uruchurtu, "Four-point correlators with higher weight superconformal primaries in the AdS/CFT Correspondence," *JHEP* **0903** (2009) 133, arXiv:0811.2320 [hep-th].

[75] E. Buchbinder and A. Tseytlin, "On semiclassical approximation for correlators of closed string vertex operators in AdS/CFT," *JHEP* **1008** (2010) 057, `arXiv:1005.4516 [hep-th]`.

[76] L. I. Uruchurtu, "Next-next-to-extremal Four Point Functions of N=4 1/2 BPS Operators in the AdS/CFT Correspondence," *JHEP* **1108** (2011) 133, `arXiv:1106.0630 [hep-th]`.

[77] F. Dolan, M. Nirschl, and H. Osborn, "Conjectures for large N superconformal N=4 chiral primary four point functions," *Nucl.Phys.* **B749** (2006) 109–152, `arXiv:hep-th/0601148 [hep-th]`.

[78] E. D'Hoker, D. Z. Freedman, and L. Rastelli, "AdS / CFT four point functions: How to succeed at z integrals without really trying," *Nucl.Phys.* **B562** (1999) 395–411, `arXiv:hep-th/9905049 [hep-th]`.

[79] S. Raju, "New Recursion Relations and a Flat Space Limit for AdS/CFT Correlators," *Phys.Rev.* **D85** (2012) 126009, `arXiv:1201.6449 [hep-th]`.

[80] S. Raju, "Recursion Relations for AdS/CFT Correlators," *Phys.Rev.* **D83** (2011) 126002, `arXiv:1102.4724 [hep-th]`.

[81] J. Penedones, "Writing CFT correlation functions as AdS scattering amplitudes," *JHEP* **1103** (2011) 025, `arXiv:1011.1485 [hep-th]`.

[82] M. S. Costa, J. Penedones, D. Poland, and S. Rychkov, "Spinning Conformal Correlators," *JHEP* **1111** (2011) 071, `arXiv:1107.3554 [hep-th]`.

[83] M. S. Costa, J. Penedones, D. Poland, and S. Rychkov, "Spinning Conformal Blocks," *JHEP* **1111** (2011) 154, `arXiv:1109.6321 [hep-th]`.

[84] I. Balitsky, "Mellin representation of the graviton bulk-to-bulk propagator in AdS," *Phys.Rev.* **D83** (2011) 087901, `arXiv:1102.0577 [hep-th]`.

[85] L. Susskind, "Holography in the flat space limit," `arXiv:hep-th/9901079 [hep-th]`.

[86] J. Polchinski, "S matrices from AdS space-time," `arXiv:hep-th/9901076 [hep-th]`.

[87] M. Gary, S. B. Giddings, and J. Penedones, "Local bulk S-matrix elements and CFT singularities," *Phys.Rev.* **D80** (2009) 085005, arXiv:0903.4437 [hep-th].

[88] I. Heemskerk, J. Penedones, J. Polchinski, and J. Sully, "Holography from Conformal Field Theory," *JHEP* **0910** (2009) 079, arXiv:0907.0151 [hep-th].

[89] A. L. Fitzpatrick, E. Katz, D. Poland, and D. Simmons-Duffin, "Effective Conformal Theory and the Flat-Space Limit of AdS," *JHEP* **1107** (2011) 023, arXiv:1007.2412 [hep-th].

[90] T. Okuda and J. Penedones, "String scattering in flat space and a scaling limit of Yang-Mills correlators," *Phys.Rev.* **D83** (2011) 086001, arXiv:1002.2641 [hep-th].

[91] A. L. Fitzpatrick and J. Kaplan, "Scattering States in AdS/CFT," arXiv:1104.2597 [hep-th].

[92] M. Gary and S. B. Giddings, "The Flat space S-matrix from the AdS/CFT correspondence?," *Phys.Rev.* **D80** (2009) 046008, arXiv:0904.3544 [hep-th].

[93] S. B. Giddings, "Flat space scattering and bulk locality in the AdS / CFT correspondence," *Phys.Rev.* **D61** (2000) 106008, arXiv:hep-th/9907129 [hep-th].

[94] M. Gary and S. B. Giddings, "Constraints on a fine-grained AdS/CFT correspondence," arXiv:1106.3553 [hep-th].

[95] A. L. Fitzpatrick and J. Kaplan, "Analyticity and the Holographic S-Matrix," *JHEP* **1210** (2012) 127, arXiv:1111.6972 [hep-th].

[96] A. L. Fitzpatrick and J. Kaplan, "Unitarity and the Holographic S-Matrix," *JHEP* **1210** (2012) 032, arXiv:1112.4845 [hep-th].

[97] A. L. Fitzpatrick and J. Kaplan, "AdS Field Theory from Conformal Field Theory," *JHEP* **1302** (2013) 054, arXiv:1208.0337 [hep-th].

[98] J. M. Drummond, J. M. Henn, and J. Trnka, "New differential equations for on-shell loop integrals," *JHEP* **1104** (2011) 083, `arXiv:1010.3679 [hep-th]`.

[99] L. J. Dixon, J. M. Drummond, and J. M. Henn, "The one-loop six-dimensional hexagon integral and its relation to MHV amplitudes in N=4 SYM," *JHEP* **1106** (2011) 100, `arXiv:1104.2787 [hep-th]`.

[100] L. Ferro, "Differential equations for multi-loop integrals and two-dimensional kinematics," `arXiv:1204.1031 [hep-th]`.

[101] A. I. Davydychev, "Some exact results for N point massive Feynman integrals," *J.Math.Phys.* **32** (1991) 1052–1060.

[102] A. I. Davydychev and R. Delbourgo, "A Geometrical angle on Feynman integrals," *J.Math.Phys.* **39** (1998) 4299–4334, `arXiv:hep-th/9709216 [hep-th]`.

[103] L. Mason and D. Skinner, "Amplitudes at Weak Coupling as Polytopes in AdS_5," *J.Phys.* **A44** (2011) 135401, `arXiv:1004.3498 [hep-th]`.

[104] O. Schnetz, "The geometry of one-loop amplitudes," `arXiv:1010.5334 [hep-th]`.

[105] M. F. Paulos, "Loops, Polytopes and Splines," `arXiv:1210.0578 [hep-th]`.

[106] N. Arkani-Hamed, J. L. Bourjaily, F. Cachazo, A. Hodges, and J. Trnka, "A Note on Polytopes for Scattering Amplitudes," *JHEP* **1204** (2012) 081, `arXiv:1012.6030 [hep-th]`.

[107] A.B.Goncharov, "Volumes of hyperbolic manifolds and mixed tate motives," *arXiv:alg-geom/9601021* (1996) .

[108] M. Spradlin and A. Volovich, "Symbols of One-Loop Integrals From Mixed Tate Motives," *JHEP* **1111** (2011) 084, `arXiv:1105.2024 [hep-th]`.

[109] V. Del Duca, C. Duhr, and V. A. Smirnov, "The massless hexagon integral in $D = 6$ dimensions," *Phys.Lett.* **B703** (2011) 363–365, `arXiv:1104.2781 [hep-th]`.

[110] V. Del Duca, C. Duhr, and V. A. Smirnov, "The One-Loop One-Mass Hexagon Integral in D=6 Dimensions," *JHEP* **1107** (2011) 064, `arXiv:1105.1333 [hep-th]`.

[111] V. Del Duca, L. J. Dixon, J. M. Drummond, C. Duhr, J. M. Henn, *et al.*, "The one-loop six-dimensional hexagon integral with three massive corners," *Phys.Rev.* **D84** (2011) 045017, `arXiv:1105.2011 [hep-th]`.

[112] S. Caron-Huot and K. J. Larsen, "Uniqueness of two-loop master contours," *JHEP* **1210** (2012) 026, `arXiv:1205.0801 [hep-ph]`.

[113] M. S. Costa, V. Goncalves, and J. Penedones, "Conformal Regge theory," *JHEP* **2012** (2012) 091, `arXiv:1209.4355 [hep-th]`.

[114] Z. Bern, L. J. Dixon, and D. A. Kosower, "Dimensionally regulated pentagon integrals," *Nucl.Phys.* **B412** (1994) 751–816, `arXiv:hep-ph/9306240 [hep-ph]`.

[115] P. Heslop and V. V. Khoze, "Analytic Results for MHV Wilson Loops," *JHEP* **1011** (2010) 035, `arXiv:1007.1805 [hep-th]`.

[116] L. F. Alday, "Some analytic results for two-loop scattering amplitudes," *JHEP* **1107** (2011) 080, `arXiv:1009.1110 [hep-th]`.

[117] P. Heslop and V. V. Khoze, "Wilson Loops @ 3-Loops in Special Kinematics," *JHEP* **1111** (2011) 152, `arXiv:1109.0058 [hep-th]`.

[118] T. Goddard, P. Heslop, and V. V. Khoze, "Uplifting Amplitudes in Special Kinematics," *JHEP* **1210** (2012) 041, `arXiv:1205.3448 [hep-th]`.

[119] S. Laporta and E. Remiddi, "Analytic treatment of the two loop equal mass sunrise graph," *Nucl.Phys.* **B704** (2005) 349–386, `arXiv:hep-ph/0406160 [hep-ph]`.

[120] S. Weinberg, "Photons and Gravitons in s Matrix Theory: Derivation of Charge Conservation and Equality of Gravitational and Inertial Mass," *Phys.Rev.* **135** (1964) B1049–B1056.

[121] A. Sen, "Asymptotic Behavior of the Sudakov Form-Factor in QCD," *Phys.Rev.* **D24** (1981) 3281.

[122] G. F. Sterman, "Summation of Large Corrections to Short Distance Hadronic Cross-Sections," *Nucl.Phys.* **B281** (1987) 310.

[123] S. Catani and L. Trentadue, "Resummation of the QCD Perturbative Series for Hard Processes," *Nucl.Phys.* **B327** (1989) 323.

[124] J. C. Collins, "Sudakov form-factors," *Adv.Ser.Direct.High Energy Phys.* **5** (1989) 573–614, `arXiv:hep-ph/0312336 [hep-ph]`.

[125] L. Magnea and G. F. Sterman, "Analytic continuation of the Sudakov form-factor in QCD," *Phys.Rev.* **D42** (1990) 4222–4227.

[126] S. Catani and L. Trentadue, "Comment on QCD exponentiation at large x," *Nucl.Phys.* **B353** (1991) 183–186.

[127] S. Catani, "The Singular behavior of QCD amplitudes at two loop order," *Phys.Lett.* **B427** (1998) 161–171, `arXiv:hep-ph/9802439 [hep-ph]`.

[128] G. F. Sterman and M. E. Tejeda-Yeomans, "Multiloop amplitudes and resummation," *Phys.Lett.* **B552** (2003) 48–56, `arXiv:hep-ph/0210130 [hep-ph]`.

[129] J. L. Bourjaily, A. DiRe, A. Shaikh, M. Spradlin, and A. Volovich, "The Soft-Collinear Bootstrap: N=4 Yang-Mills Amplitudes at Six and Seven Loops," *JHEP* **1203** (2012) 032, `arXiv:1112.6432 [hep-th]`.

[130] J. Golden and M. Spradlin, "Collinear and Soft Limits of Multi-Loop Integrands in N=4 Yang-Mills," *JHEP* **1205** (2012) 027, `arXiv:1203.1915 [hep-th]`.

[131] N. Arkani-Hamed, F. Cachazo, C. Cheung, and J. Kaplan, "The S-Matrix in Twistor Space," *JHEP* **1003** (2010) 110, `arXiv:0903.2110 [hep-th]`.

[132] A. P. Hodges, "Twistor diagrams for all tree amplitudes in gauge theory: A Helicity-independent formalism," `arXiv:hep-th/0512336 [hep-th]`.

[133] N. Arkani-Hamed, J. Bourjaily, F. Cachazo, and J. Trnka, "Local Spacetime Physics from the Grassmannian," *JHEP* **1101** (2011) 108, `arXiv:0912.3249 [hep-th]`.

[134] N. Arkani-Hamed, J. Bourjaily, F. Cachazo, and J. Trnka, "Unification of Residues and Grassmannian Dualities," *JHEP* **1101** (2011) 049, `arXiv:0912.4912 [hep-th]`.

[135] L. Dolan and P. Goddard, "Gluon Tree Amplitudes in Open Twistor String Theory," *JHEP* **0912** (2009) 032, `arXiv:0909.0499 [hep-th]`.

[136] M. Spradlin and A. Volovich, "From Twistor String Theory To Recursion Relations," *Phys.Rev.* **D80** (2009) 085022, `arXiv:0909.0229 [hep-th]`.

[137] D. Nandan, A. Volovich, and C. Wen, "A Grassmannian Etude in NMHV Minors," *JHEP* **1007** (2010) 061, `arXiv:0912.3705 [hep-th]`.

[138] J. L. Bourjaily, J. Trnka, A. Volovich, and C. Wen, "The Grassmannian and the Twistor String: Connecting All Trees in N=4 SYM," *JHEP* **1101** (2011) 038, `arXiv:1006.1899 [hep-th]`.

[139] M. Bullimore, L. Mason, and D. Skinner, "Twistor-Strings, Grassmannians and Leading Singularities," *JHEP* **1003** (2010) 070, `arXiv:0912.0539 [hep-th]`.

[140] D. Nguyen, M. Spradlin, A. Volovich, and C. Wen, "The Tree Formula for MHV Graviton Amplitudes," *JHEP* **1007** (2010) 045, `arXiv:0907.2276 [hep-th]`.

[141] M. Bullimore, "Inverse Soft Factors and Grassmannian Residues," *JHEP* **1101** (2011) 055, `arXiv:1008.3110 [hep-th]`.

[142] D. C. Dunbar, J. H. Ettle, and W. B. Perkins, "The n-point MHV one-loop Amplitude in N=4 Supergravity," *Phys.Rev.Lett.* **108** (2012) 061603, `arXiv:1111.1153 [hep-th]`.

[143] D. C. Dunbar, J. H. Ettle, and W. B. Perkins, "Constructing Gravity Amplitudes from Real Soft and Collinear Factorisation," *Phys.Rev.* **D86** (2012) 026009, `arXiv:1203.0198 [hep-th]`.

[144] A. Hodges, "New expressions for gravitational scattering amplitudes," `arXiv:1108.2227 [hep-th]`.

[145] A. Hodges, "A simple formula for gravitational MHV amplitudes," `arXiv:1204.1930 [hep-th]`.

[146] C. Boucher-Veronneau and A. J. Larkoski, "Constructing Amplitudes from Their Soft Limits," *JHEP* **1109** (2011) 130, arXiv:1108.5385 [hep-th].

[147] W. van Neerven, "INFRARED BEHAVIOR OF ON-SHELL FORM-FACTORS IN A N=4 SUPERSYMMETRIC YANG-MILLS FIELD THEORY," *Z.Phys.* **C30** (1986) 595.

[148] J. Drummond and J. Henn, "All tree-level amplitudes in N=4 SYM," *JHEP* **0904** (2009) 018, arXiv:0808.2475 [hep-th].

[149] J. Maldacena and A. Zhiboedov, "Form factors at strong coupling via a Y-system," *JHEP* **1011** (2010) 104, arXiv:1009.1139 [hep-th].

[150] A. Brandhuber, B. Spence, G. Travaglini, and G. Yang, "Form Factors in N=4 Super Yang-Mills and Periodic Wilson Loops," *JHEP* **1101** (2011) 134, arXiv:1011.1899 [hep-th].

[151] A. Brandhuber, O. Gurdogan, R. Mooney, G. Travaglini, and G. Yang, "Harmony of Super Form Factors," *JHEP* **1110** (2011) 046, arXiv:1107.5067 [hep-th].

[152] L. Bork, D. Kazakov, and G. Vartanov, "On MHV Form Factors in Superspace for $\backslash = 4$ SYM Theory," *JHEP* **1110** (2011) 133, arXiv:1107.5551 [hep-th].

[153] A. Brandhuber, G. Travaglini, and G. Yang, "Analytic two-loop form factors in N=4 SYM," *JHEP* **1205** (2012) 082, arXiv:1201.4170 [hep-th].

[154] L. Bork, "On NMHV form factors in N=4 SYM theory from generalized unitarity," *JHEP* **1301** (2013) 049, arXiv:1203.2596 [hep-th].

[155] B. Eden, P. Heslop, G. P. Korchemsky, and E. Sokatchev, "The super-correlator/super-amplitude duality: Part I," *Nucl.Phys.* **B869** (2013) 329–377, arXiv:1103.3714 [hep-th].

[156] B. Eden, P. Heslop, G. P. Korchemsky, and E. Sokatchev, "The super-correlator/super-amplitude duality: Part II," *Nucl.Phys.* **B869** (2013) 378–416, arXiv:1103.4353 [hep-th].

[157] L. J. Dixon, E. N. Glover, and V. V. Khoze, "MHV rules for Higgs plus multi-gluon amplitudes," *JHEP* **0412** (2004) 015, `arXiv:hep-th/0411092 [hep-th]`.

[158] J. Drummond, M. Spradlin, A. Volovich, and C. Wen, "Tree-Level Amplitudes in N=8 Supergravity," *Phys.Rev.* **D79** (2009) 105018, `arXiv:0901.2363 [hep-th]`.

[159] R. Kallosh and T. Kugo, "The Footprint of E(7(7)) amplitudes of N=8 supergravity," *JHEP* **0901** (2009) 072, `arXiv:0811.3414 [hep-th]`.

[160] S. He and H. Zhu, "A Note on Single Soft Scalar Emission of N=8 SUGRA and E(7)(7) Symmetry," *JHEP* **1007** (2010) 025, `arXiv:0812.4533 [hep-th]`.

[161] J. Broedel and L. J. Dixon, "R**4 counterterm and E(7)(7) symmetry in maximal supergravity," *JHEP* **1005** (2010) 003, `arXiv:0911.5704 [hep-th]`.

[162] G. Bossard, C. Hillmann, and H. Nicolai, "E7(7) symmetry in perturbatively quantised N=8 supergravity," *JHEP* **1012** (2010) 052, `arXiv:1007.5472 [hep-th]`.

[163] M. B. Green, J. G. Russo, and P. Vanhove, "Ultraviolet properties of maximal supergravity," *Phys.Rev.Lett.* **98** (2007) 131602, `arXiv:hep-th/0611273 [hep-th]`.

[164] Z. Bern, J. Carrasco, L. J. Dixon, H. Johansson, D. Kosower, *et al.*, "Three-Loop Superfiniteness of N=8 Supergravity," *Phys.Rev.Lett.* **98** (2007) 161303, `arXiv:hep-th/0702112 [hep-th]`.

[165] Z. Bern, J. Carrasco, L. J. Dixon, H. Johansson, and R. Roiban, "Manifest Ultraviolet Behavior for the Three-Loop Four-Point Amplitude of N=8 Supergravity," *Phys.Rev.* **D78** (2008) 105019, `arXiv:0808.4112 [hep-th]`.

[166] Z. Bern, J. Carrasco, L. J. Dixon, H. Johansson, and R. Roiban, "The Ultraviolet Behavior of N=8 Supergravity at Four Loops," *Phys.Rev.Lett.* **103** (2009) 081301, `arXiv:0905.2326 [hep-th]`.

[167] L. J. Dixon, "Ultraviolet Behavior of N = 8 Supergravity," arXiv:1005.2703 [hep-th].

[168] J. Drummond, P. Heslop, and P. Howe, "A Note on N=8 counterterms," arXiv:1008.4939 [hep-th].

[169] N. Beisert, H. Elvang, D. Z. Freedman, M. Kiermaier, A. Morales, *et al.*, "E7(7) constraints on counterterms in N=8 supergravity," *Phys.Lett.* **B694** (2010) 265–271, arXiv:1009.1643 [hep-th].

[170] R. Kallosh, "The Ultraviolet Finiteness of N=8 Supergravity," *JHEP* **1012** (2010) 009, arXiv:1009.1135 [hep-th].

[171] M. Spradlin, A. Volovich, and C. Wen, "Three Applications of a Bonus Relation for Gravity Amplitudes," *Phys.Lett.* **B674** (2009) 69–72, arXiv:0812.4767 [hep-th].

[172] F. A. Berends, W. Giele, and H. Kuijf, "On relations between multi - gluon and multigraviton scattering," *Phys.Lett.* **B211** (1988) 91.

[173] V. Nair, "A Note on MHV amplitudes for gravitons," *Phys.Rev.* **D71** (2005) 121701, arXiv:hep-th/0501143 [hep-th].

[174] J. Bedford, A. Brandhuber, B. J. Spence, and G. Travaglini, "A Recursion relation for gravity amplitudes," *Nucl.Phys.* **B721** (2005) 98–110, arXiv:hep-th/0502146 [hep-th].

[175] H. Elvang and D. Z. Freedman, "Note on graviton MHV amplitudes," *JHEP* **0805** (2008) 096, arXiv:0710.1270 [hep-th].

[176] L. Mason and D. Skinner, "Gravity, Twistors and the MHV Formalism," *Commun.Math.Phys.* **294** (2010) 827–862, arXiv:0808.3907 [hep-th].

[177] N. Bjerrum-Bohr, P. H. Damgaard, B. Feng, and T. Sondergaard, "Gravity and Yang-Mills Amplitude Relations," *Phys.Rev.* **D82** (2010) 107702, arXiv:1005.4367 [hep-th].

[178] N. Bjerrum-Bohr, P. H. Damgaard, B. Feng, and T. Sondergaard, "New Identities among Gauge Theory Amplitudes," *Phys.Lett.* **B691** (2010) 268–273, arXiv:1006.3214 [hep-th].

[179] B. Feng and S. He, "KLT and New Relations for N=8 SUGRA and N=4 SYM," *JHEP* **1009** (2010) 043, `arXiv:1007.0055 [hep-th]`.

[180] Z. Bern, L. J. Dixon, M. Perelstein, and J. Rozowsky, "Multileg one loop gravity amplitudes from gauge theory," *Nucl.Phys.* **B546** (1999) 423–479, `arXiv:hep-th/9811140 [hep-th]`.

[181] B. Feng, S. He, R. Huang, and Y. Jia, "Note on New KLT relations," *JHEP* **1010** (2010) 109, `arXiv:1008.1626 [hep-th]`.

[182] K. Symanzik, "On Calculations in conformal invariant field theories," *Lett.Nuovo Cim.* **3** (1972) 734–738.

[183] A. Hodges, "Eliminating spurious poles from gauge-theoretic amplitudes," `arXiv:0905.1473 [hep-th]`.

[184] J. L. Bourjaily, "Efficient Tree-Amplitudes in N=4: Automatic BCFW Recursion in Mathematica," `arXiv:1011.2447 [hep-ph]`.

[185] H. Elvang, Y.-t. Huang, and C. Peng, "On-shell superamplitudes in N <4 SYM," *JHEP* **1109** (2011) 031, `arXiv:1102.4843 [hep-th]`.